Estimating the Effects of Orography on Precipitation Levels in the Ibrahim River Basin, Lebanon

by

Jessica L. Fox

B.S. Civil and Environmental Engineering
Massachusetts Institute of Technology, 2000

Submitted to the Department of Civil and Environmental Engineering in Partial Fulfillment of the Requirements for the degree of

Master of Engineering in Civil and Environmental Engineering
at the
Massachusetts Institute of Technology

June 2001

Signature of author:_____
Department of Civil and Environmental Engineering
May 11, 2001

Certified by:_____
Professor Rafael L. Bras
Professor of Civil and Environmental Engineering
and Earth, Atmosphere, and Planetary Sciences
Thesis Supervisor

Accepted by:_____
Professor Oral Buyukozturk
Chairman, Committee on Graduate Studies

Estimating the Effects of Orography on Precipitation Levels in the Ibrahim River Basin, Lebanon

by

Jessica L. Fox

Submitted to the Department of Civil and Environmental Engineering on May 11, 2001 in Partial Fulfillment of the Requirements for the degree of Master of Engineering in Civil and Environmental Engineering

Abstract

The Middle Eastern country of Lebanon was plagued with a devastating civil war from 1975 to 1990. In the years since, the country has begun examining its environmental resources in an attempt to rebuild the nation. During this assessment, it has become clear that during the war much of the precipitation data has been lost and the weather stations destroyed. Precipitation data is an important factor in all forms of environmental assessments. It is necessary for understanding pollution runoff, drinking water resources, and erosion. Using geographic information systems, this thesis models the precipitation in the Ibrahim River basin, north of Beirut. The model uses the climatologic and orographic characteristics of the basin in order to estimate the precipitation in the basin.

Thesis Supervisor: Professor Rafael L. Bras
Title: Professor of Civil and Environmental Engineering and Earth, Atmosphere, and Planetary Sciences

Acknowledgements

I would like to thank:

Professor Bras, for making me work for it.

Pete Shanahan, for finding a solution to every problem.

Eric Adams, for all of your help and advice.

Manal Moussallem, for being a fabulous social and academic coordinator.

Everyone at the Ministry of the Environment and the American University of Beirut for your all your help.

The Powerpuff girls, for all your help here and abroad.

and Ethan, my family, and my friends, for keeping me sane.

TABLE OF CONTENTS

TABLE OF FIGURES

Chapter 1 - Introduction

Reliable weather data is not collected in many countries and any existing data can be unavailable due to limits on the public access to records. The Middle Eastern country of Lebanon faces both of these problems today as a result of a fifteen-year civil war. Many reports from before the war were destroyed along with the instruments to conduct further studies. In the years since, as emphasis has been placed on rebuilding the country, searching for or replacing scientific data has not been a priority. As a result, it is difficult to find recent, consistent environmental data.

However, the government in Lebanon is beginning to be concerned with the effects of the war and reconstruction on the natural resources in the country. The Ministry of the Environment of Lebanon, has begun to perform baseline pollution surveys of various water bodies in the hopes of preventing further damage and reversing the environmental effects of the war. What they have found is a lack of basic precipitation data, hindering modeling and estimation efforts.

1.1 Scope of Work

In order to assist the Ministry of the Environment, this thesis will explore the use of a theoretically based model with a Geographic Information System (GIS) to estimate spatial precipitation. The model will be used to estimate this precipitation on a daily scale. Daily precipitation can then be aggregated into monthly and yearly precipitation totals, which can be compared to other available estimates. Should this method work, it would be an inexpensive way to provide badly needed input to many ongoing and planned environmental studies.

The structure of the following chapters is described here. Chapter 2 will present the recent history of Lebanon in order to illuminate the reasons for the data availability problems in the country. It will then provide background information about the location chosen as a case study, including a discussion of the known precipitation data for the region.

In Chapter 3, the method of precipitation estimation is described. The causes of the orographic effect and a derivation of a theoretical formula are presented in order to provide a basis for the estimation model. The estimation model and method are then explained.

Chapter 4 presents the results of the model and discusses the findings. Conclusions are given in Chapter 5.

Chapter 2 - Background

2.1 *History of Lebanon*

Located in the Middle East, Lebanon is surrounded by the Mediterranean Sea to the West, Syria to the North and East, and Israel to the South (Figure 1). Since its creation in 1920, Lebanon has been repeatedly afflicted with political instability, war, and economic devastation. The most recent war, between 1975 and 1990, devastated the social, economic, and political structure of this once prosperous nation (Nauphal, 1997).

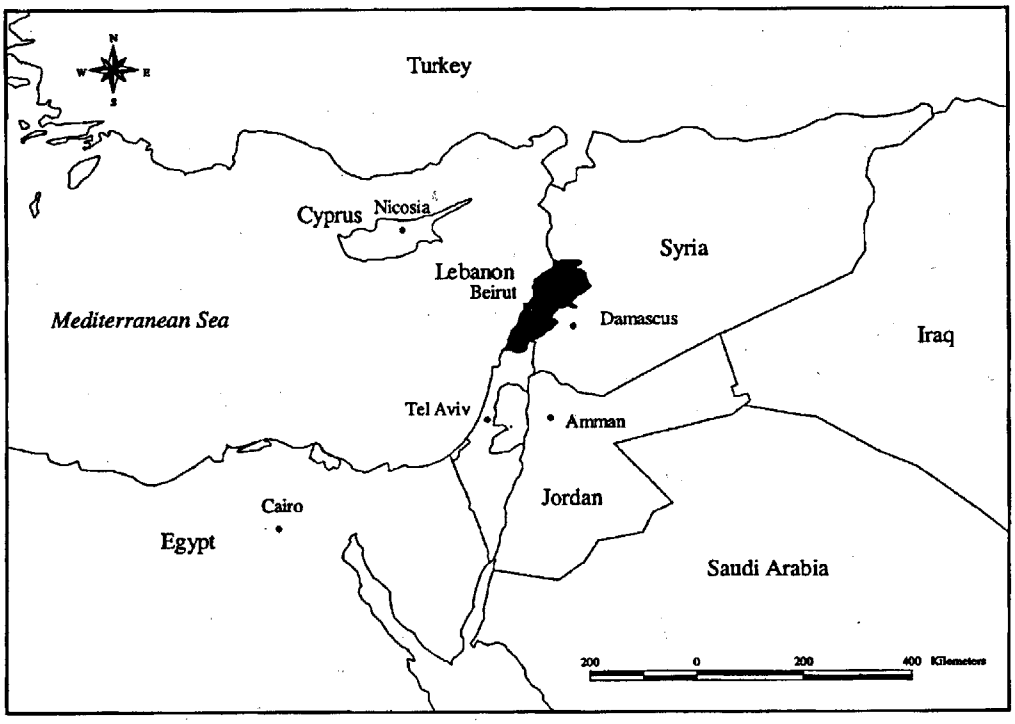

Figure 1 - Map of Middle East

(El Fadel, et al., 2000)

2.1.1 Causes of War

During the Ottoman Empire, portions of what is now Lebanon (Sildon, Tripoli, and Beirut) were under direct Ottoman rule. These areas were inhabited by the dominant orthodox religions of the Byzantine and Islamic empires. The rest of Lebanon, however, maintained only indirect Ottoman rule and became a haven for persecuted Christian and Muslim sects; including the Maronites, Druzes, and Shi'a (Nauphal, 1997).

When the Ottoman Empire was dismantled during World War I, the League of Nations gave France control of Syria and Lebanon. The Republic of Lebanon was formally created in 1926, bringing together the two previously isolated communities of differing religions (orthodox and heterodox sects). Because the two groups had enjoyed separate histories and socio-economic systems, this combination is noted as the root cause of the subsequent civil wars (Nauphal, 1997).

There was soon a power struggle between the Lebanese nationalists (Christians), the French supported groups (Maronites), and the Arab nationalists (Muslims). The Lebanese nationalists wanted an independent Lebanon. The French helped the Maronites implement their political program throughout the country, but with borders differing from what was desired by the Lebanese nationalists. The Arab nationalists wanted Lebanon to become part of a larger Arab-Islamic empire. This divide jeopardized the legitimacy of the republic (Nauphal, 1997).

There are many potential causes of the 1975-1990 civil war in Lebanon. The inequities in cultural group representation in the government, army, and eventually in wealth contributed to a general struggle within the country. Another contributor is that Lebanon was used as a "surrogate battleground" for the foreign conflicts between the Palestinians, Israelis, and Syrians. Displaced Palestinians from the creation of Israel became increasingly militarized and launched guerrilla operations from Lebanon (Nauphal, 1997).

The intentions of the neighboring nations for the state of Lebanon also led to war. Syria has never accepted the sovereignty given to Lebanon by France, believing it to be a province of its own country. Additionally, Israel desired to end the Palestinian terrorist groups within Lebanon as well as expand its territory (Nauphal, 1997).

Internal and external tensions within the country reached a breaking point in 1975, inciting the civil war (Nauphal, 1997).

2.1.2 The 1975-1990 Civil War

The war began in 1975 when the main Christian party accused the Palestinians of violating the sovereignty of the State. Violence soon spread to the entire country, generally between the militias of the pro-Palestinian groups and the Israeli supported Christian group. In 1976, the Palestine Liberation Organization (PLO) joined the war on the Palestinian side while Syria joined to oppose the Palestinians. Two years later, following a bomb attack near Tel Aviv, Israel invaded Lebanon to eliminate the Palestinian bases in the southern region of the country. The United Nations then entered Lebanon to replace the Israeli army (Nauphal, 1997).

In July 1981, the United States stepped in to mediate a cease-fire agreement between Israel and the PLO. However, in 1982 Israel invaded again, surrounding the capital of Beirut and pushing the PLO into Syria (Nauphal, 1997).

The war continued until 1991, when Syria and Lebanon signed a Treaty of Brotherhood, Cooperation, and Coordination and a Pact of Defense and Security, which outlined peace between the two nations. However, despite these peace accords, Israel occupied southern Lebanon until the year 2000 and approximately 40,000 Syrian soldiers remain in the country today (Nauphal, 1997).

In the years since the war, Lebanon has worked to rebuild the infrastructure and economy of the nation. Although relations with Syria and Israel are still tense, there has been relative peace since 1990 (Nauphal, 1997).

Ten years after the war, the reconstruction of infrastructure in the country is well underway and the government of Lebanon is now beginning to become concerned with its environmental resources. During the war, people understandably did not focus on environmental issues. Without a secure government, houses, industries and businesses were built without permits or any means of waste control. After the war, the correction of these past environmental wrongs was not a high priority. In the past few years scientists and governmental offices in Lebanon have begun to study the state of the

environment. However, they are finding that much of the data has been lost and the means to take new measurements have yet to be rebuilt.

2.2 Ibrahim River Basin

The Ibrahim River basin, located in rural central Lebanon, 20 kilometers north of Beirut, is of specific interest to the Ministry of the Environment. The agency is performing an environmental baseline study on the watershed in the hopes of restoring the environment of the basin and attracting tourists to its dramatic and beautiful natural environment. This thesis will focus on the Ibrahim River basin as it is an area of active research and any resulting data will be immediately useful to the Lebanese government.

In the 1970s, before the civil war, the Lebanese government had hoped to build additional dams along the Ibrahim River to aid in hydroelectric power generation and water resource management. Although these plans were never implemented, the scientific reports that were to provide a basis for the dam design are still available (Papazian, 1981; Electrowatt, 1981). In addition, there is one study performed after the war regarding flow in the Ibrahim River (Bureau D'Etudes Hydrauliques, 1994). The data contained within these reports is sparse, but gives a broad range of information regarding the geological, hydrological, and climatic features of the basin.

2.2.1 Watershed Description

The Ibrahim River basin is 330 square kilometers, stretching from the Western slope of Mount Lebanon to the Mediterranean sea (Figure 2). The mountain range frames the Eastern rim of the basin and the terrain slopes downward from an elevation of 2625 meters to sea level. The area is characterized by steep mountain ridges divided by narrow, deep valleys (Papazian, 1981).

At the northern border of the watershed is the drainage basin of Nahr el-Djoz, and at the southern border is the basin of Nahr el-Kelb. Towards the east are the Yammouneh basin and the Nahr Litani Basin. The crest of Mount Lebanon forms the eastern border, which

is 27 kilometers long. The elevation of this rim decreases from the North to South, from 2625 meters to 1875 meters (Papazian, 1981).

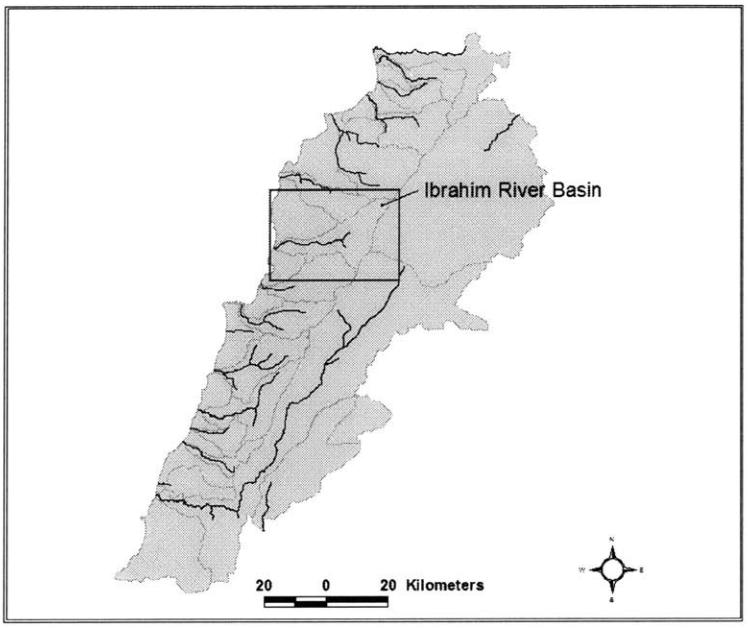

Figure 2 - Location of Ibrahim River Basin
(Based on GIS data from the Lebanese Ministry of the Environment)

The majority of the drainage basin is comprised of steep-sided mountain ridges. A large portion of the drainage basin lies on a high plateau, extending between the branch of the river and the Eastern rim of the basin. This high plateau, which forms Jebel Mneitri, is rectangular, having a surface area of 200 square kilometers (Papazian, 1981). Elevation of the plateau varies between 1200 and 2500 kilometers and is covered by snow from December first until the beginning of April (Bureau D'Etudes Hydrauliques, 1994).

2.2.2 River Statistics

The Ibrahim River (Figure 3) is one of fifteen major rivers in Lebanon. It originates at the crest of Mount Lebanon, at an elevation of 1250 meters from a natural spring in the Afqa Cave formation. Flowing westward, it is joined by a major tributary, the Roueiss River at 1170 meters, and a few smaller tributaries along its length before

emptying into the Mediterranean Sea. The river experiences highly seasonal flow, with high flow in the winter and little flow in the summer (Papazian, 1981).

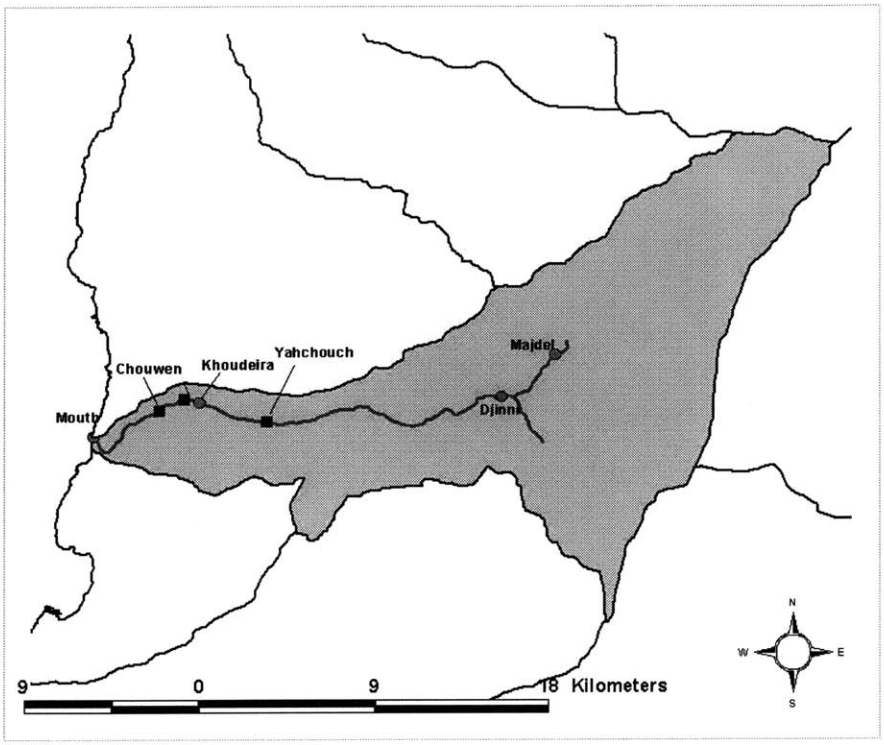

Figure 3 – Sampling Locations along the Ibrahim River
Sampling Locations shown as circles, dams shown as squares

The Ministry of Public Works of Lebanon installed three gauging stations along The Ibrahim River in July of 1939. One was installed near the Khoudeira bridge (at an elevation of 135 m), the second between the present hydroelectric power plants at Yahchouch (elevation of 150 m), and the third at Khoudeira or Bezhel (elevation 86 m). During the fall of 1951, the Ministry of Public Works put in a fourth gauging station, located just downstream the village of Mougheire at Majdel (elevation of 1200 m), and a fifth station located between the confluence of the Roueiss River and Ibrahim River branches at Dijinni (elevation of 775 m) (Papazian, 1981). Another station was built at the mouth of the river. These gauging stations were not monitored during the civil war, and are no longer in operation. The exact positions of these descriptive locations are also not known. Flow data from these stations is summarized in the table below.

Table 1 – Flow Recording at Gauging Station

Flow Recorded at Gauging Station (m^3/s)				
	Majdel	Djinni	Khouaira	Mouth
September	0.20	1.38	1.95	2.06
October	0.30	1.29	2.00	2.12
November	0.30	2.26	3.04	3.22
December	0.35	3.19	7.36	7.79
January	0.30	6.00	13.21	13.98
February	0.30	15.33	16.19	17.04
March	8.00	13.99	27.49	29.09
April	13.50	30.76	38.45	40.69
May	10.00	26.42	28.58	30.24
June	3.00	11.21	10.29	10.89
July	0.50	3.57	4.29	4.54
August	0.20	1.76	2.39	2.53
Yearly Average	3.08	10.05	13.24	13.68

Madjel measurements based on data averaged over the period 1952-1953. Dijinni, Khouaira, and Mouth measurements based on data averaged over the period 1940-1942. (From Papazian, 1981)

2.2.3 Climate within the Basin

The weather in the Ibrahim river basin is that of a typical Mediterranean climate. This characteristic seasonal pattern, experienced by most regions along the Mediterranean Sea, is typified by mild, windy, wet winters and hot, dry summers (Air Ministry, Meteorological Office, p. 3) . The winter (October – May) is characterized by short duration, high-intensity rainfalls, while there is essentially no precipitation during the rest of the year (El-Fadel, et. al., 2000).

The mouth of the river is located in a semi-tropical zone, while the area around the source is considerably cooler. The temperature within the basin spans from approximately 10°C (January) to 24°C (July and August) at low elevations, and from approximately 6.7°C (January) to 23.3°C (August) at high elevations (Papazian, 1981).

The prevailing winds in the region are westerly, carrying moisture from the Mediterranean Sea (El-Fadel, et al., 2000).

The humidity along the coast of Lebanon is relatively high throughout the year, with a continuous influx of moist air from the Mediterranean. In the winter, the Mediterranean cyclonic disturbances produce precipitation. In the summer, the hot, humid air remains along the coast, maintaining high humidity (Papazian, 1981).

The precipitation in the basin ranges from an average of 1000 millimeters at low elevations to 1400 millimeters at high elevations. The average precipitation over the whole surface of the basin is estimated to be 1300 millimeters (Papazian, 1981).

2.2.4 Precipitation Data

There are two existing contour maps of spatial variations in precipitation over the Ibrahim River Basin (Figure 4 and Figure 5). This section describes this data and examines the complications of contour maps based on raingauge measurement.

Figure 4 is a isohyetal map (contours of precipitation) of annual precipitation based on rainfall gauges in the Ibrahim River Basin. It is important to note that the legend (in French) in Figure 4 indicates a monthly (*mensuelles*) time scale for the contours. Weather station measurements show magnitudes of 900-1400mm/month of rain, which are unheard of in the region and would be much more realistic as annual totals (Papazian, 1981). It is thus assumed that Figure 4 is intended to show annual total precipitation contours.

The contours of Figure 4 show a strong correlation between elevation and precipitation levels. Rainfall levels at the mouth of the river are approximately 900mm/yr, while the magnitude increases to a peak of approximately 1400mm/yr in the eastern-central portion of the basin. The totals received in the eastern basin decrease from this peak to 1000mm/yr. The eastward bends in the lines are similar to contours of elevations (shown in 3.3.3.2), indicating a direct increase in rainfall with elevation.

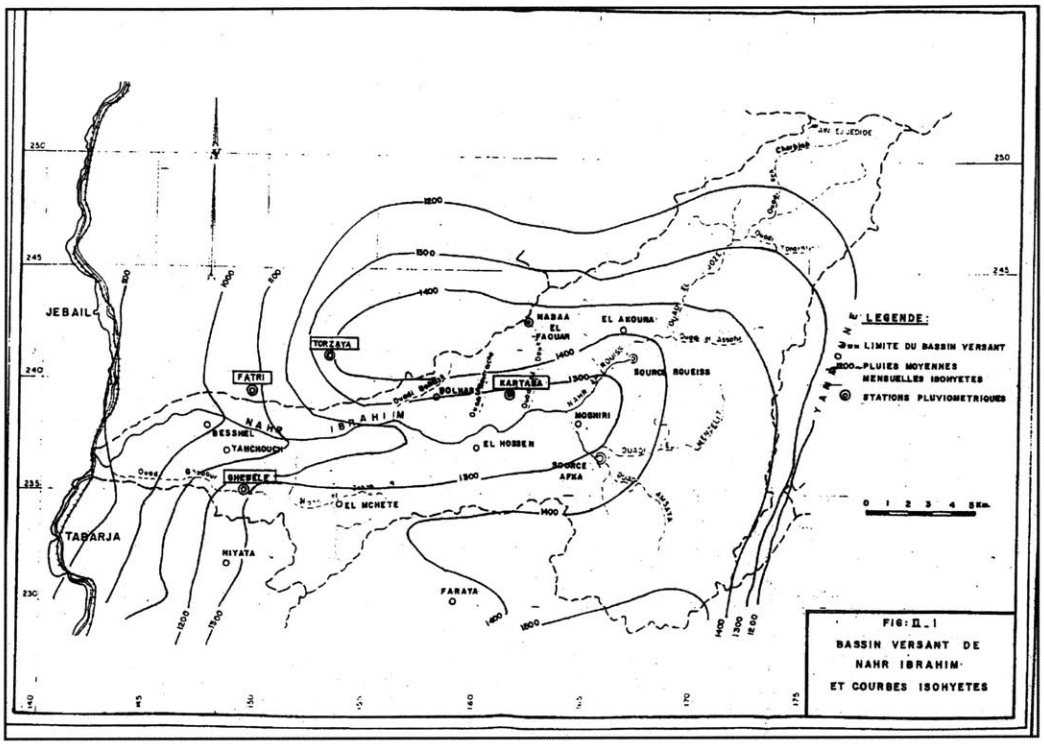

Figure 4 – Isohyetal Map of annual precipitation in the Ibrahim River Basin (From Bureau D'Etudes Hydrauliques, 1994)

Figure 5 is also an isohyetal map of annual precipitation in the Ibrahim River Basin. In this interpretation, the precipitation levels at the mouth of the river are roughly 1000mm/yr and increase towards the east to a peak after which they decrease gradually. While the peak precipitation is also 1400mm/yr, Figure 5 indicates that the majority of the central basin receives this maximum precipitation. The relatively straight contours show that there is an elevation impact on precipitation, reflected in the increasing trends to the east. Nevertheless, the elevation effects seen are smoothed and smaller scale than the changes in elevation.

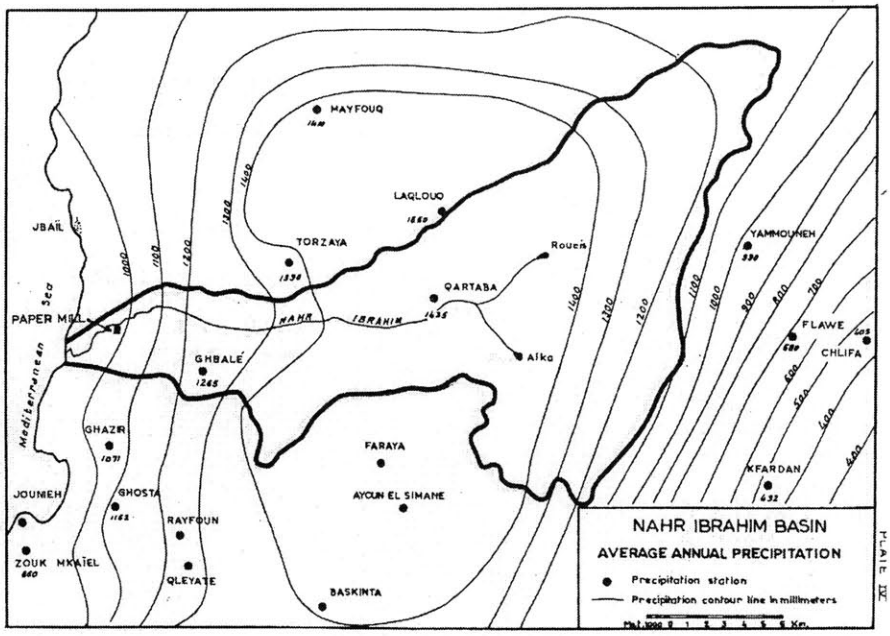

Figure 5 - Isohyetal Map of annual precipitation in the Ibrahim River Basin (From Papazian, 1981)

The measurements leading to these contour maps are based on only a small number of raingage stations. Figure 5 is derived from only two weather stations within the basin (at Qartaba and Ghbale) and Figure 4 only five. Such small data sets will inevitably result in varying results depending heavily on the judgement of the interpreter. The orographic effect, which governs precipitation levels in the mountainous Ibrahim River basin, is a complex problem that is especially difficult to consistently interpolate by hand based on few widely spaced data points.

The installation of a greater number of weather stations will not necessarily provide enough information to correct for the problems of interpretation because of the nature of raingage measurements. The accuracy of estimating any regional precipitation based on existing raingage measurements is difficult because of the wide variations in the spatial distribution of precipitation (Shih, 1990). In regions of significantly varying terrain, the problem becomes even more complex due to the impact of elevation on precipitation. Spatial variations of climatic elements can show differences over distances of only 100 meters, a much smaller distance than typical raingage network spacing (Barry, p. 83).

Although the raingage remains the standard method of rainfall measurement, the developing techniques of remote sensing and geographic information systems (GIS) modeling could be capable of providing a more accurate, rapid, and comprehensive picture of regional precipitation distribution (Shih, 1990). The goal of this thesis is to evaluate a theoretical method to estimate spatial orographic precipitation as well as provide a better source of precipitation data in a more accessible format to the Ministry of the Environment in Lebanon.

Chapter 3 - Precipitation Estimation

3.1 The Orographic Effect

In large, mountainous basins, such as the Ibrahim River watershed, spatial variations in precipitation levels are largely dependent on the topographic features of the area. Regional weather systems interact with the terrain in a relationship known as the "orographic effect" (Singh, 1997). The net result of this effect is a long term increase in mean precipitation with elevation on the windward slope of the mountain (Dingman, 1994, p. 95).

The orographic effect occurs when horizontally moving air currents are blocked by a vertical topographic barrier, such as a mountain, and are forced upward over the barrier (See Figure 6). This lifting brings the air mass to a region of lower pressure and lower temperature causing the air to be cooled adiabatically. As the air cools, it is no longer able to maintain water in its vapor state, forcing it to precipitate. The clouds and precipitation caused by this orographic lifting form along the windward side of the mountain. However, as the air mass falls over the leeward side of the barrier, the air experiences adiabatic warming and the precipitation dissipates rapidly (Dingman, 1994, p95-97).

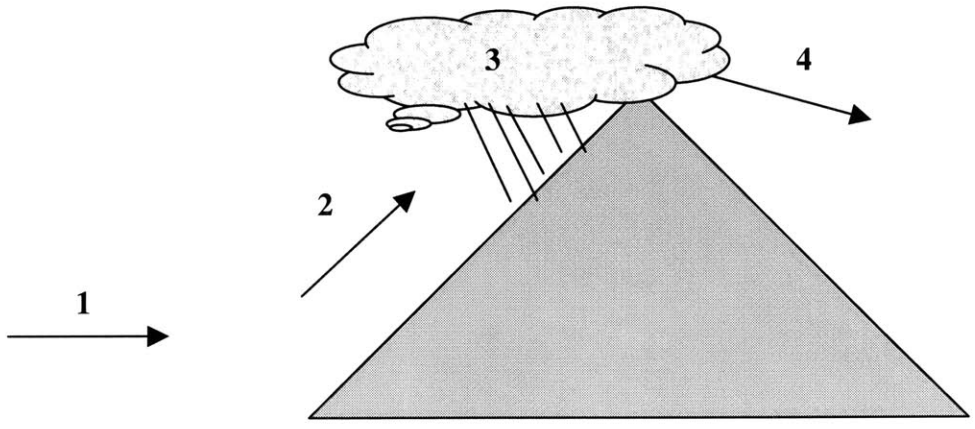

Figure 6 - Schematic of the orographic effect.

As a horizontal wind from a preexisting storm front (1) encounters a barrier, it is forced upward (2). The uplift causes adiabatic cooling, forming clouds and precipitation (3). The air mass warms as it descends over the lee side of the mountain and the precipitation disperses (4).

In general, orographic effects are the result of preexisting precipitation fronts interacting with topography, rather than a separate precipitation generating process. Thus, instead of creating new systems, the effect is to either increase the time over which precipitation falls as elevation increases, or to increase the intensity with which the precipitation falls at all elevations. In either case, the orographic effect is responsible for most of the spatial variation in precipitation in regions of significant topography. The amount of precipitation generated through orographic effects depends on characteristics of the air mass, variations in terrain, large-scale pressure patterns, extent of vertical lifting, and microphysical processes within the cloud structure (Barry, 1992, p225-226).

Although the existence of the orographic effect is well documented, predicting the resulting variation in precipitation levels is a complicated problem. The level of precipitation does not necessarily increase continuously with elevation. In fact, it is more likely that above a certain altitude precipitation begins to decrease (Singh, 1997).

There are two major categories of data necessary for estimating this orographic precipitation. The first is the topographic features of the mountain: including elevation, orientation, slope, and leeward or windward side position. The second is the climatic characteristics of the basin: including atmospheric conditions, wind speed, wind direction, and regional precipitation (Taher, 1998).

In order to fully model the orographic effect, it is necessary to manage each of these parameters for each spatial coordinate. Such a procedure requires a system that is able to handle an enormous amount of data that varies with geography. The most suitable tool to address this problem is Geographic Information Systems (GIS) technology, a type of mapping software that is able to link a database of information to the corresponding geographic location.

This thesis uses GIS technology in order to spatially calculate the amount of precipitation over the Ibrahim River basin using the software package ArcView 3.2 and the companion Spatial Analyst. The Ministry of the Environment in Lebanon provided elevation GIS data of the Ibrahim River basin, making this type of modeling possible.

3.2 Model of Orographic Precipitation

F. Baopu (1995) derived an equation for precipitation intensity (P) as a function of climatologic and topographic characteristics. The formula projects precipitation intensity at the base of the mountain to locations of differing characteristics at varying elevations.

The basic assumption made in the derivation of this formula is that the change of water content in a cloud is the difference between the flux of water vapor transported into the cloud through orographic lifting (Q) and the water leaving the cloud as precipitation (P), shown in Equation 1.

$$\frac{dW}{dt} = Q - P \tag{1}$$

The crux of the derivation was to determine the magnitude of the orographic lifting water flux, Q.

This was done by first finding the uplifting component of the wind based on the wind speed and direction, and the mountain orientation and slope. To solve for the uplift velocity, it is necessary to determine the component of wind perpendicular to the slope (V_n') and the vertical component of that vector (V_g).

As a wind (V) intercepts the mountain face at any angle, only the portion that is directed perpendicularly towards the slope will contribute to uplifting. This component (V_n') was determined by multiplying the wind velocity vector (V) by the cosine of the angle between the wind direction (θ) and the mountain orientation (β) (Figure 7):

$$V_n' = V \cos(\theta - \beta) = V \cos \sigma \tag{2}$$

The vertical component (V_g) of this portion of the wind is the force that contributes to orographic lifting (Baopu, 1995). The result of these trigonometric calculations is the relationship describing the orographic lifting velocity (Figure 8):

$$V_g = \frac{V}{2}\cos\sigma\sin\alpha \tag{3}$$

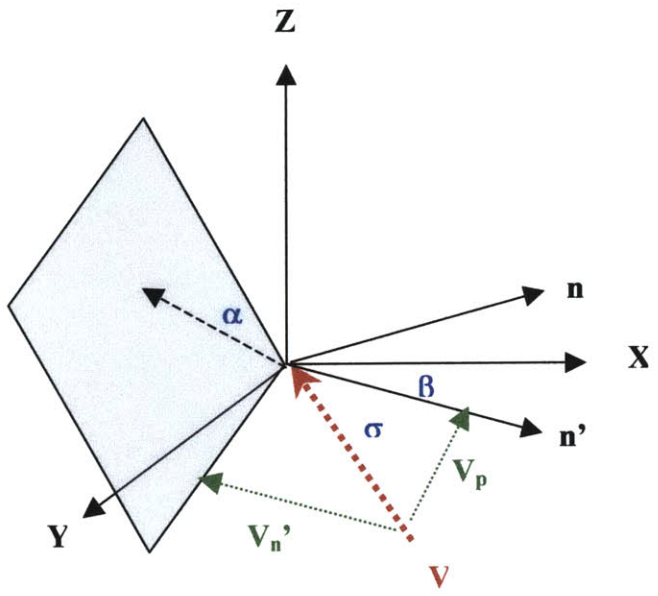

Figure 7 – Vector diagram for wind velocity vector (V)
The gray polygon indicates the mountain face at a slope α. (Based on figure in Baopu, 1995)

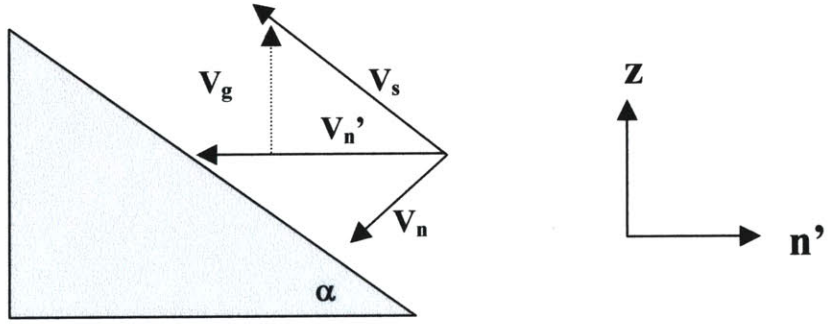

Figure 8 – Component diagram of wind (Vn') vector intercepting the mountain slope.
(Based on figure in Baopu, 1995)

The saturated vapor pressure (E_s) (in mm) can be expressed as a function of temperature (T) (in degrees Celsius) through the relationship known as Magnus' formula:

$$E_s = 4.6\exp\left(\frac{17.15T}{235+T}\right) \tag{4}$$

Using Equation 4, the saturated vapor pressure (E_s) at any height (z) above the foot of the mountain can be expressed as:

$$E_s = E_{s0}\exp[-\mu_1 rz - \mu_2(T_0 - rz)rz] \tag{5}$$

where $\mu_1 = \frac{17.15}{235+T_0}$, $\mu_2 = \frac{17.15}{(235+T_0)^2}$, T_0 is the temperature at the foot of the mountain, and r is the lapse rate of temperature (defined with the standard value of 0.6°C/100m). Under atmospheric conditions, the μ_1 term of Equation 5 is much larger than the μ_2 term.

Vapor pressure (E) can also be expressed as a function of height (z) by the empirical formula:

$$E = E_0 e^{-cz} \tag{6}$$

where the variable c is a meteorological parameter, the value of which was found to be 0.44km^{-1} (Barry, 1992, p. 27).

The ratio between Equation 6 and Equation 5 is the relationship between relative humidity (R) and height (z):

$$R = \frac{E}{E_s} \approx R_0 e^{(\mu_1 r - c)z} \tag{7}$$

where R_0 is the relative humidity at the foot of the mountain. The condensation level (Z_c) is defined as the elevation at which the relative humidity (R) is equal to 1. Applying this definition to Equation 7, it is possible to solve for Z_c:

$$Z_c = \ln R_0^{-1/\mu_1 r - c} \tag{8}$$

When air rises to an altitude below the condensation level, it is cooled by a dry adiabatic process. The temperature of the air lifted from the height of the base of the mountain (Z_0) to a new height Z ($Z = Z_0+h$) decreases by $r_d h$ (where r_d is the adiabatic lapse rate of temperature, defined with the standard values of 1°C/100m). The lowered temperature (T) can be expressed as:

$$T = (T_0 - rZ_0) - r_d h = T_0 - r(z-h) - r_d h = T_0 - rz - (r_d - r)h \tag{9}$$

Inserting Equation 9 into Magnus' formula (Equation 4) yields:

$$E_s = E_{s0} \exp[-\mu_1 rz - \mu_1 (r_d - r)h] \tag{10}$$

By equating Equation 10 and Equation 6 and incorporating them into Equation 8, the condensation level (Z_c) at height (h) can now be shown to be:

$$Z_c = \frac{\delta}{c} \ln R_0^{-1} - \frac{s}{c} h \tag{11}$$

where $\delta = \dfrac{c}{u_1 r - c}$, $s = \delta u_1 (r_d - r)$, and $u_1 = \dfrac{17.15}{235 + T_0}$.

The vapor pressure at the condensation level derived in Equation 11 (E_c) is:

$$E_c = E_0 e^{-cZ_c} = E_0 R_0^{\delta} e^{sh} \tag{12}$$

It follows that the absolute humidity at the condensation level (a_c) can be found as:

$$a_c = a_0 R_0^{\delta} e^{sh} \tag{13}$$

where a_0 is the absolute humidity at the foot of the mountain.

With the orographic lifting velocity, it is possible to calculate the velocity of ascent of air (V_z). This value is defined as the negative of the partial derivative of the condensation level (Equation 11) with respect to t:

$$V_z = \frac{s}{c} V_g \tag{14}$$

The amount of moisture being transported upward (F) is $F = a_c V_z$, which can be expressed as:

$$F = \frac{s a_0 R_0^{\delta}}{c} V g e^{sh} \tag{15}$$

The flux of water from lower altitudes is small or near zero once the uplifted air mass reaches saturation. Therefore, the general flux density (Q(h)) is equal to F below this saturation elevation (h*) and is equal to zero above it. To satisfy these conditions, Q must be equal to the upward flux (F) multiplied by a function g(h) which approaches 1 when the height (h) is less than or equal to h* and approaches 0 when the height is greater than h*. The g(h) function is defined as:

$$g(h) = \left[1 + f e^{mb(h-h^*)}\right]^{-((1/m)+1)} \tag{16}$$

where m is a fitting parameter, which Baopu chose to be 200 based on a calibration of the formula. The variable f is a dimensionless parameter that signifies whether the point is on the leeward (f = 0) or windward side of the mountain (f = 1). Based on the orientation of the basin, the solution assumes that all points within the basin can be estimated as facing windward. The parameter b is determined later.

The value of h* can be determined by setting the condensation elevation equal to the height (Z_c=h) in the established definition of condensation level (Equation 11).

$$h^* = \frac{\ln R_0^{-1}}{\mu_1 r_d - c} \tag{17}$$

Finally, Equations 15 and 16 were related to determine the uplifting water flux.

$$Q(h) = F \cdot g(h) = \frac{s a_0 R_0^{\delta} V g}{(c[1 + f e^{mb(h-h^*)}])^{1/m+1}} e^{sh} \tag{18}$$

If it is assumed that the rate at which cloud water is converted to precipitation does not change significantly with orography, it follows that the ratio between precipitation intensity (P) and cloud water content (W) is the same at all locations within the basin (Equation 19).

$$\frac{P}{W} = \frac{P_0}{W_0}$$

or

$$P = kW, \quad k = \frac{P_0}{W_0} \tag{19}$$

where k is assumed constant.

It follows that:

$$\frac{dw}{dt} = \frac{1}{k}\frac{dP}{dt} = \frac{1}{k}\frac{dP}{dh}\frac{dh}{dt} = \frac{V_g}{k}\frac{dP}{dh} \tag{20}$$

where t is the time needed to for the air mass to uplift from the foot of the mountain to height (h), and $h=V_g t$.

Substituting Equation 20 and Equation 18 into Equation 1 yields a relationship between height (h) and precipitation intensity (P):

$$\frac{dP}{dh} + \frac{k}{V_g}P - \left(\frac{ksa_0 R_0^{\delta}}{c} \frac{e^{sh}}{(1 + fe^{mb(h-h^*)})^{(1/m)+1}} \right) = 0 \tag{21}$$

Solving for this differential equation yields an expression for precipitation intensity (P)[1].

$$P = e^{-qh}\left\{ P_0 + M\left[\frac{e^{bh}}{\left(1 + fe^{mb(h-h^*)}\right)^{1/m}} - \frac{1}{\left(1 + fe^{-mbh^*}\right)^{1/m}} \right] \right\} \tag{22}$$

with

$$q = \frac{k}{V_g} \qquad k = \frac{P_0}{W_0}$$

$$M = \frac{ksa_0 R_0^{\delta}}{bc} \qquad s = \delta u_1 (r_d - r)$$

$$\delta = \frac{c}{u_1 r - c} \qquad u_1 = \frac{17.15}{235 + T_0}$$

[1] Errors were found in some formulas as published by Baopu (1995). The formula shown here is the corrected version, see Appendix A for further explanation.

$$h^* = \frac{\ln R_0^{-1}}{(u_1 r_d - c)} \qquad b = q + s$$

where:

Climatic Parameters:

P_0	precipitation intensity at the foot of the mountain
W_0	cloud water content at the foot of the mountain
a_0	absolute humidity at the foot of the mountain
R_0	relative humidity at the foot of the mountain
T_0	temperature at the foot of the mountain

Topographic Parameters:

α	slope of the mountain
σ	angle between wind and slope directions
h	elevation
f	dimensionless parameter (equal to 0 on a leeward slope, and 1 on a windward slope)

General Parameters:

r	lapse rate of temperature
r_d	dry adiabatic lapse rate of temperature
m, c	parameters

(Baopu, 1995)

The base case conditions of this formula show that when the elevation is zero (h = 0), the precipitation at that elevation is equal to that of the precipitation at the base of the mountain ($P = P_0$). Also, when there is not precipitation at the base of the mountain ($P_0 = 0$), there is never precipitation in the basin (P = 0).

3.3 Method

Equation 22 was chosen because it is able to determine the precipitation intensity at any position in a region given the slope, aspect, and elevation of the location. Such a system is very suitable for GIS technology and the determination of small scale spatial variations in precipitation. By applying the equation to a dense number of locations within the

Ibrahim River Basin, it will be possible to create a map of precipitation as it varies with geography.

The first step in implementing this method is to establish a baseline location and time scale for the model. The next step is to establish the values for the climatic parameters at the base of the mountain, especially precipitation. Each parameter must then be either calculated or estimated for the final step of solving the formula for a grid of geographic locations within the basin.

3.3.1 Baseline Climatic Parameters

There are a large number of climatic parameters from the foot of the mountain required to solve the equation. However, the Ibrahim River Basin is located in a relatively remote region and no consistent climatic data has been collected. The only location in Lebanon that has a sufficient amount of data is the large city of Beirut. In order to continue with this model, it is necessary to assume that climatic characteristics for Beirut can be approximated as the parameters at the foot of the mountain.

This assumption can be justified through a number of supporting factors. Both Beirut and the mouth of the river are in similar geographical locations. They are both situated along the coast of the Mediterranean, at similar elevations of approximately sea level. The winds in the region flow from the west towards the east, thus intercepting both locations from the same direction and without interference. Additionally, the distance between the two is 20 kilometers, a relatively small separation. Finally, a large scale precipitation contour map (Figure 9) shows the relative amounts of precipitation received by the two locations to be the same.

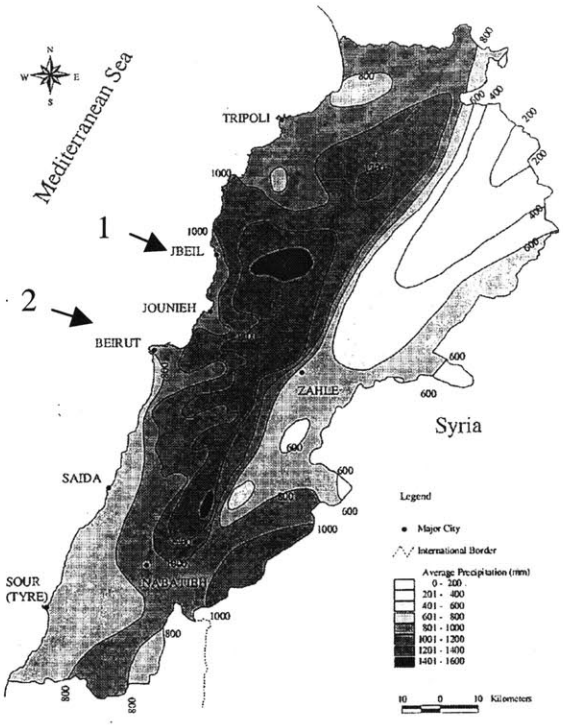

Figure 9 – Isohyetal Map of Lebanon

This map shows precipitation contours of Lebanon, indicating that both the mouth of the river (arrow 1) and Beirut (arrow 2) are within the same contour line.

(El Fadel, et al., 2000)

3.3.2 Time Scale Determination

The ideal time scale on which to model precipitation would be hourly. This resolution would be able to capture the diurnal cycles of many of the climatic data as well as more accurately simulate individual rainfall events. However, it was not possible to obtain hourly precipitation data in Beirut. Beirut does have daily precipitation data and hence this work focuses on estimate daily precipitation over the Ibrahim River Basin.

To use Equation 22 to estimate daily precipitation, it is necessary to show that the climatic parameters do not vary greatly during a 24-hour period. Figure 10, Figure 11, and Figure 12 show the daily fluctuations of several key parameters for the first day of each month for the year 1998 (http://www.aub.edu.lb/fea/weather, visited 3/8/2001). Although there are diurnal fluctuations, particularly in temperature and relative humidity, it was assumed that the variations were small enough to use daily averages of the

meteorological parameters in Equation 22 in order to derive representative daily precipitation estimates.

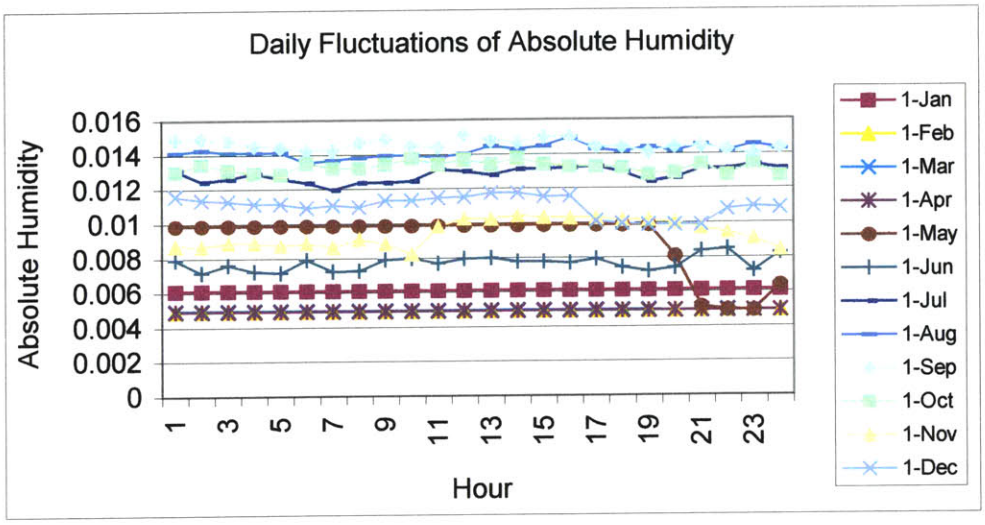

Figure 10 - Daily fluctuations of absolute humidity in Beirut

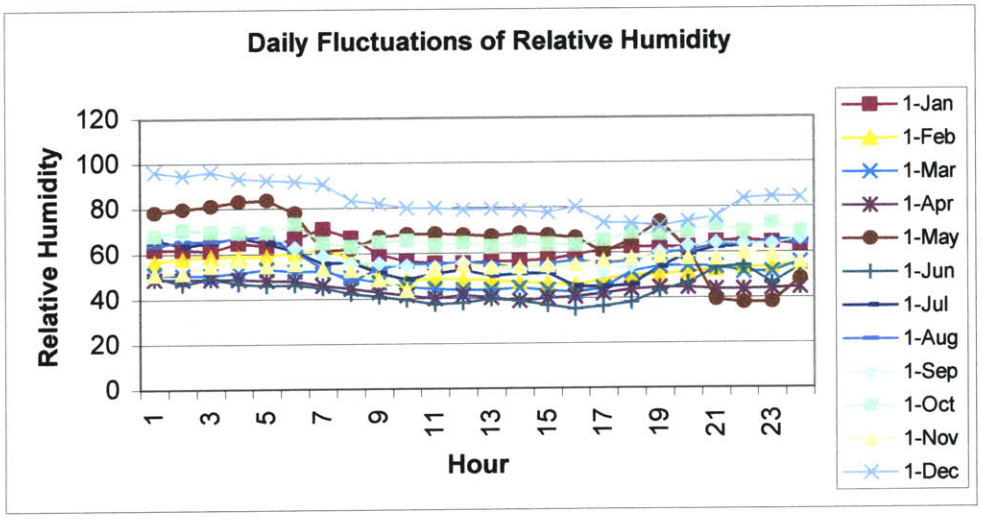

Figure 11 - Daily Fluctuations of Relative Humidity in Beirut

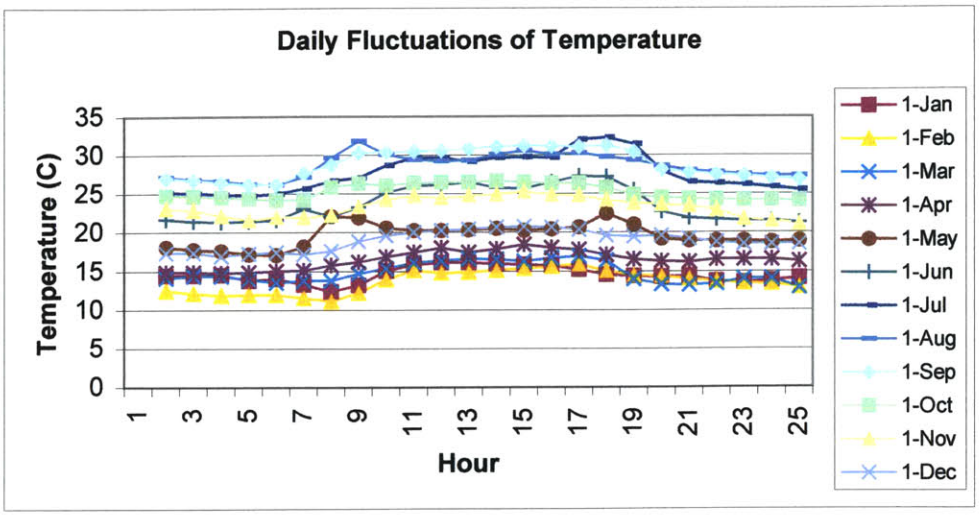

Figure 12 - Daily Fluctuations of Temperature in Beirut

3.3.3 Parameter Estimation

With these assumptions in place, it is now possible to estimate the parameters to solve for Equation 22.

3.3.3.1 Climatic Parameters

Using the baseline location and time scale established above, the daily values of absolute humidity (a_0), relative humidity (R_0), temperature (T), precipitation (P_0), wind speed (V), and wind direction (θ) for Beirut were obtained from the American University of Beirut (http://www.aub.edu.lb/fea/weather/, visited 3/8/2001).

It was only possible to acquire daily Beirut climatic information for the period between May, 1998 and April, 1999. Although this represents a full year, the period unfortunately is extremely dry compared to the average precipitation levels (Figure 13). Therefore, the results will not be representative of a typical year of rainfall over the basin.

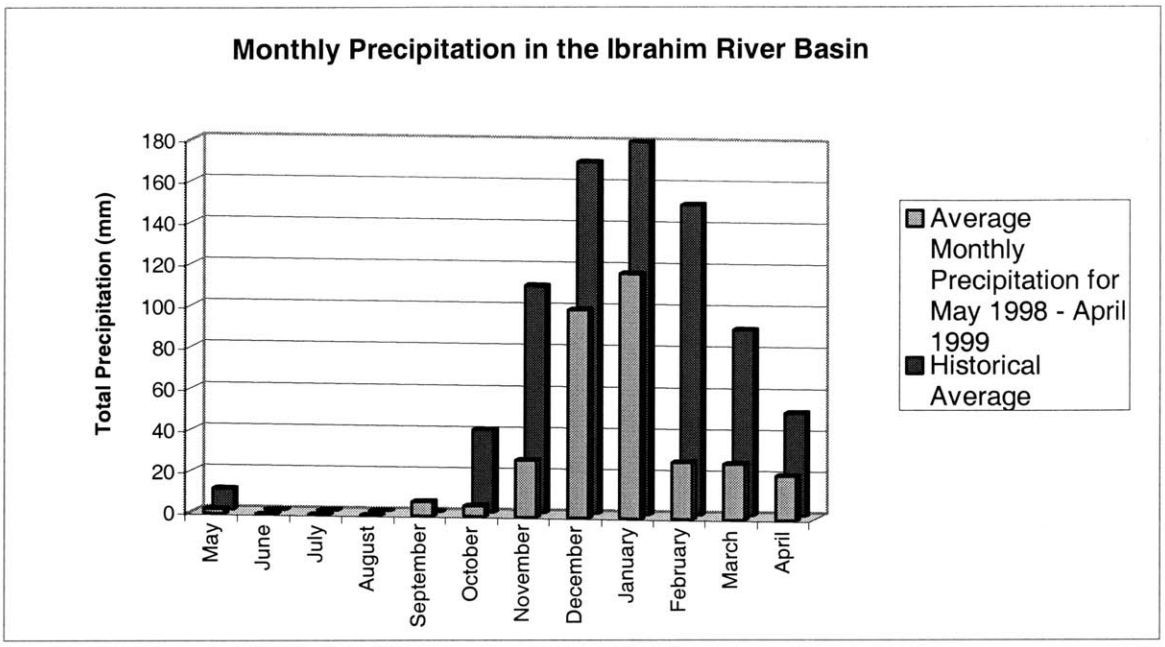

Figure 13 - A comparison of the Beirut precipitation data used in the model (foreground) to the historical average of the precipitation in the city (background).

The amount of precipitation received for the dates used in the model is well below the average except for the month of September. Based on data from Electrowatt, 1981 and weatherbase.com[2].

3.3.3.2 Topographic Parameters

The topographic parameters of the basin were determined using the Spatial Analyst extension to ArcView GIS. Known elevation contour data was transformed into a gridded version of the basin, which can then be operated on by features of the software.

The first step in preparing the data for the model was to convert a GIS elevation contour line layer obtained from the Ministry of the Environment into a grid with an average elevation value assigned to each cell. Such a grid is known in GIS as a Digital Elevation Model (DEM).

A free program distributed on the internet by researchers at the University of Ottawa, polyxyz.ave[3] enables ArcView to step through the X, Y coordinates of the contour layer,

[2] http://www.weatherbase.com/weather/weatherall_c.php3?s=000104&refer=, visited 4/20/2001

determining the location of the points on the contour lines, and assigning the appropriate elevation (Z). The output of this program is a comma delimited text file which can then imported into ArcView. The result of this transformation is a grid of 110x172 cells with an averaged elevation value for each cell, shown in Figure 14.

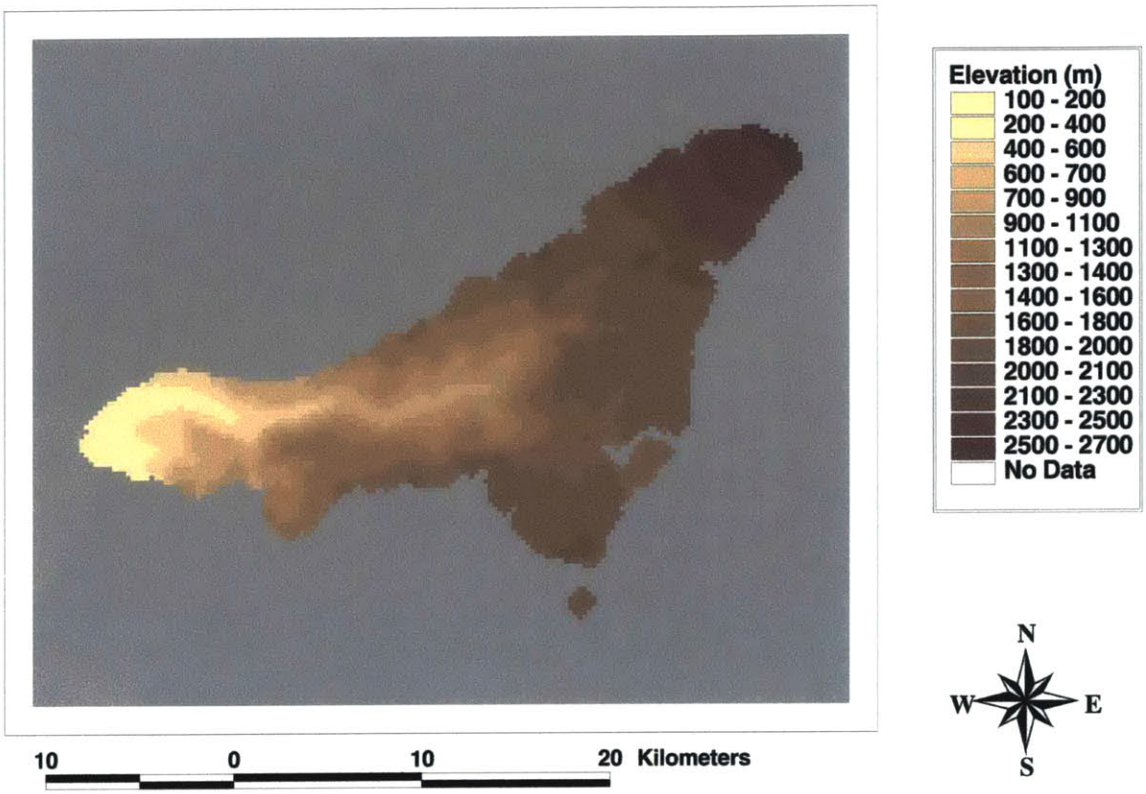

Figure 14 – Elevation grid

One problem with this method is that areas that are located between widely spaced contour lines are not defined by the polyxyz program. It would be possible to assign values for these spaces by creating a lower resolution grid. However, since the undefined regions are small and located along the boundary at the eastern edge of the basin (visible as a highly irregular boundary in three locations), it was decided that this correction would not be worth the loss of resolution.

---

[3] http://www.uottawa.ca/academic/arts/geographie/lpcweb/sections1/software/xyzclips/polyxyz.htm, visited 2/16/2001

Using this DEM, features within Spatial Analyst can easily solve for the slope and aspect (orientation of the mountain) within each grid cell. The results are shown in Figure 15 and Figure 16.

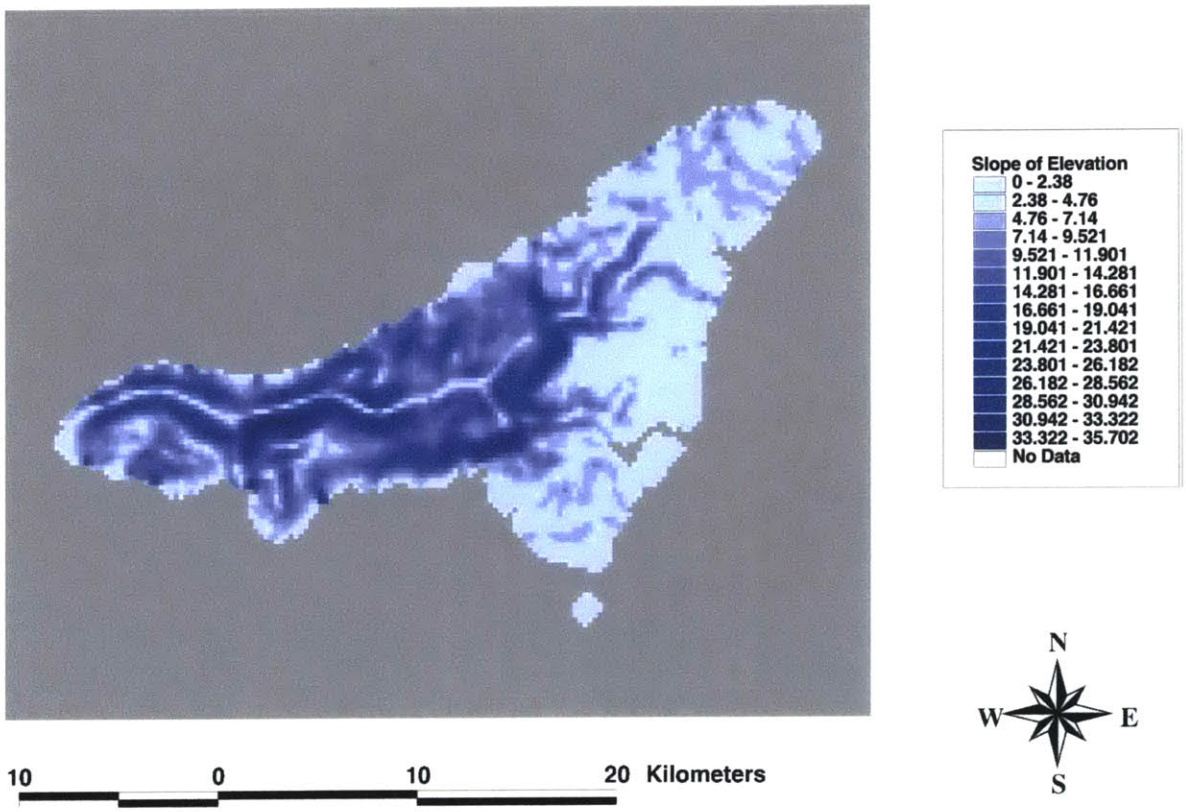

Figure 15 - Slope grid – slopes shown in percent

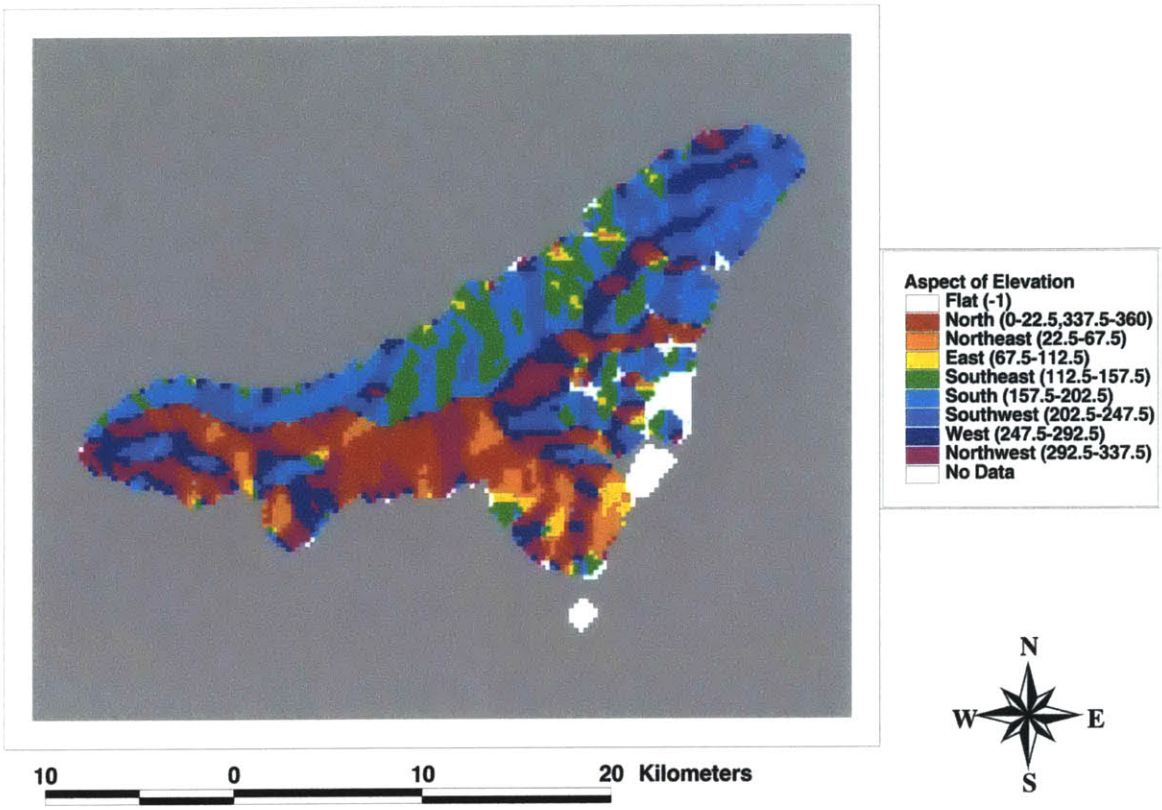

Figure 16 - Aspect grid – aspect shown in degrees

3.3.4 Calculations

Within the Spatial Analyst program, there is a function called "map calculator" that allows arithmetic operations on and with grid layers such as those calculated for elevation, slope, and aspect. By inputting formulas for the variables in Equation 22 (definitions shown in Table 2), as well as the estimated climatic parameters into this map calculator, it was possible to create a final grid layer in which every cell contained the average precipitation for the area contained in that cell. This method was then repeated for each of the 67 rainy days in the May 1998 – April 1999 time period, creating an atlas of the precipitation for that year. The final result was a set of 67 maps, each showing geographically the precipitation levels for that day. The map calculator was again used to aggregate the daily precipitation grids into monthly and yearly levels.

Table 2 - Map Calculator Expressions

Variable	Map Calculator Definition
[slope (degrees)]	([slope]/100).Atan
[Vg]	([slope (degrees)]*2).Sin * ([Aspect]*3.1415/180-**θ**).Cos * **V**/2
[q]	([Vg].Pow(-1)*__k__)
[b]	[q]+ **s**
[M]	([b].Pow(-1)*__k__*__s__*__ao__*__Ro__^**δ**/__c__)
[1st Term]	([b] * [Elevation]).Exp / (([b] *([Elevation] – **h***)*__m__).Exp+1).Pow(1/__m__)
[2nd Term]	(((-[b]*__m__*__h__*).Exp + 1).Pow(1/__m__)).Pow(-1)
Precipitation	([q] * [Elevation]).Exp * ([M] *([1st term] - [2nd term])+**Po**)

Variables shown in bold indicate that the values must be entered into ArcView, rather than being determined by the map calculator.

Because the aspect is not defined (i.e. the land is flat) in some areas, a few cells are also undefined. Another feature of Spatial Analyst, neighborhood statistics, was used to assign a distance-averaged value to the cells based on neighboring cells, thus defining these regions. Also, to present the data such that each day or month can be compared to any other, a graduated color scheme spanning the entire range of precipitation values was employed.

Chapter 4 - Results

The results of this model are given in the Appendices: the yearly aggregate, in Appendix B, the monthly aggregates in Appendix C, and the daily precipitation calculations in Appendix D. A copy of the ArcView project file will remain with the Department of Civil and Environmental Engineering at MIT. In general, the model seems to estimate precipitation well. The results are reasonable, and are supported by the minimal existing data.

4.1 Low Daily Precipitation

Many days in the Spring and Autumn received very small precipitation totals, in the fractions of millimeters. Because this thesis designed all of the daily precipitation maps to be directly comparable, such small variations in precipitation are not evident in the color schemes of the maps.

April 8, 1999

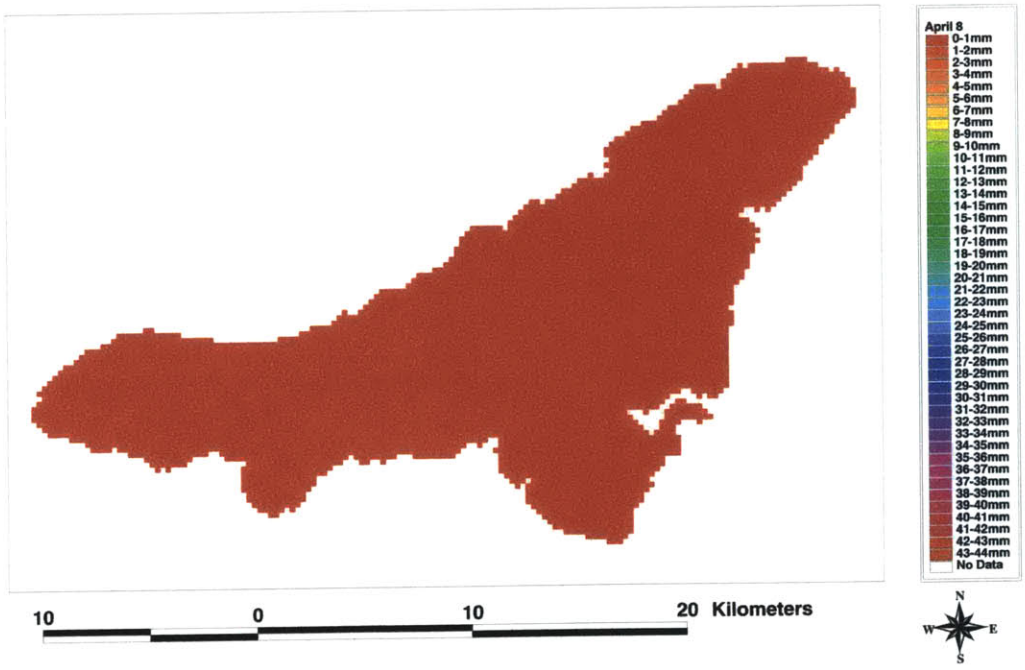

Figure 17 – Daily precipitation for April 8, 1999

Thus, days receiving little precipitation appear to be all one color (red), indicating precipitation in the 0-1mm range. An example, shown in Figure 17, is April 8, 1999.

4.2 *Effects of Orography*

As expected, precipitation follows elevation closely. One example, shown in Figure 18, is the daily precipitation estimate for March 25. The precipitation pattern is similar to the elevation map shown in Figure 14.

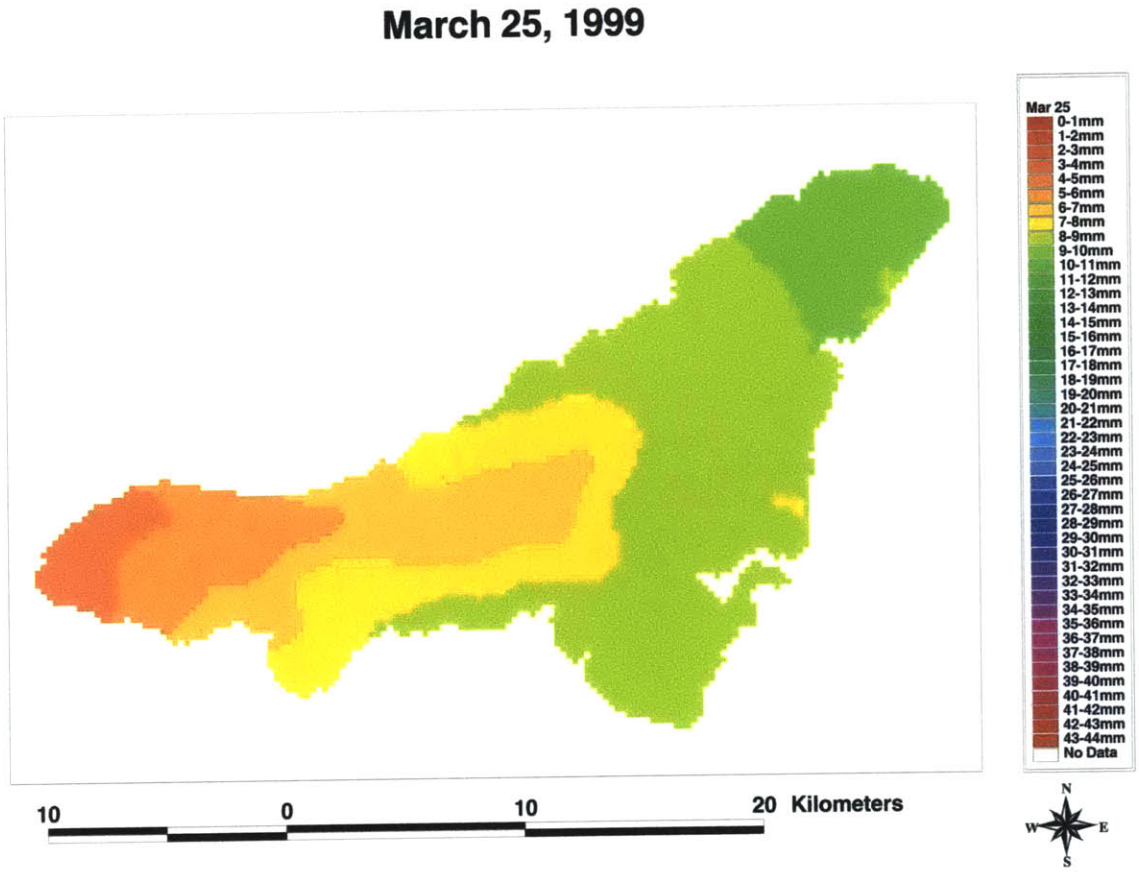

Figure 18 – Daily precipitation for March 25, 1999

The slope of the mountain also has an effect on the results of the estimation. This is also evident in Figure 18, in the northeastern region of the basin. Although the elevation is very high, and continues to increase in this region (Figure 14), the precipitation does not intensify as rapidly. This is due the low slope in the region (Figure 15). Even though the elevation is high, the orographic lifting velocity will be low with the gradual slope.

Mountain orientation also has an effect on the spatial variation of precipitation, but, it is only evident in days with high precipitation. An example of this is January 18, shown in Figure 19. One can see that there is more variation in the precipitation received throughout the basin, in comparison to the example in Figure 18. Although effects from elevation are still noticeable in the western region of the watershed, the majority of the basin has widely varied areas of rainfall. This is due to changes in terrain orientation, which affects the orographic lifting velocity.

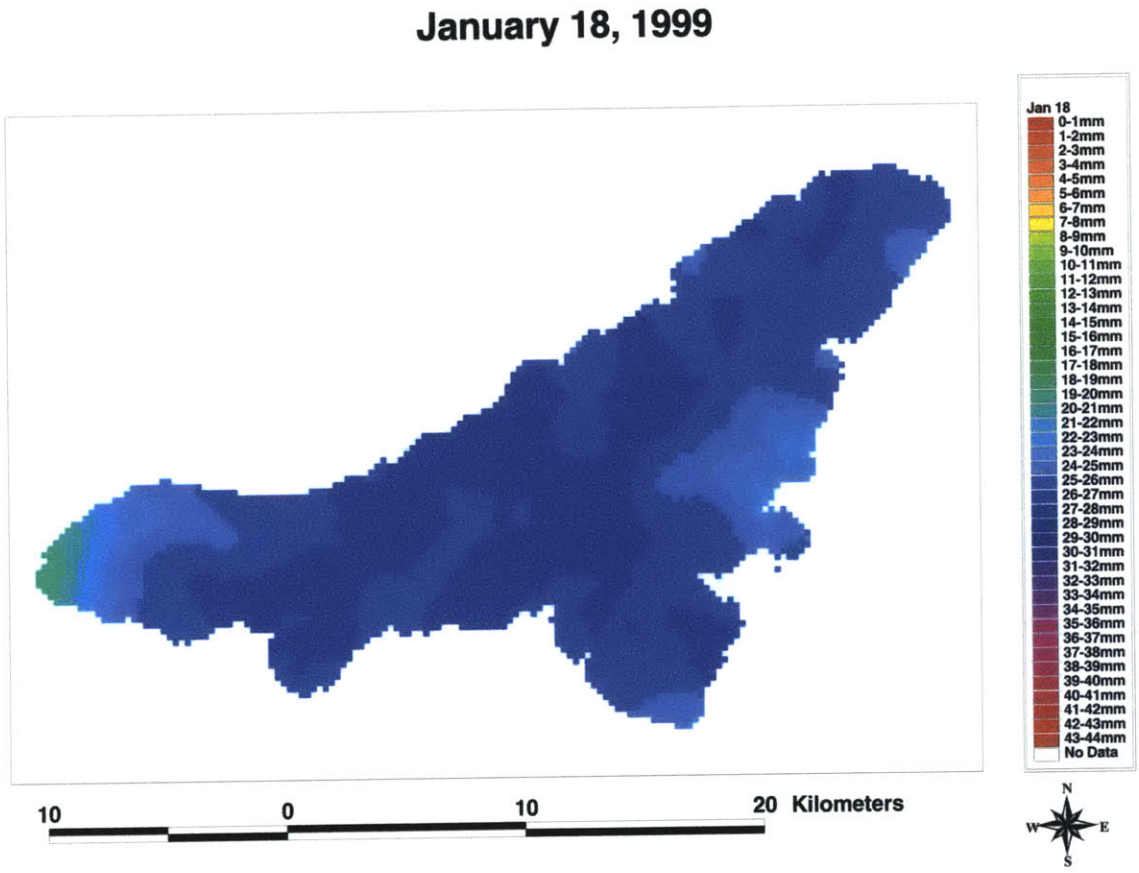

Figure 19 – Daily precipitation for January 18, 1999

4.3 Comparison to Existing Data

The annual average isohyetal maps, shown in Section 2.2.4 (Figure 4, Figure 5), can be directly compared to the yearly aggregate map shown in Appendix B and reprinted below (Figure 20). Although, as mentioned earlier, the magnitude of the yearly precipitation values found with the estimation will be well below the averaged annual totals, the shape of the variations should remain comparable.

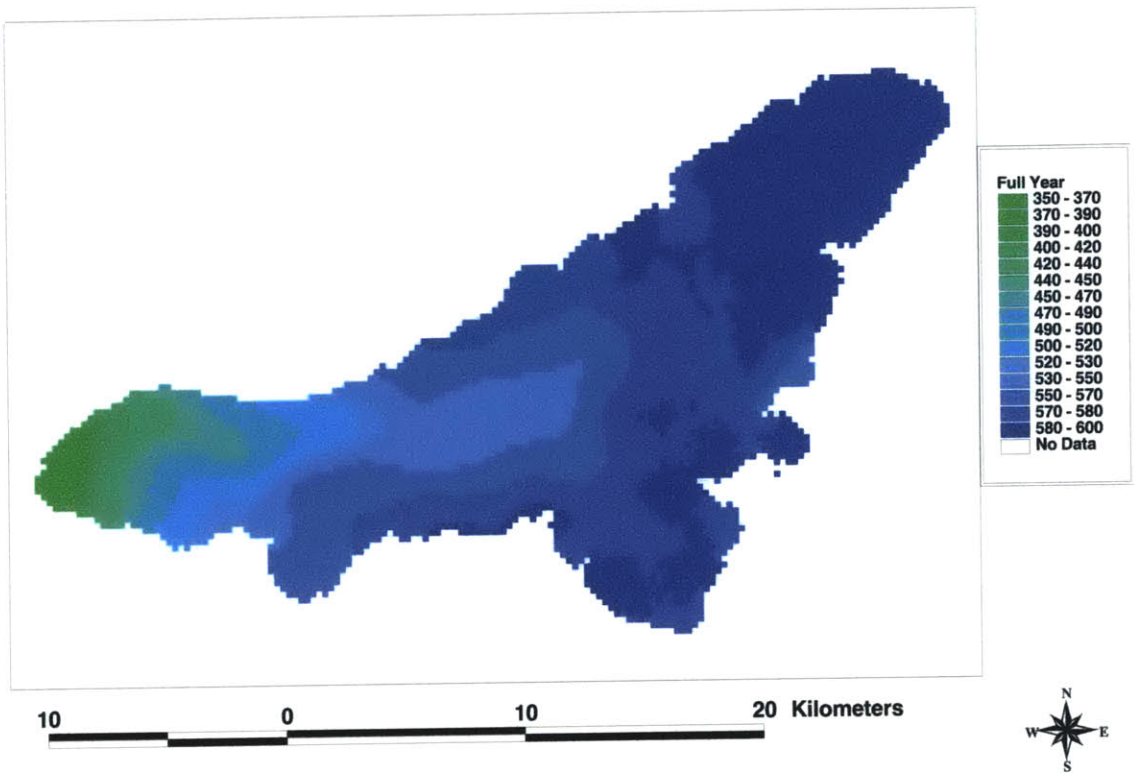

Figure 20 - Total precipitation aggregate for the 67 days of rain during the year long period between May 1998 and April 1999. Rain totals shown in mm.

Visual inspection shows that the results obtained in this thesis support the contour shape that varies with the elevation from Figure 4 rather than the relatively straight contours from Figure 5. However, the map resulting from the GIS analysis does not show a decrease in precipitation at high elevations as represented in both existing maps. Although this is a significant difference, there have never been measurements taken at these high elevations and the peak of precipitation in the basin in both Figure 4 and Figure 5 can only have been based on speculation. It is therefore difficult to determine whether the estimations performed in this thesis are, in fact, accurate without conducting additional field measurements.

The most significant difference between the existing data and the resulting map is the increase in spatial resolution in the model result. While the hand-drawn contours could

only be based on a few raingage measurements, the precipitation estimation model used in this thesis has the capability to calculate the rainfall in thousands of cells and present a more detailed picture of the distribution. However, the estimations performed here are based on even less actual data than the hand-drawn contours, making field verification of the results necessary. If this model is indeed proven to provide an accurate portrayal of spatial variations of orographic precipitation, it will be a powerful tool for generating rainfall input to environmental models.

Chapter 5 – Conclusion

The precipitation estimation model conducted in this thesis produced reasonable maps of precipitation levels for the Ibrahim River basin in Lebanon. The resulting data set of can be useful for future environmental studies of the watershed. However, there were some problems with data availability that should be addressed in future studies of precipitation.

The climatic data used to create these results did not reflect typical precipitation levels for the area and thus could not be directly compared to known data. In order for this method to become useable, it will be necessary to verify that the results are accurate. Daily precipitation and climatic measurements within the basin must be conducted to provide more consistent input and allow for direct comparison.

Until further field studies are carried out, there are several options to verify the results of the precipitation estimation model. One option is to run the model on a larger set of data to try to reproduce the known average values. However it is not clear whether such a large data set for climatic parameters exists. Future studies in this field should attempt to recover more data on the environmental characteristics of Lebanon.

Another recommendation for future studies of GIS based precipitation estimation is to verify the results of the model with stream flow measurements. The results from the model can be entered as input to a surface water flow model. By estimating or calculating a rainfall/runoff ratio, it would be possible to model the stream flow response to precipitation. Because accurate river flow measurements are easier to obtain than precipitation measurements, converting the precipitation estimation to stream flow would allow for calibration and verification of the estimation model.

References

http://www.aub.edu.lb/fea/weather visited 3/8/2001

http://www.uottowa.ca/academic/arts/geographie/lpcweb/sections1/software/xyzclips/polyxyz.htm LPC - Laboratory for Paleoclimatology and Climatology at University of Ottawa. Visited 3/9/2001

Air Ministry, Meteorological Office (1962) *Weather in the Mediterranean.* London, Her Majesty's Stationary Office.

Baopu, F., 1995: The Effects of Orography on Precipitation. *Boundary Layer Meteorology*, **75**:189-205.

Barry, Roger G. (1992) *Mountain Weather and Climate.* London, Routledge.

Broccoli, A.J. and Manabe, S., 1992: The Effects of Orography on Midlatitude Northern Hemisphere Dry Climates. *Journal of Climate*, **5**: 1181-1201.

Bureau D'Etudes Hydrauliques, 1994: *Etude Des Apports De Nahr Ibrahim.* Republique Libanaise, Ministere Des Ressources Hydrauliques et Electriques. Lebanon.

Dingman, S.L. (1994) *Physical Hydrology.* New Jersey, Prentice Hall.

Electrowatt, 1981: Relance Des Projects Hydro-Agricoles: Barrage De Iaal Dans Le Liban Nord, Barrage De Yahchouch Sur Le Nahr Ibrahim. Ministere Des Ressources Hydrauliques et Electriques. Lebanon.

El-Fadel, M. Zeinati, M., Jamali, D. 2000: Water Resources in Lebanon: Characterization, Water Balance and Constraints. *Water Resources Development*, **16**(4): 615-638.

Foufoula-Georgiou, E. and Krajewski, W. 1995: Recent Advances in Rainfall Modeling, Estimation, and Forecasting. *Reviews of Geophysics* (supplement): 1125-1137.

Huntingford, C., Blyth, E.M., Wood, N., Hewer, F.E., Grant, A., 1998: The Effects of Orography on Evapopation. *Boundary Layer Meteorology,* **86**: 487-504.

Manton, M.J., 1993: Rainfall and its Estimation. *Australian Meteorological Magazine*, **42**: 135-141.

Nauphal, Naila. 1997: *Post-war Lebanon: Women and other war-affected groups* http://www.ilo.org/public/english/employment/skills/training/publ/pub9.htm International Labor Organization. Visited 2/20/2001.

Papazian, Hratch S. 1981: *A Hydrogeological Study of the Nahr Ibrahim Basin in the Vicinity of the Paper Mill Project of Indevco in Lebanon.* Lebanon.

Patwardhan, A.S., Nieber, J.L., Johns, E.L., 1990: Effective Rainfall Estimation Methods. *Journal of Irrigation and Drainage Engineering*, **116**(2): 182-193.

Shih, S.F., 1990: Satellite Data and Geographic Information System for Rainfall Estimation. *Journal of Irrigation and Drainage Engineering*, **116**(3): 319-331.

Singh, P. and Kumar, 1997: N. Effect of Orography on Precipitation in the Western Himalayan Region. *Journal of Hydrology*, **199**: 183-206.

Taher, S. and Alshaikh, A., 1998: Spatial Analysis of Rainfall in Southwest of Saudi Arabia Using GIS. *Nordic Hydrology*, **29**(2): 91-104.

Appendix A - Letter to Editor

During the course of this thesis, it became evident that there were typographical errors in the paper containing the formula for precipitation intensity. Below is a letter that was sent to the journal containing the paper explaining the errors found. At the time of printing, no response regarding this letter has been received besides confirmation of receipt.

Jessica Fox
791 Tremont St. W210
Boston, MA 02118
foxyloxy@mit.edu

May 10, 2001

Lower Academic Publishers
C.F. van Nispen tot Sevanaer
Spuilboulevard 50
P.O. Box 17
3300 AA Dordrecht
The Netherlands

To Whom it May Concern:

I am writing in response to the article "The Effects of Orography on Precipitation" by Fu Baopu found in volume 75, page 189 of *Boundary-Layer Meteorology*. I have worked extensively with this paper and believe that I have found two critical typographical errors in the formulas derived. Jingfeng Wang, a fellow graduate student at MIT, has rederived the formulas and confirmed these apparent errors. I have been unable to locate the author on my own and hope that your publication will be able to contact him and ask him to review the paper.

On page 194, in equation (22), we believe that the formula

$$\frac{dp}{dh}+\frac{k}{V_g}P-\left(\frac{ksa_0R_0^{\delta}}{c}\frac{e^{sh}}{1+fe^{mb(h-h^*)}}\right)=0$$

should, in fact, be

$$\frac{dp}{dh}+\frac{k}{V_g}P-\left(\frac{ksa_0R_0^{\delta}}{c}\frac{e^{sh}}{(1+fe^{mb(h-h^*)})^{(1/m)+1}}\right)=0$$

And, on page 195, in equation (23), we believe that the formula

$$P = e^{-qh}\left\{P_0 + M\left[\frac{e^{sh}}{\left(1 + fe^{mb(h-h^*)}\right)^{1/m}} - \frac{1}{\left(1 + fe^{-mbh^*}\right)^{1/m}}\right]\right\}$$

Should, in fact, be

$$P = e^{-qh}\left\{P_0 + M\left[\frac{e^{bh}}{\left(1 + fe^{mb(h-h^*)}\right)^{1/m}} - \frac{1}{\left(1 + fe^{-mbh^*}\right)^{1/m}}\right]\right\}$$

Please let me know if you are either able to contact the author or otherwise verify these potential errors.

Thank You,

Jessica Fox

Masters of Engineering, 2001
Massachusetts Institute of Technology
Department of Civil and Environmental Engineering
Cambridge, MA 02139

Appendix B

Total Annual Precipitation Estimation

Total Precipitation - May 1998-April 1999

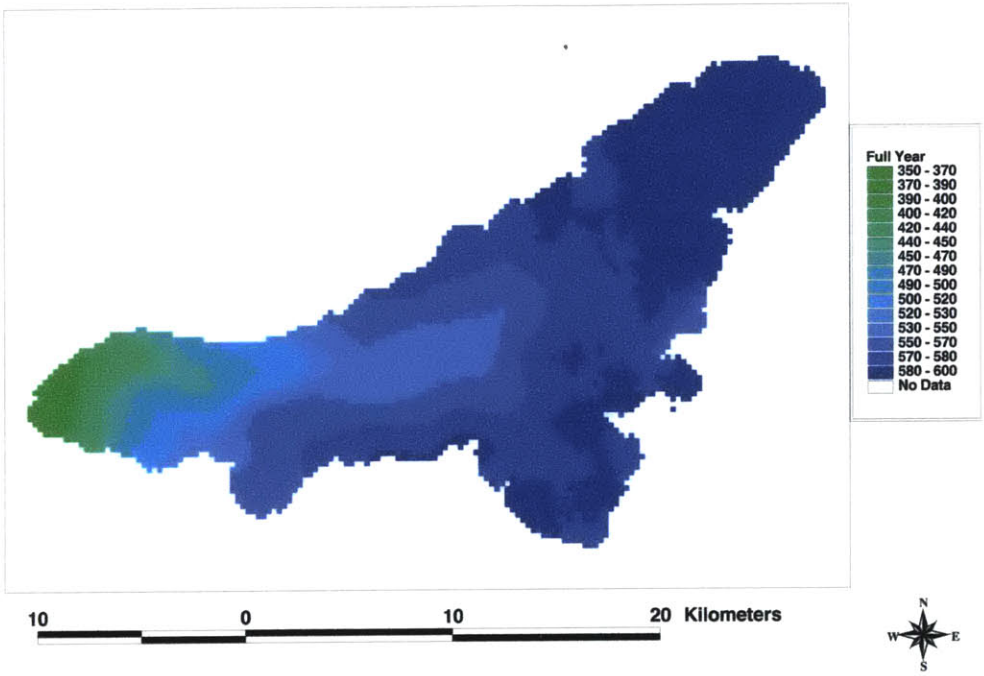

Appendix C - Monthly Precipitation Estimations

Total Precipitation - May 1998

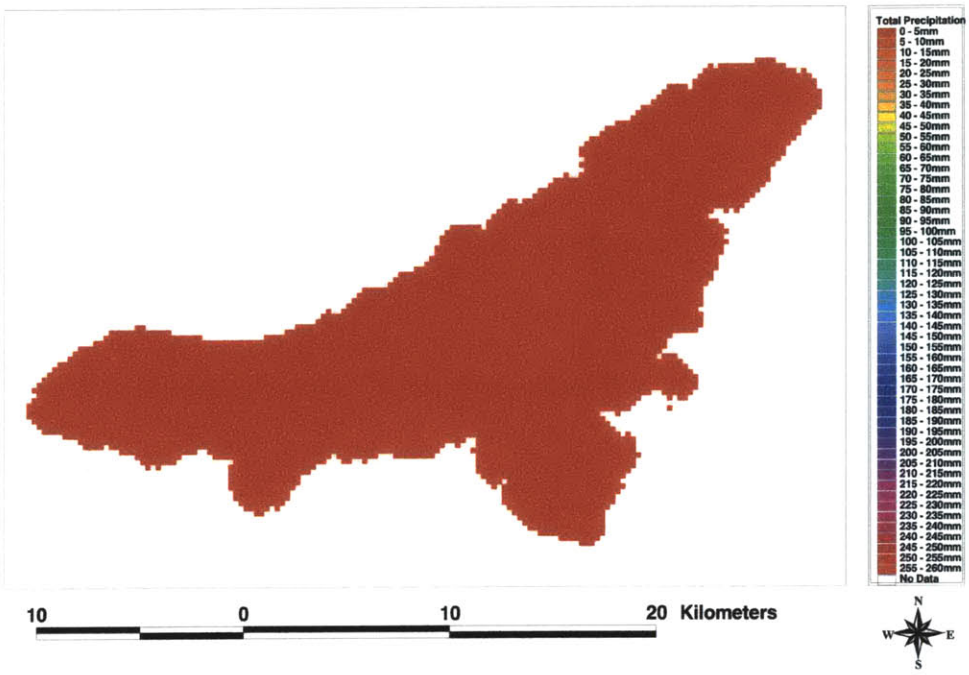

Total Precipitation - September 1998

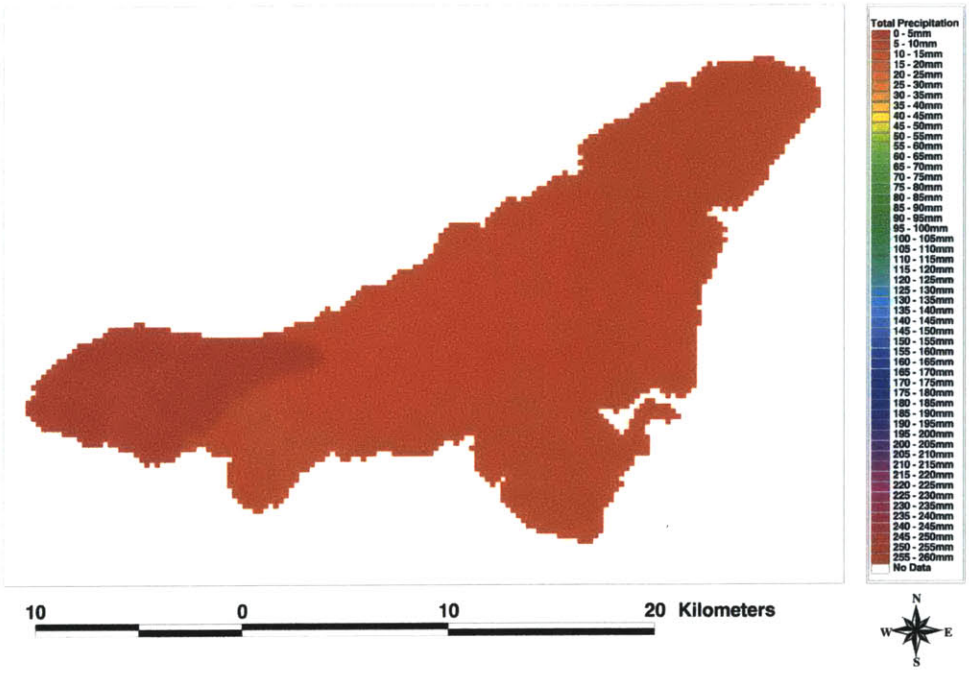

Total Precipitation - October 1998

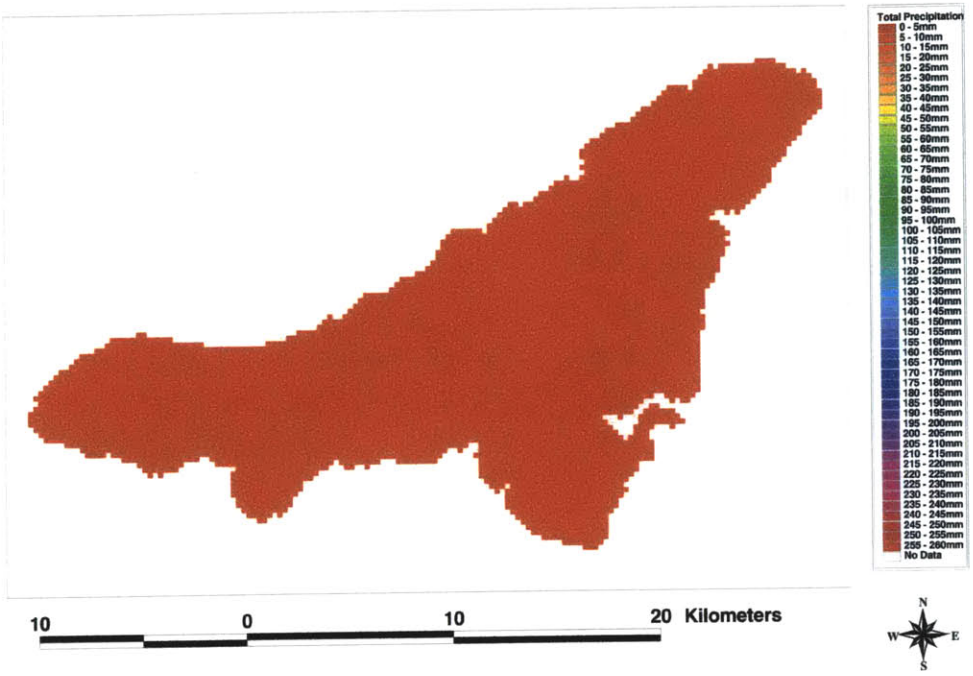

Total Precipitation - November 1998

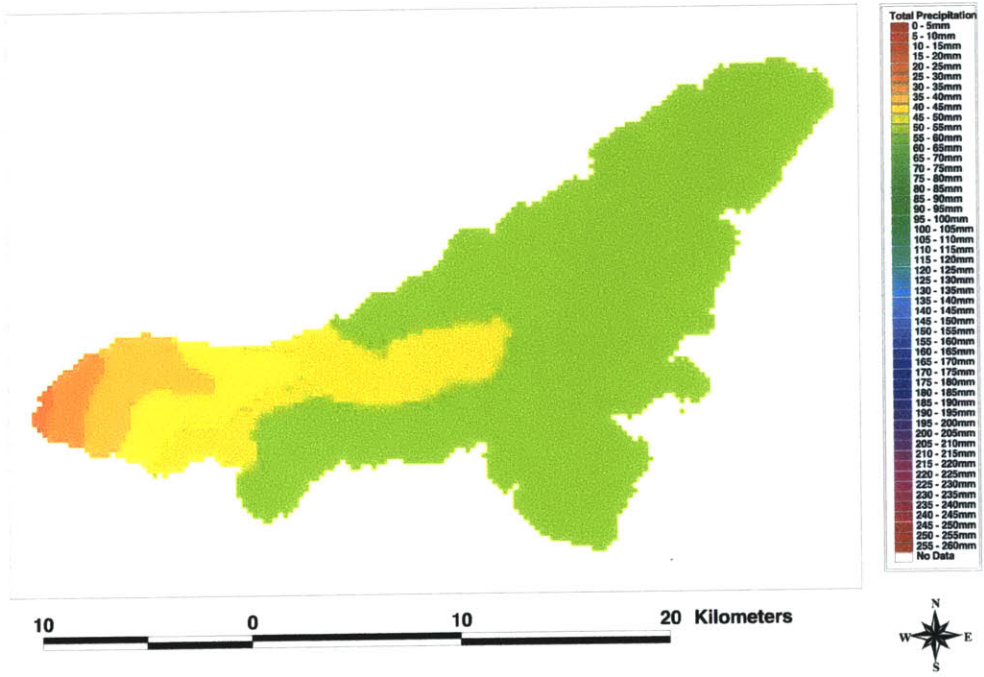

Total Precipitation - December 1998

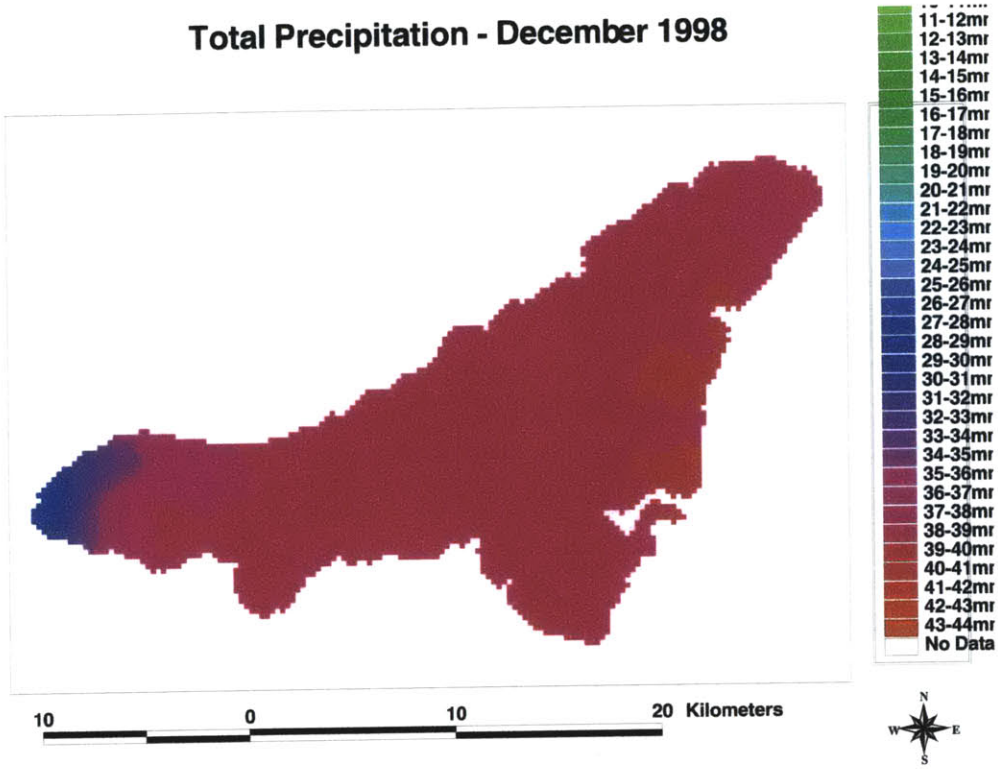

Total Precipitation - January, 1999

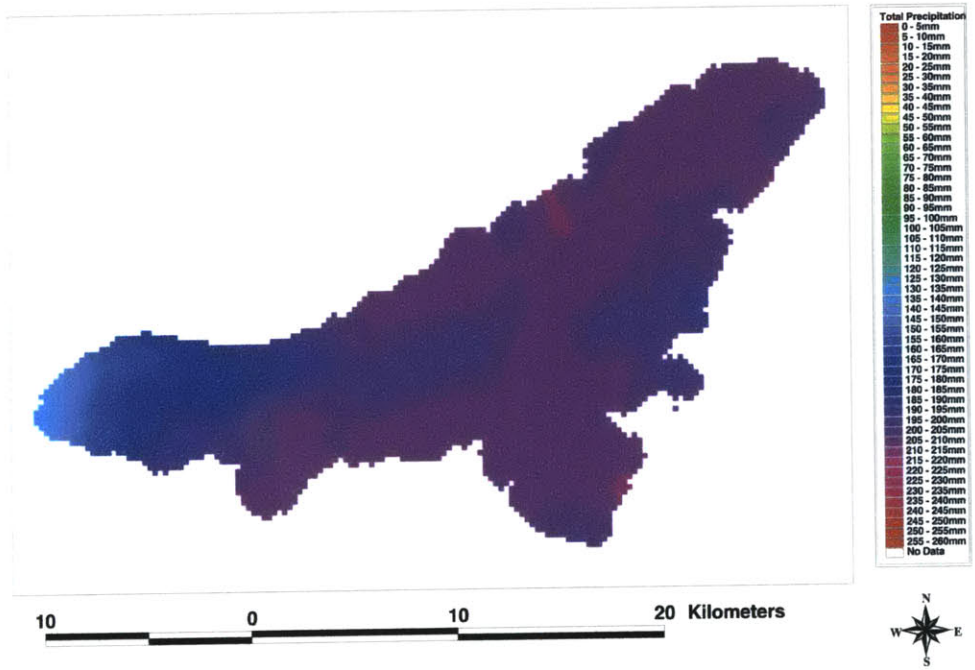

Total Precipitation - February 1999

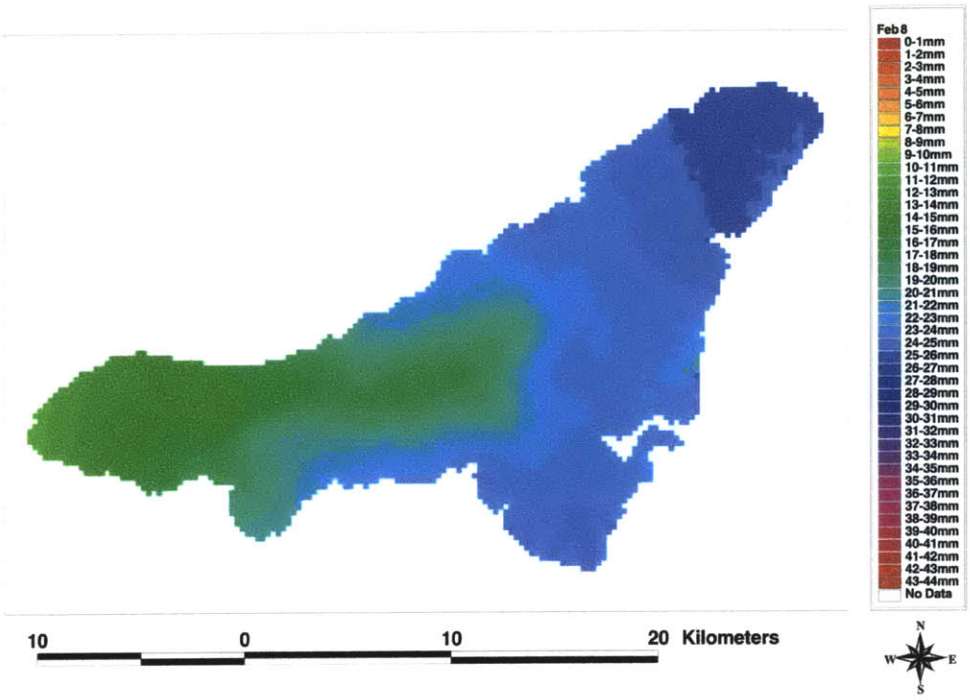

Total Precipitation - March 1999

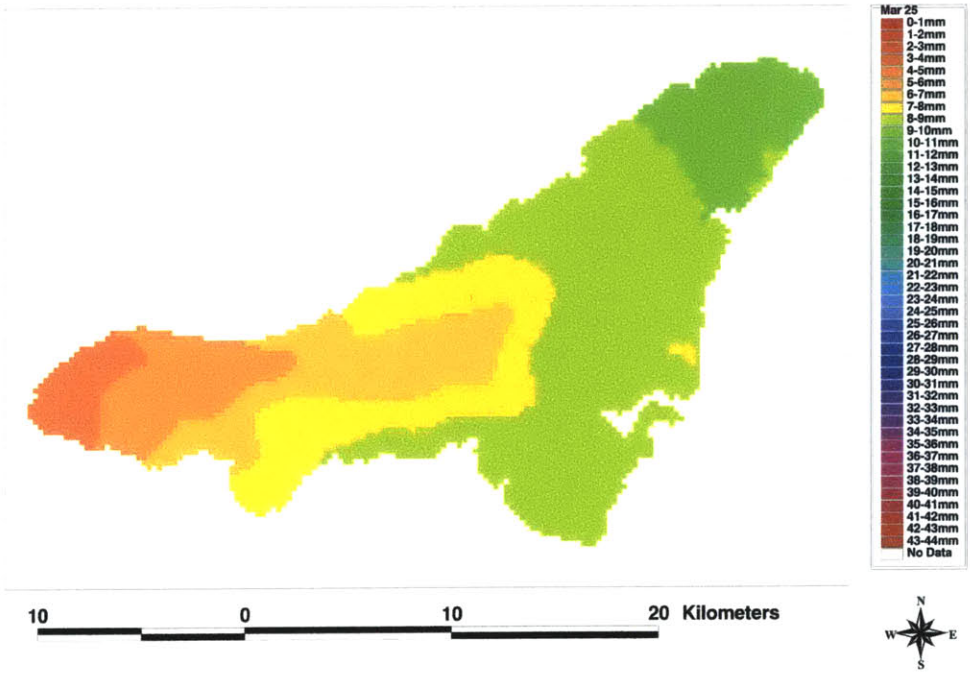

Total Precipitation - April 1999

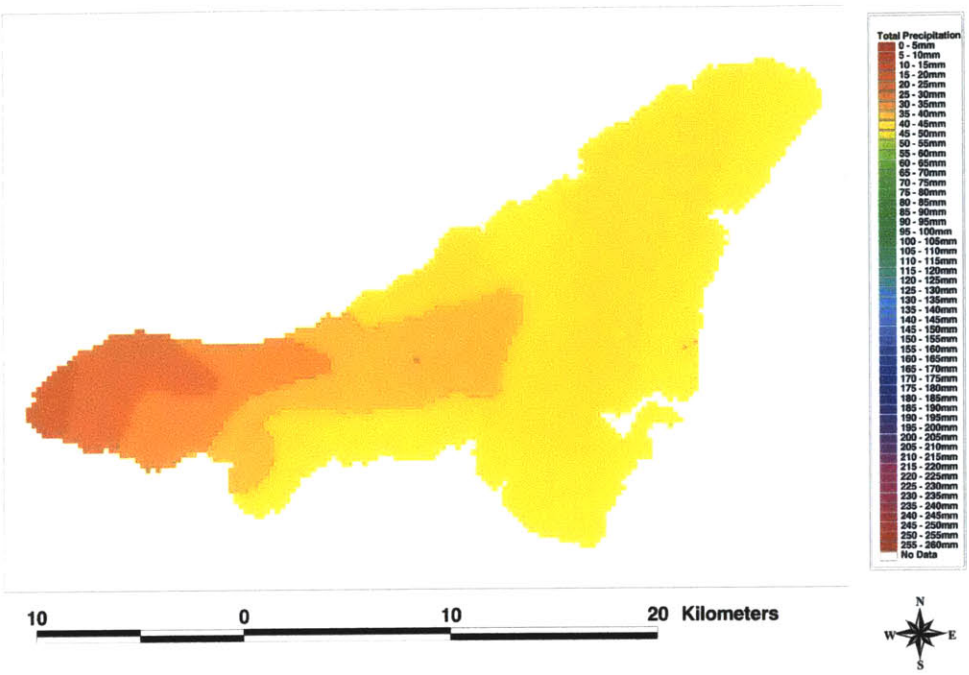

Appendix D
Daily Precipitation Estimation

May, 1998
Daily Precipitation Estimation Maps

May 10, 1998

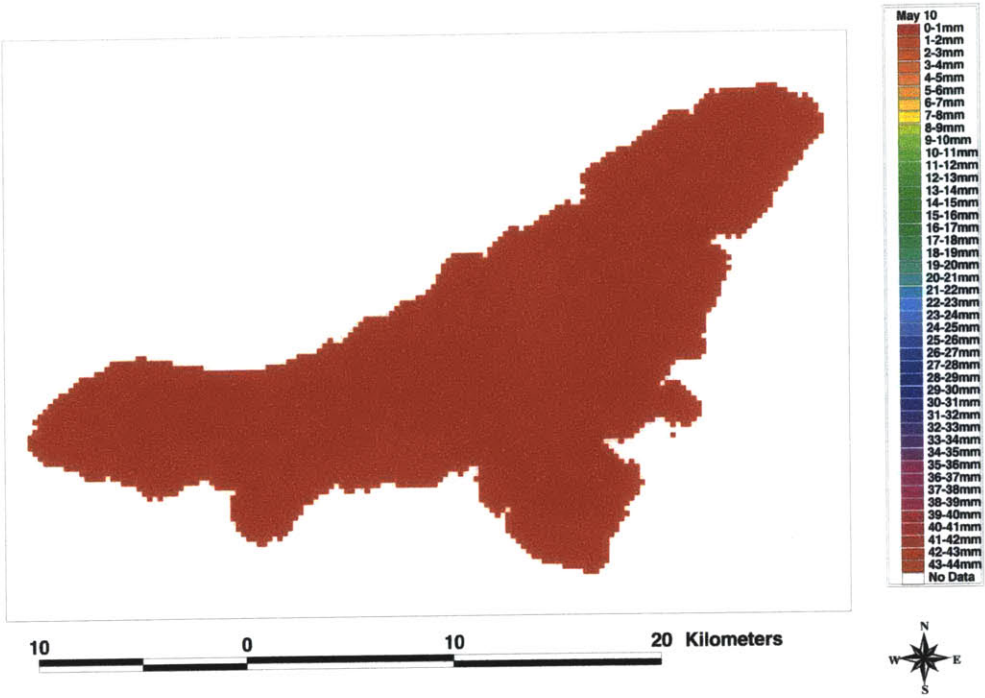

May 11, 1998

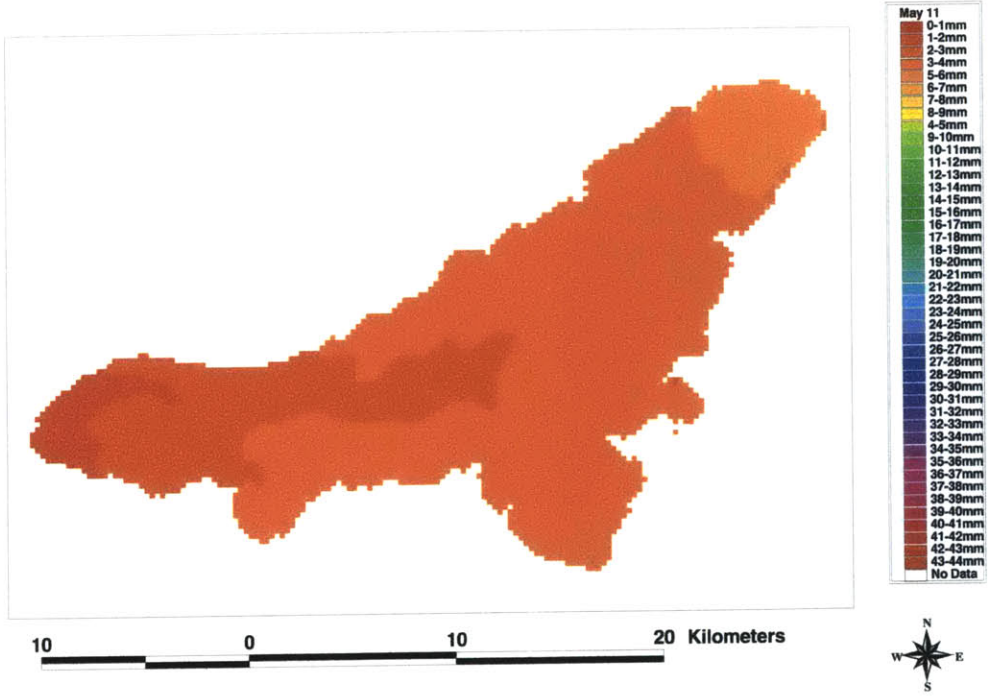

September, 1998
Daily Precipitation Estimation Maps

September 21, 1998

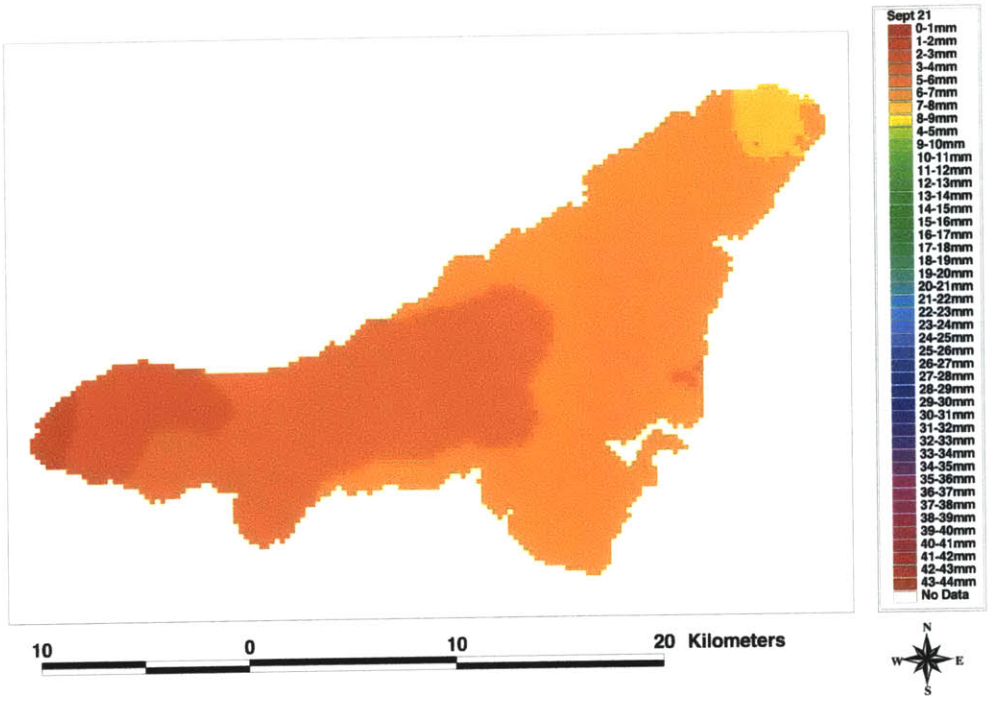

October, 1998
Daily Precipitation Estimation Maps

October 28, 1998

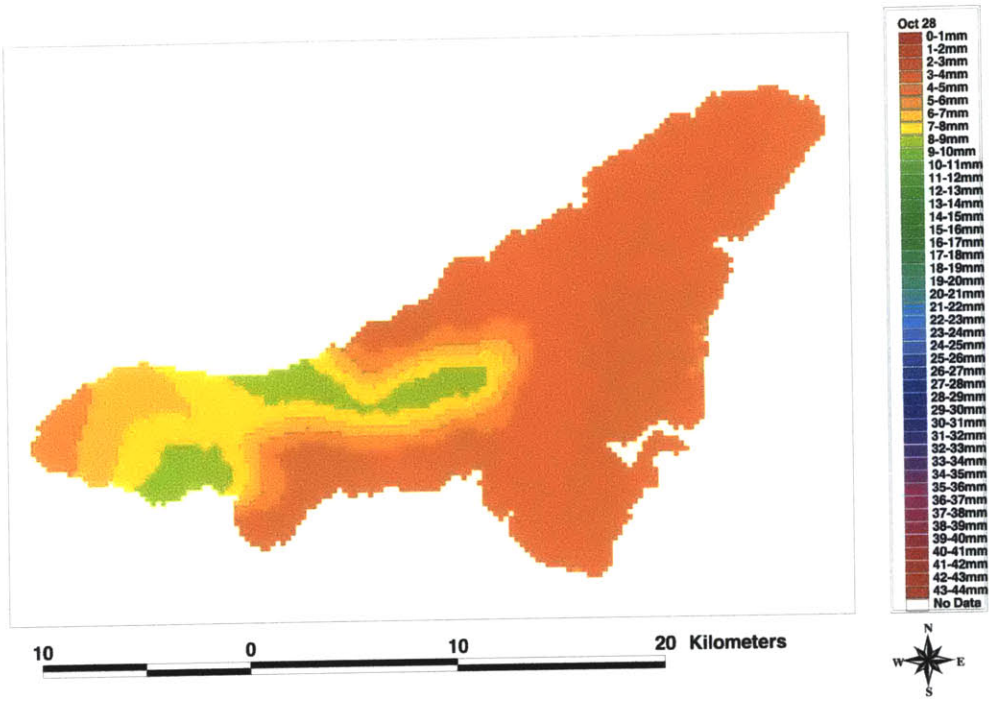

November, 1998
Daily Precipitation Estimation Maps

November 2, 1998

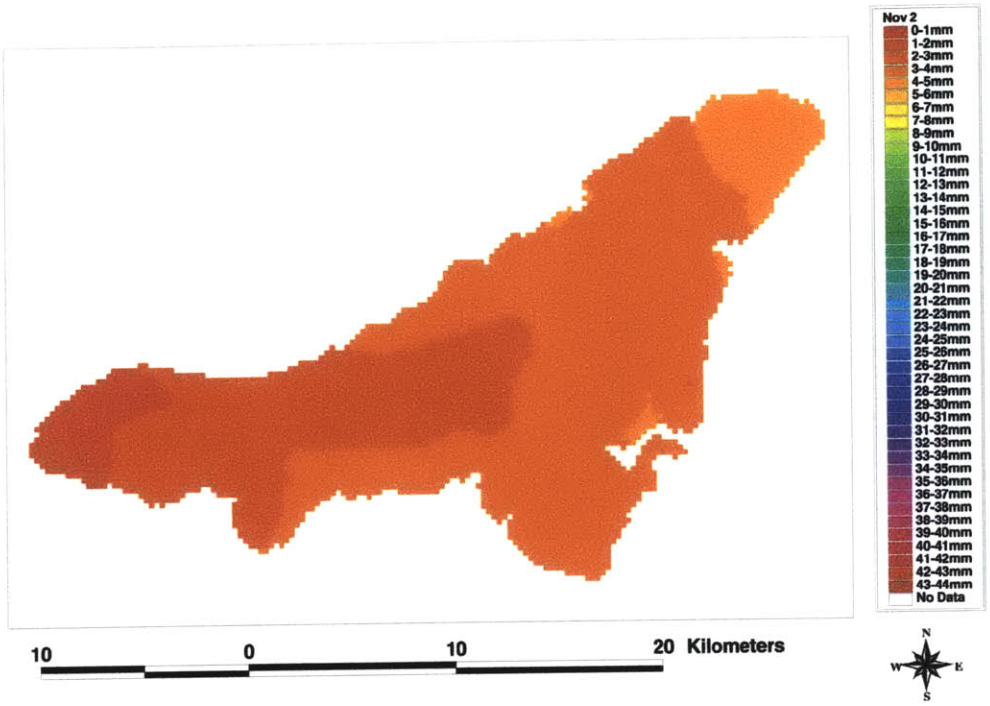

November 10, 1998

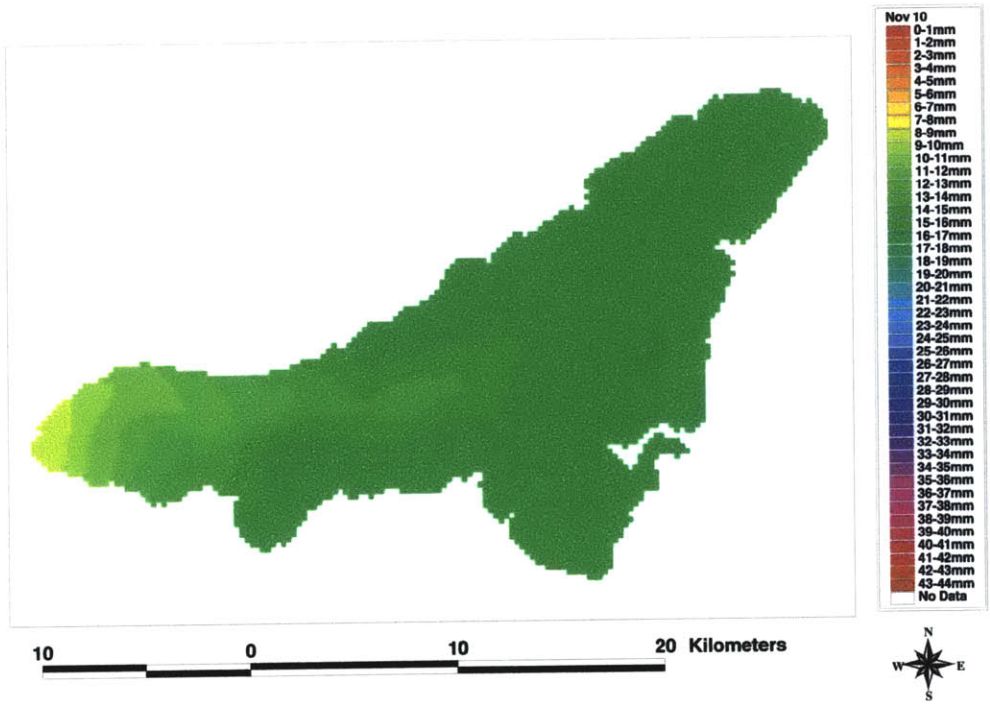

November 11, 1998

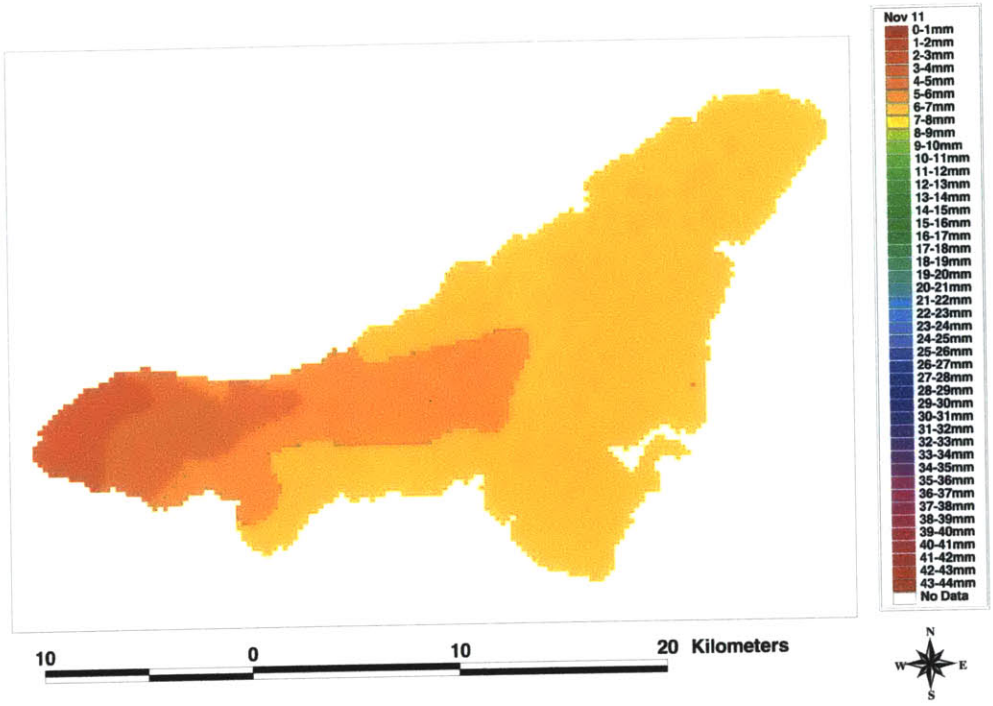

November 13, 1998

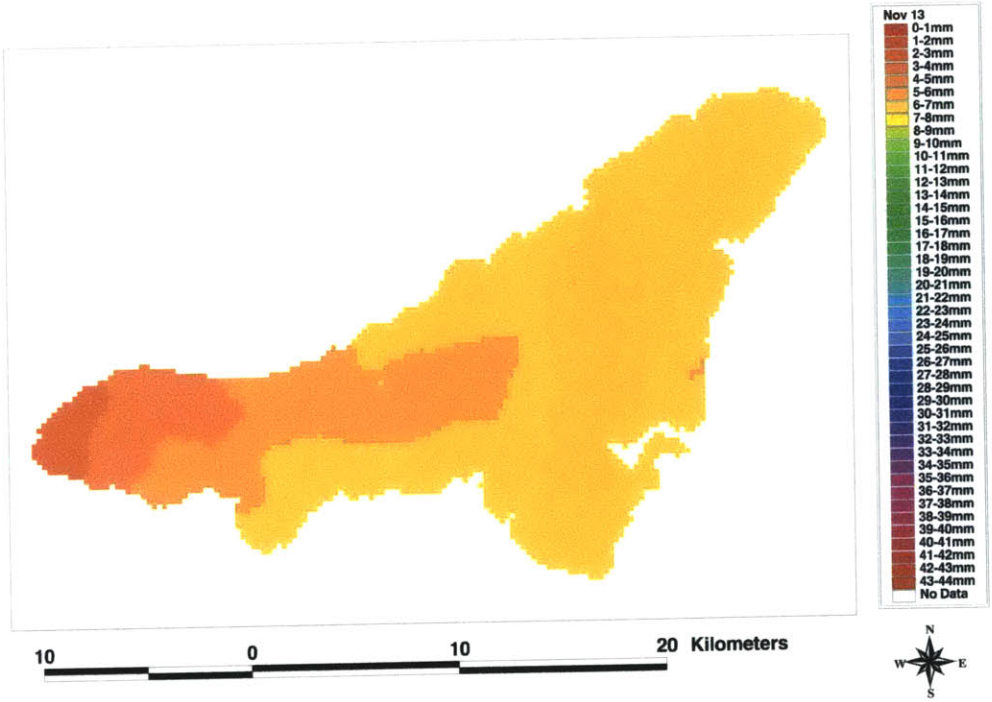

November 14, 1998

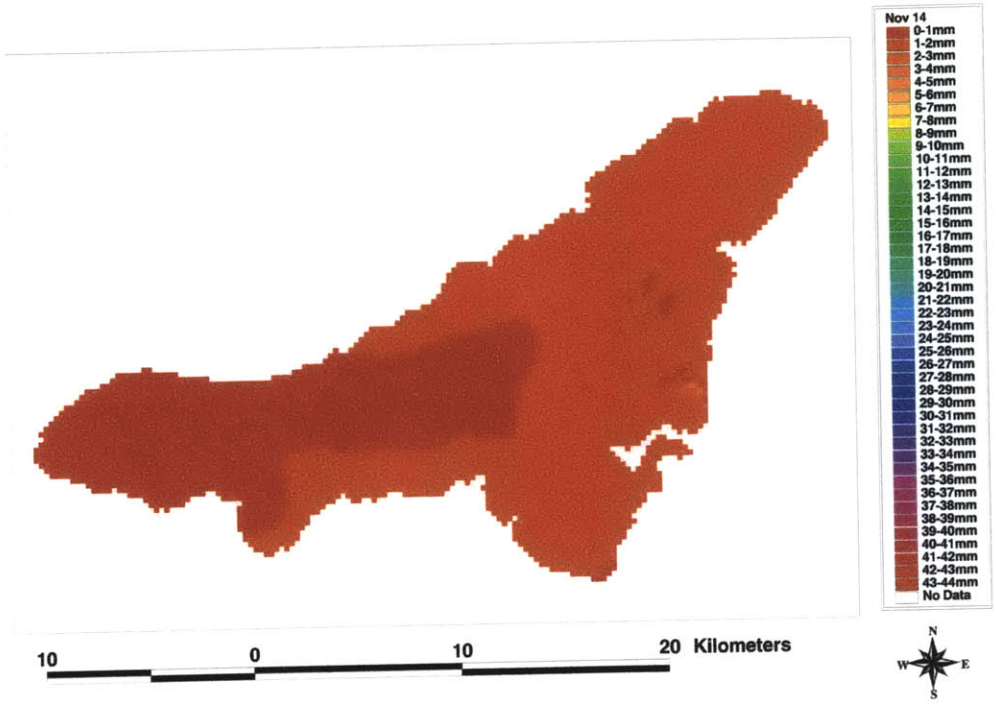

November 15, 1998

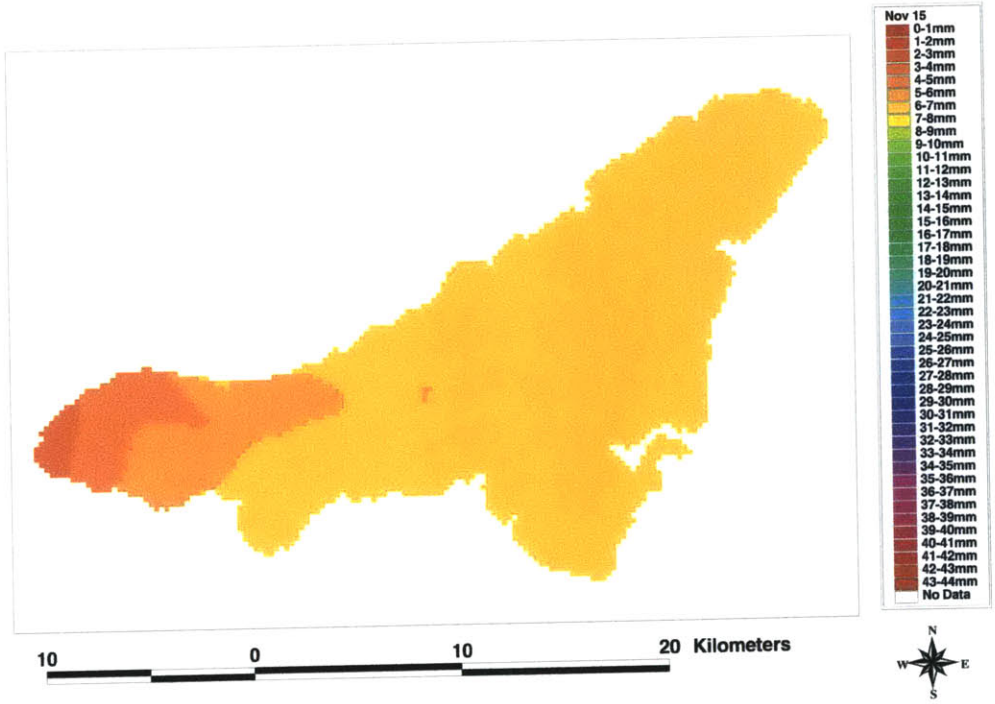

November 16, 1998

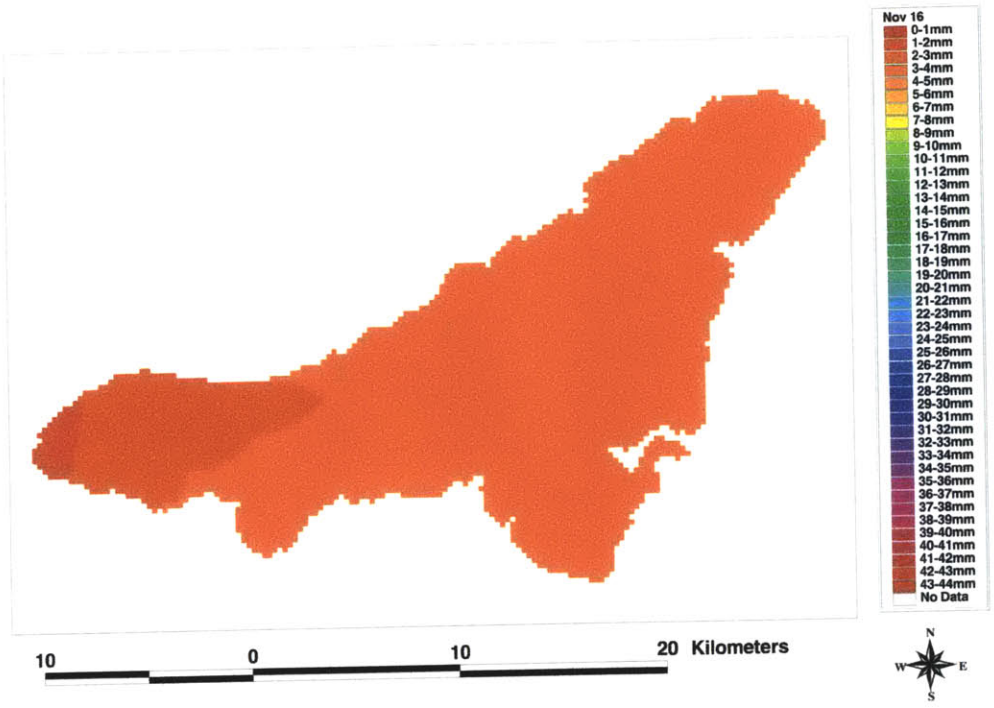

November 17, 1998

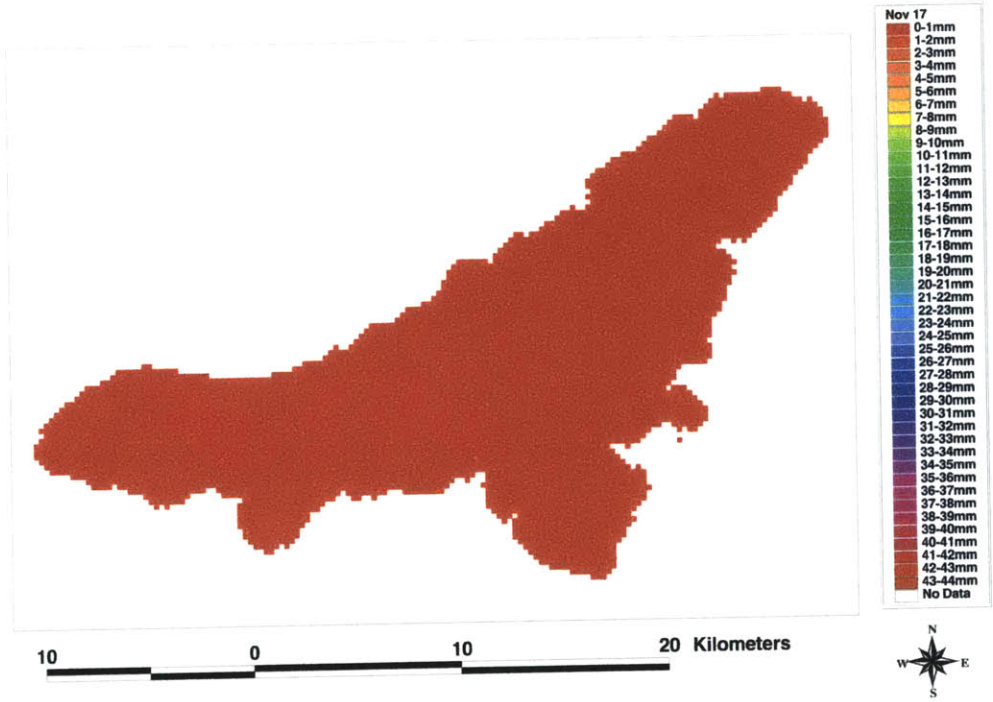

November 19, 1998

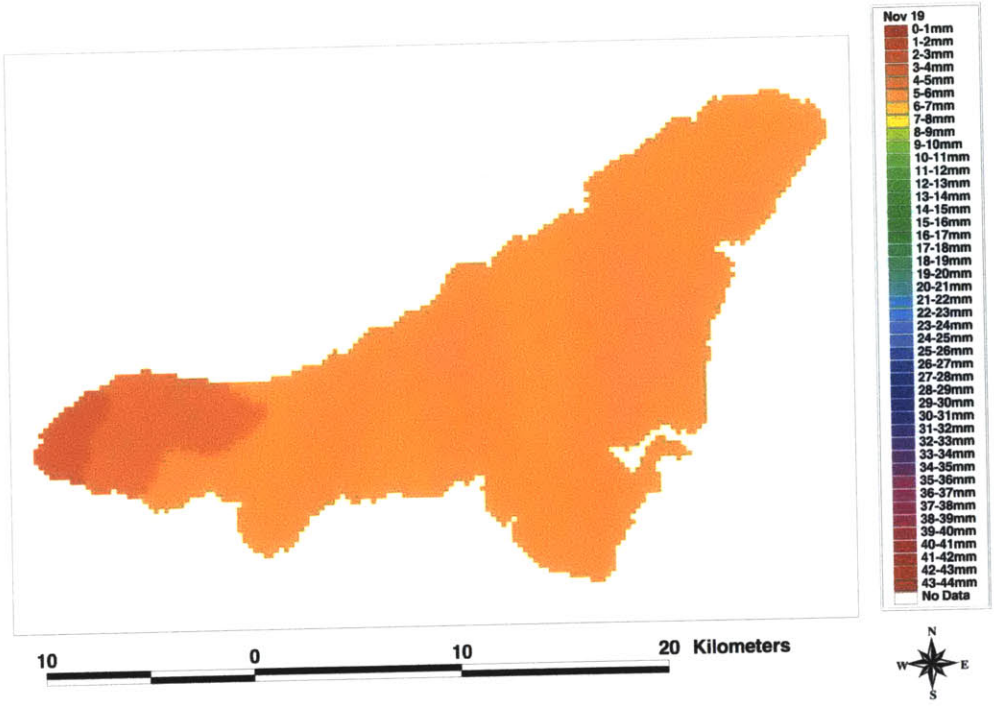

November 30, 1998

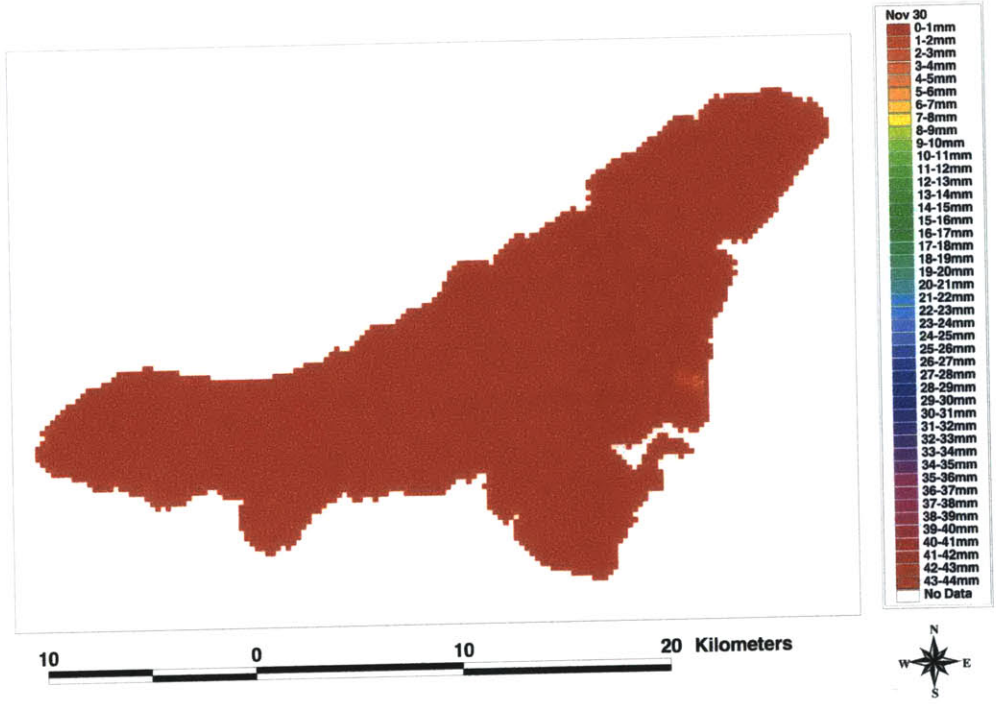

December, 1998
Daily Precipitation Estimation Maps

December 1, 1998

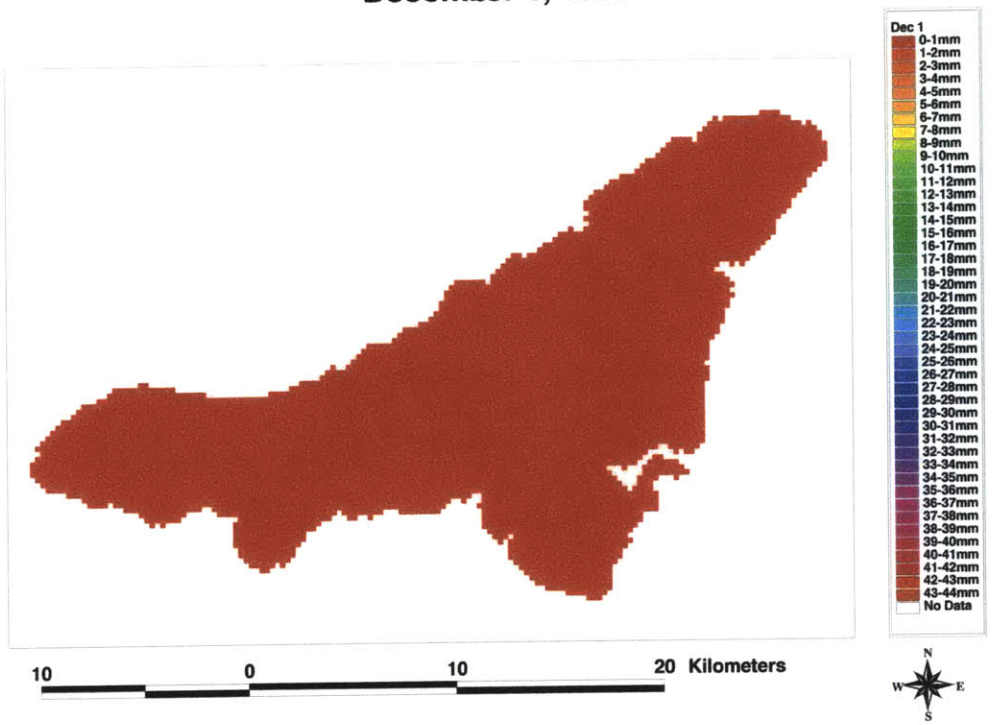

December 7, 1998

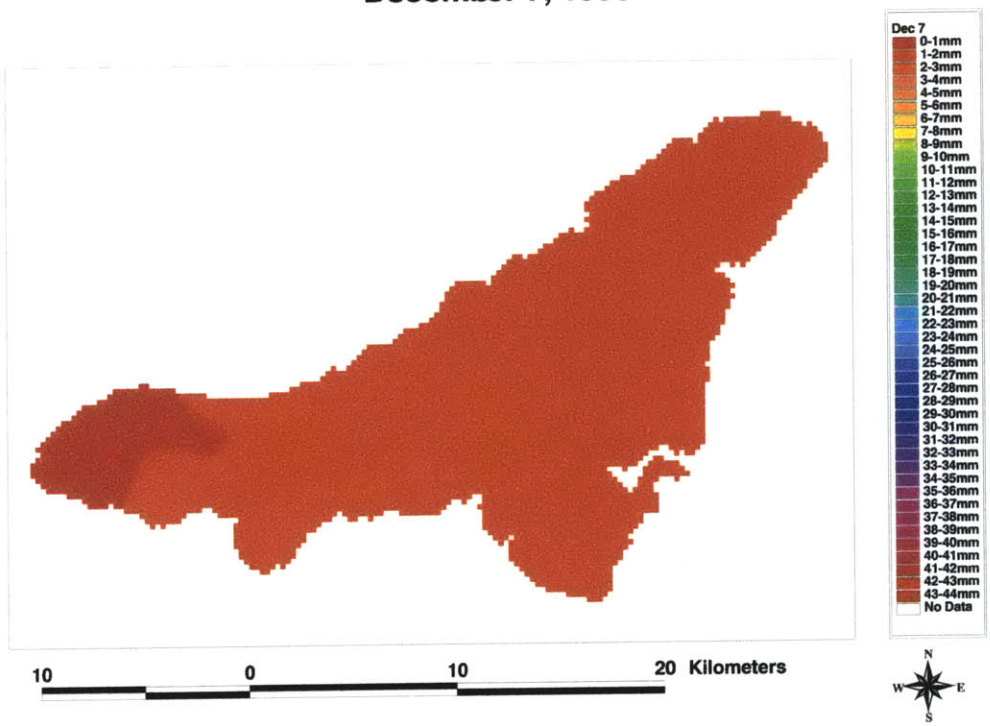

December 8, 1998

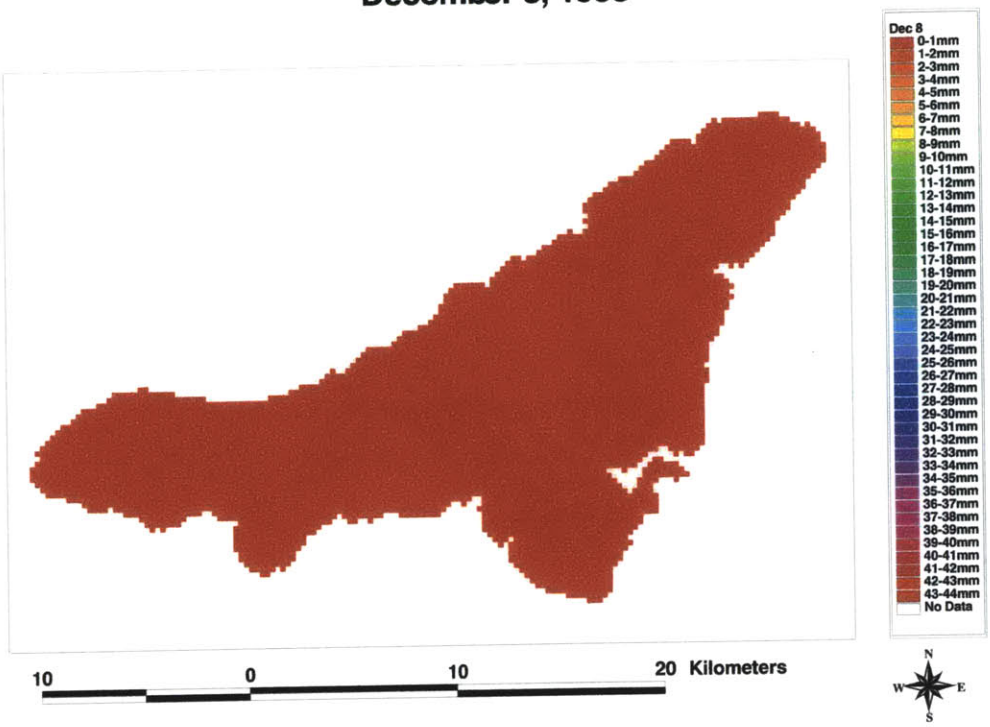

December 10, 1998

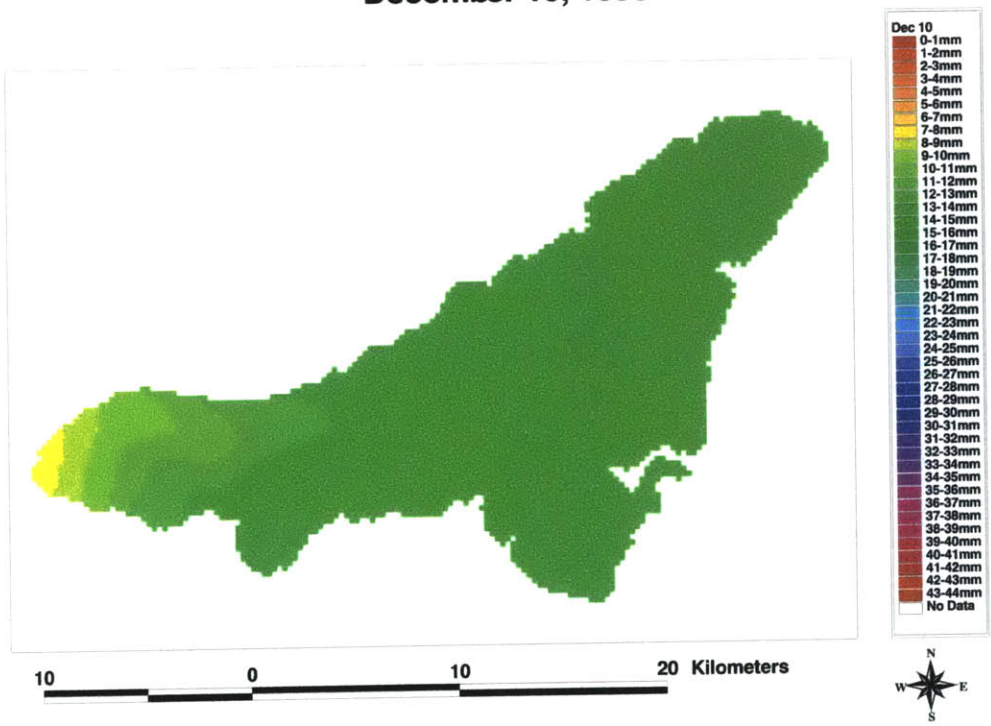

December 15, 1998

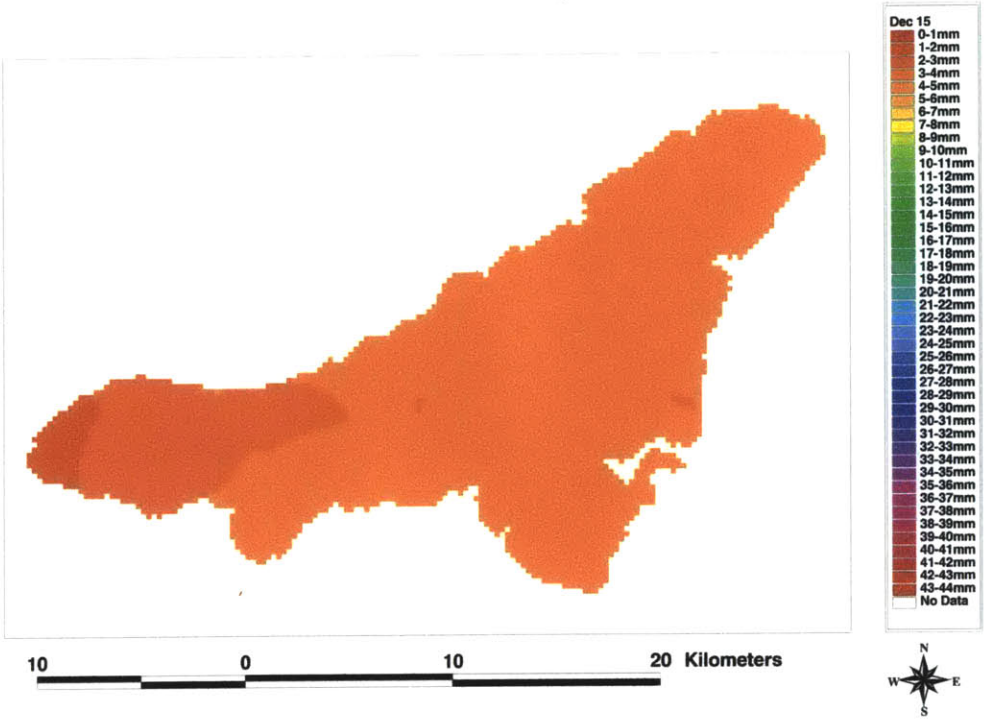

December 16, 1998

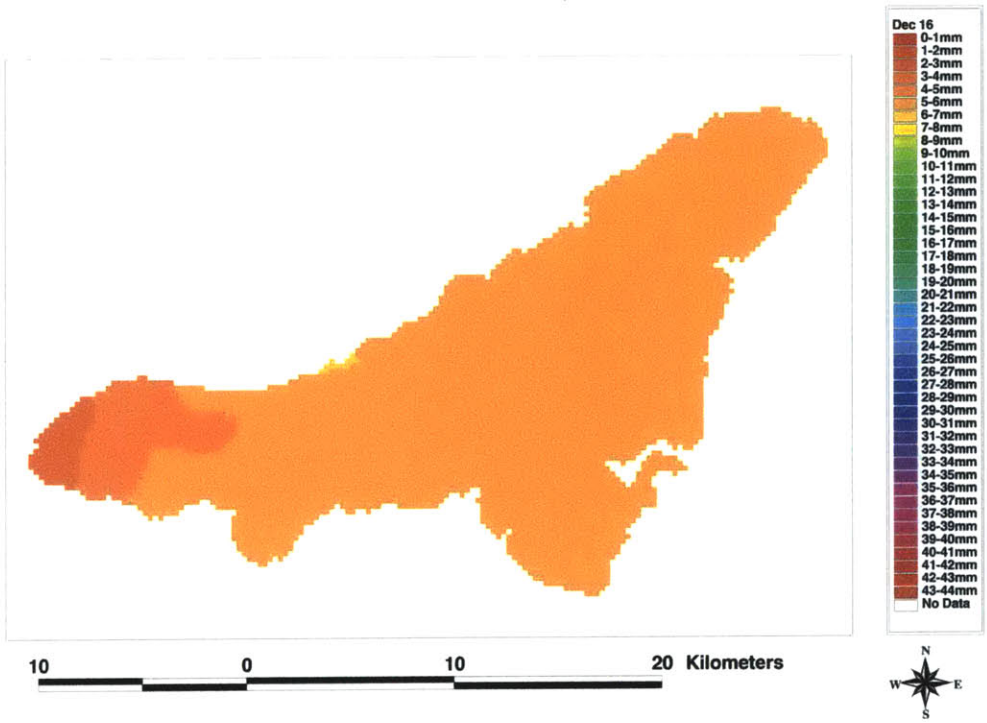

December 17, 1998

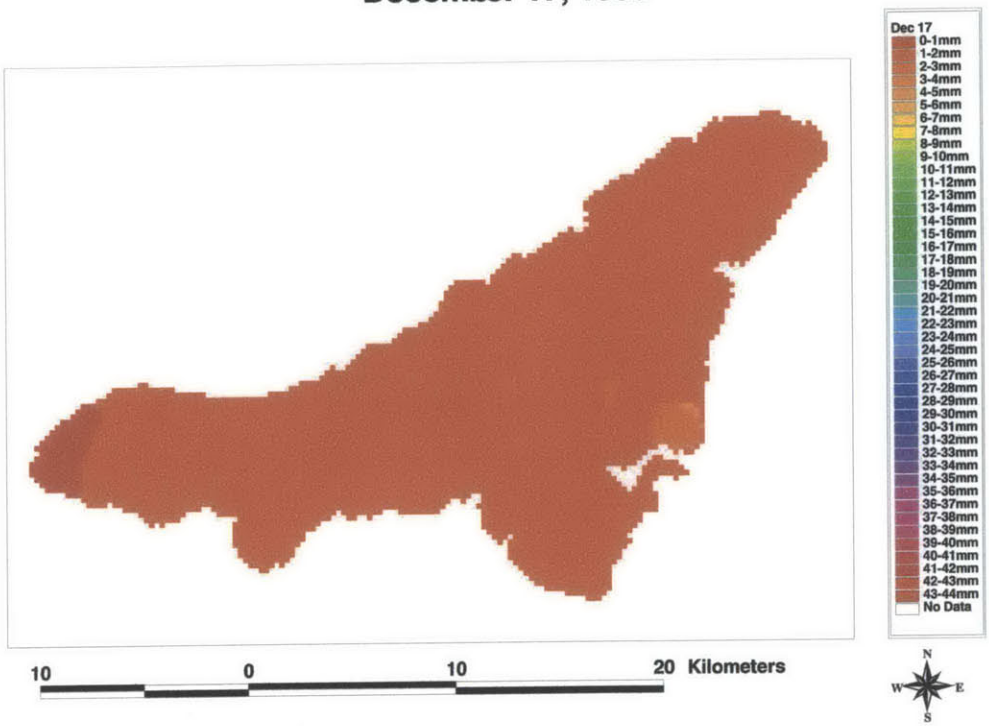

December 18, 1998

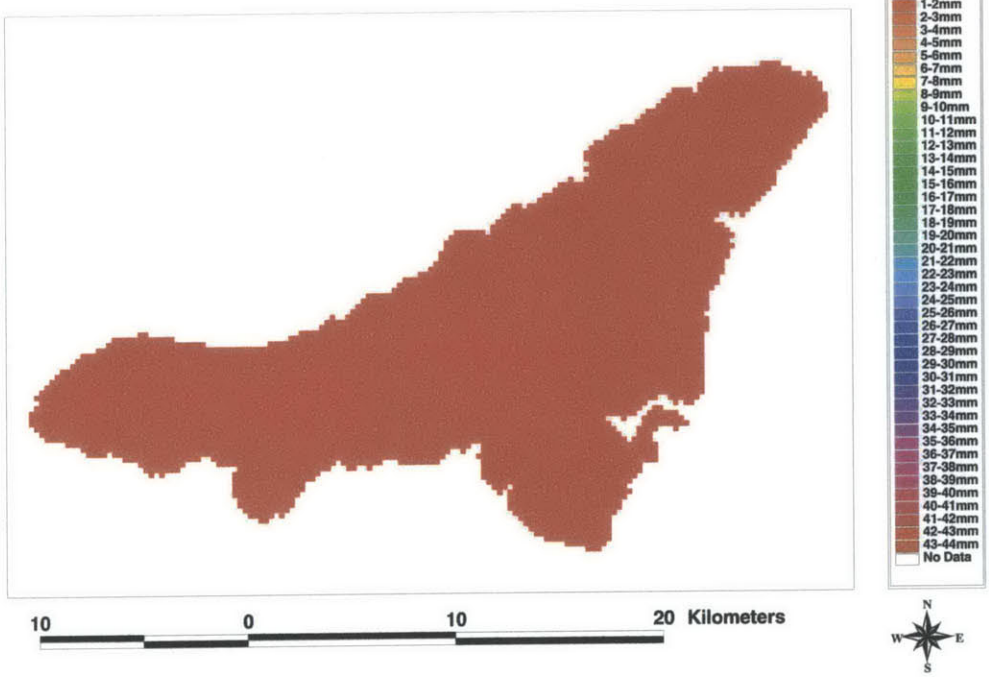

December 20, 1998

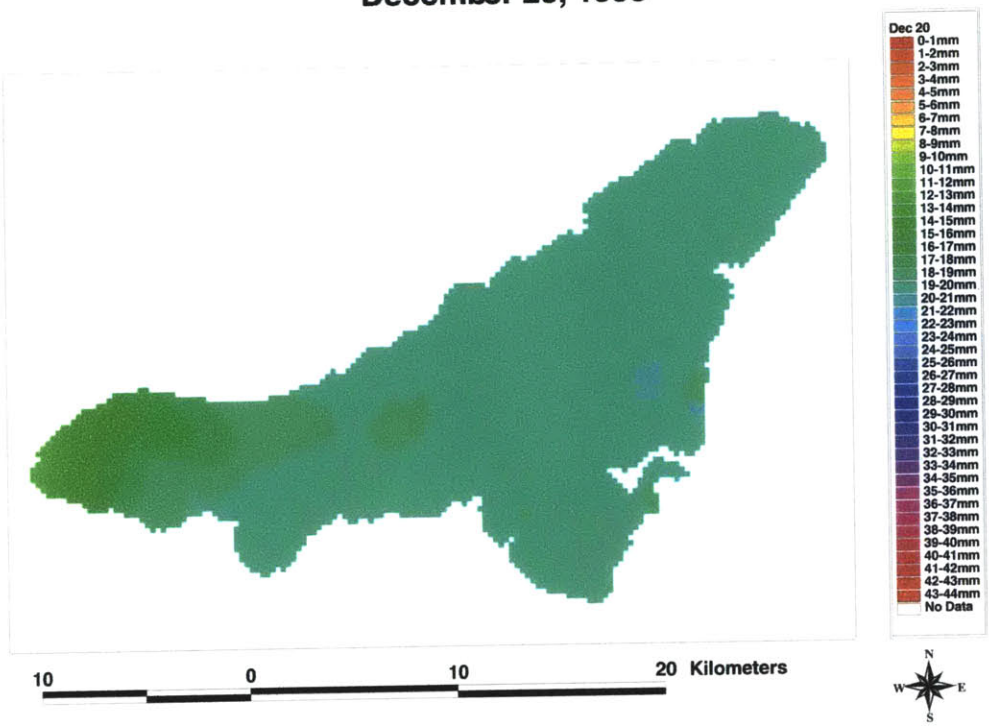

December 21, 1998

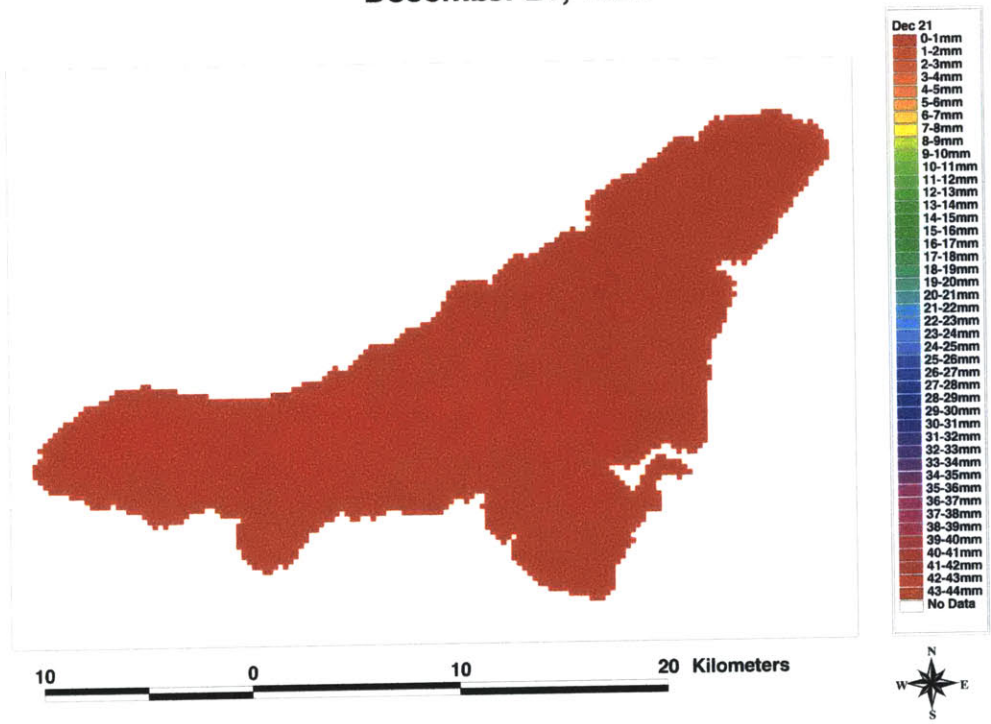

December 23, 1998

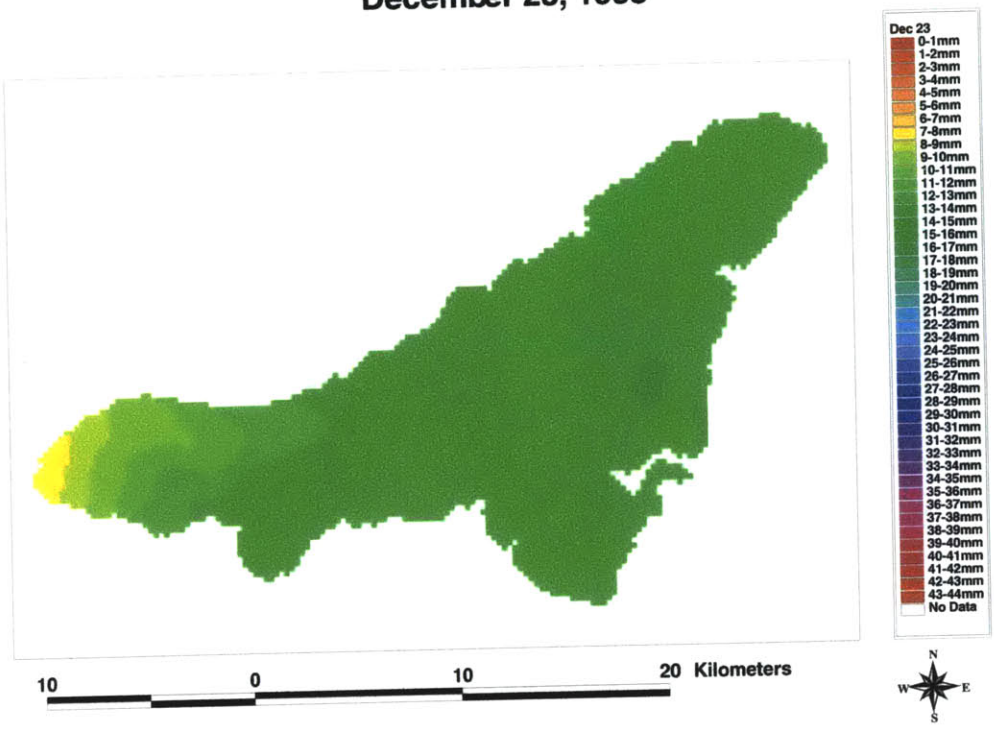

December 24, 1998

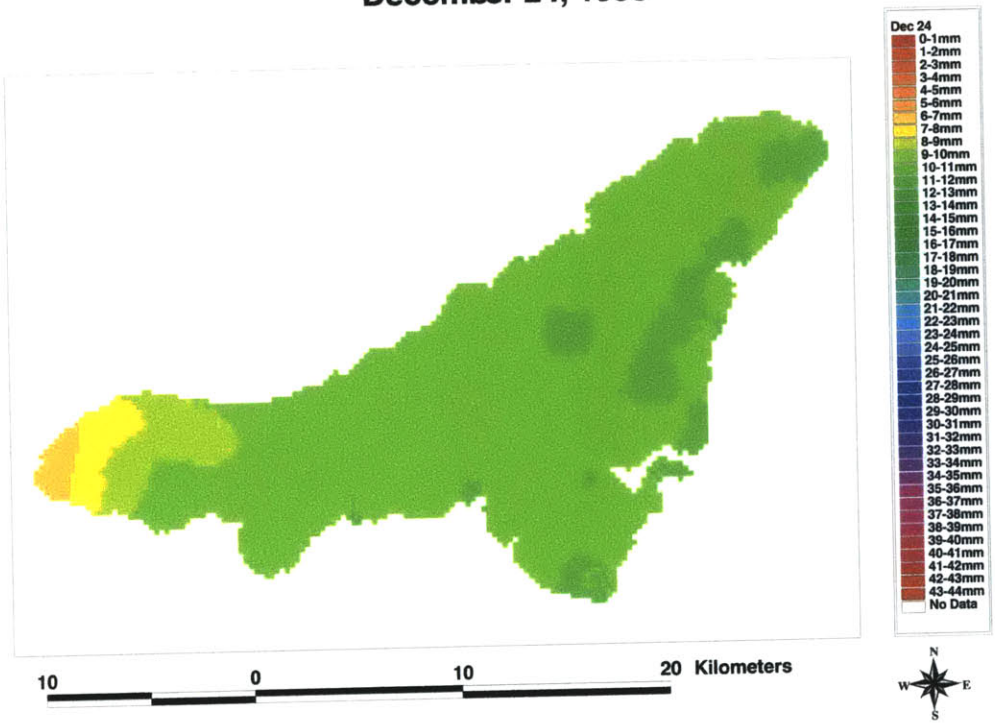

December 25, 1998

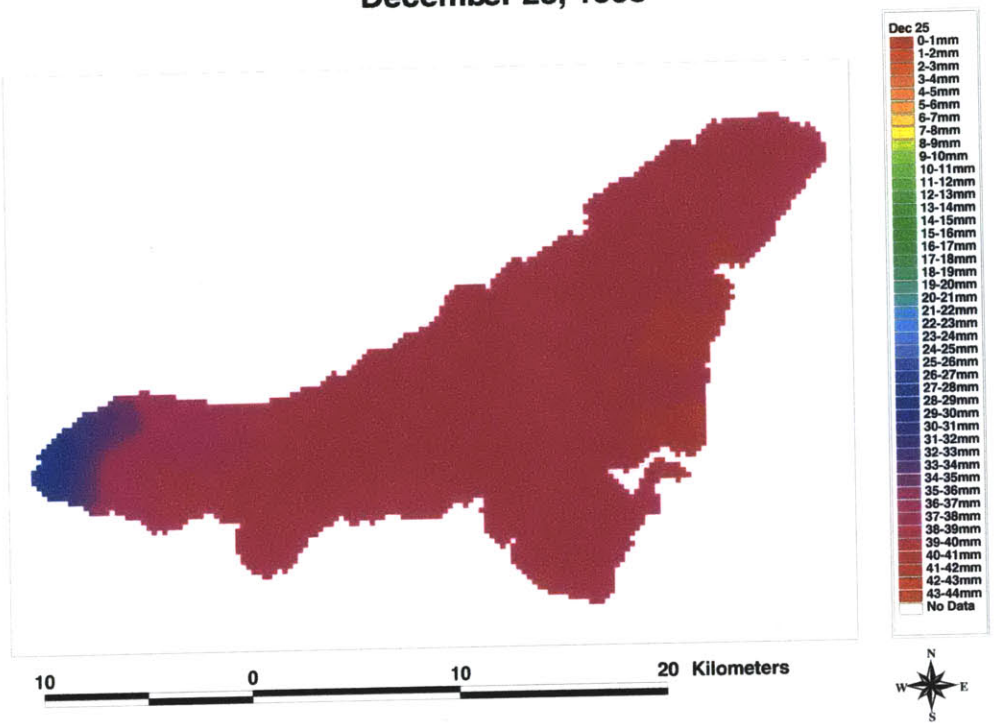

December 26, 1998

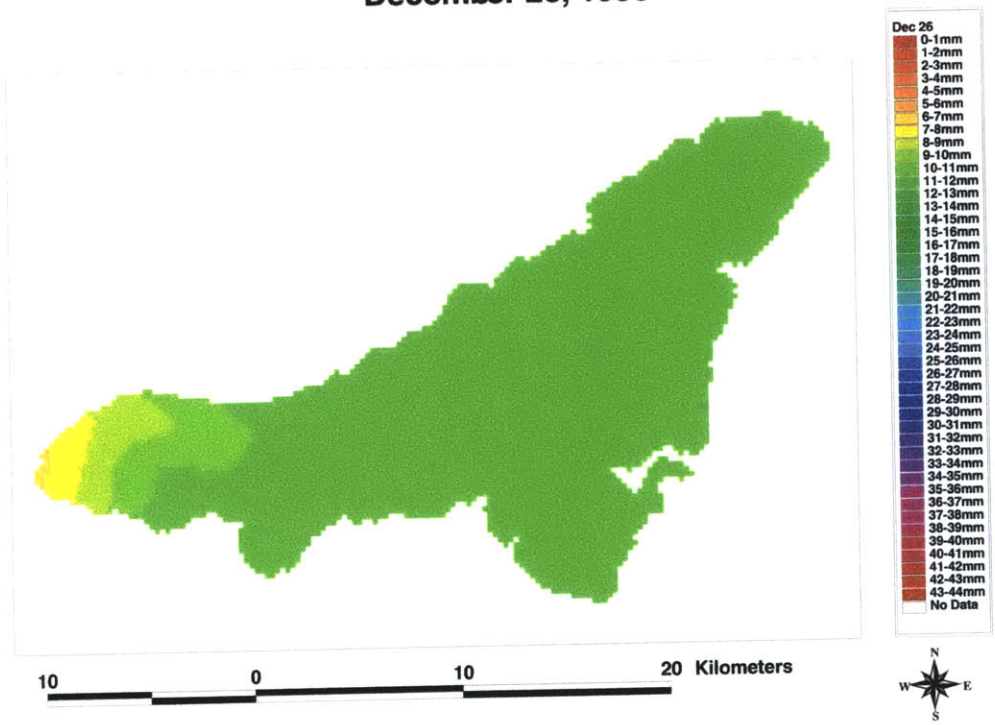

December 29, 1998

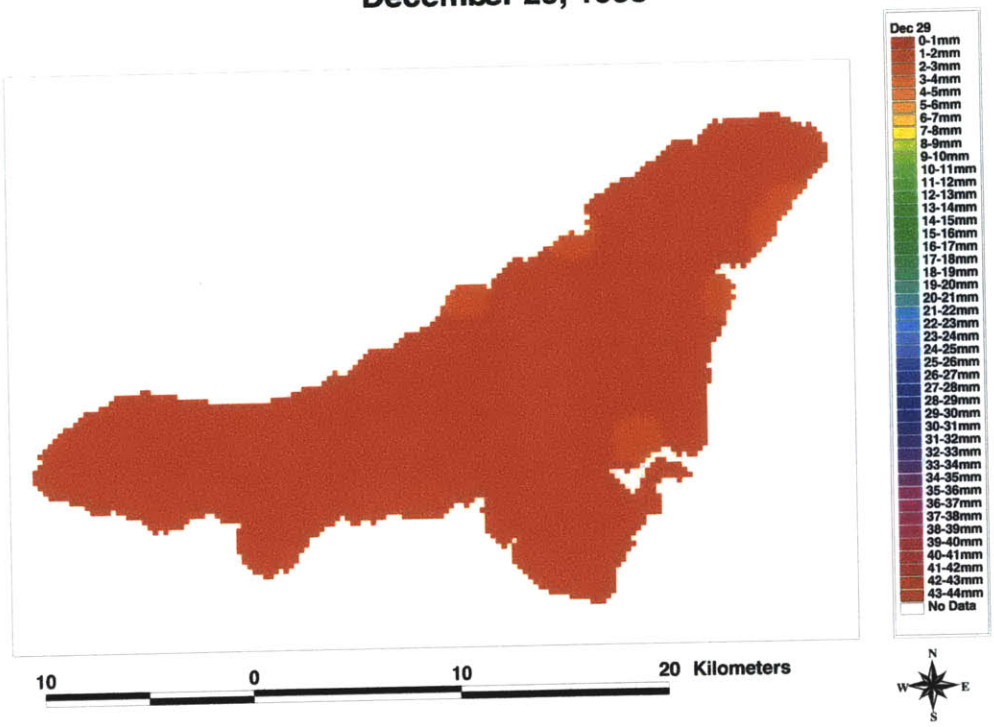

December 30, 1998

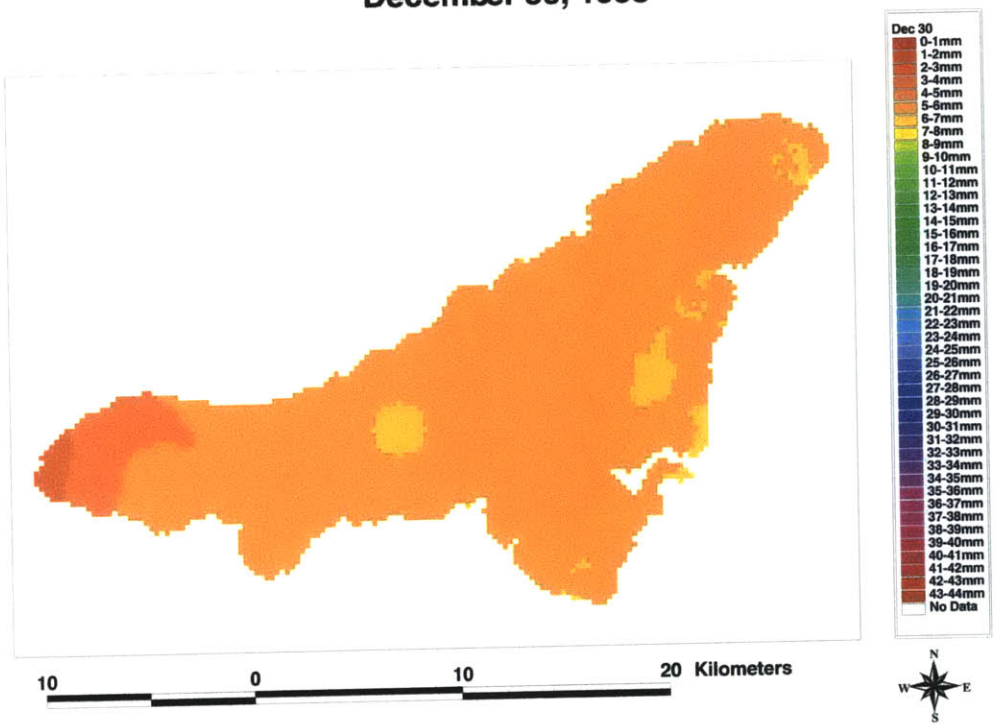

December 31, 1998

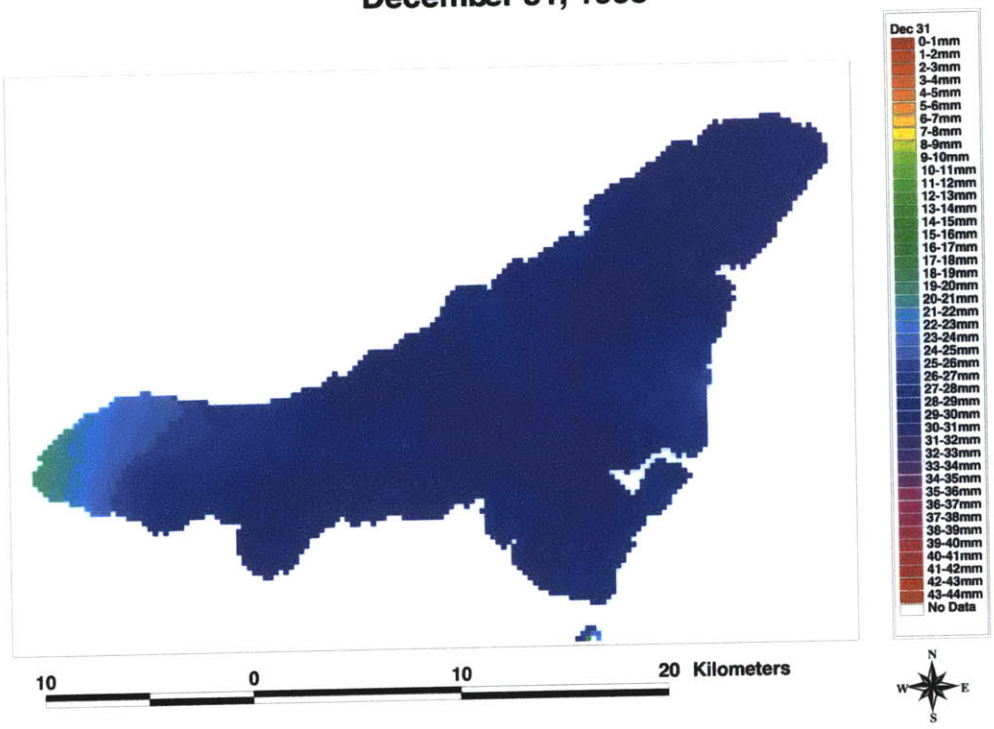

January, 1999
Daily Precipitation Estimation Maps

January 6, 1999

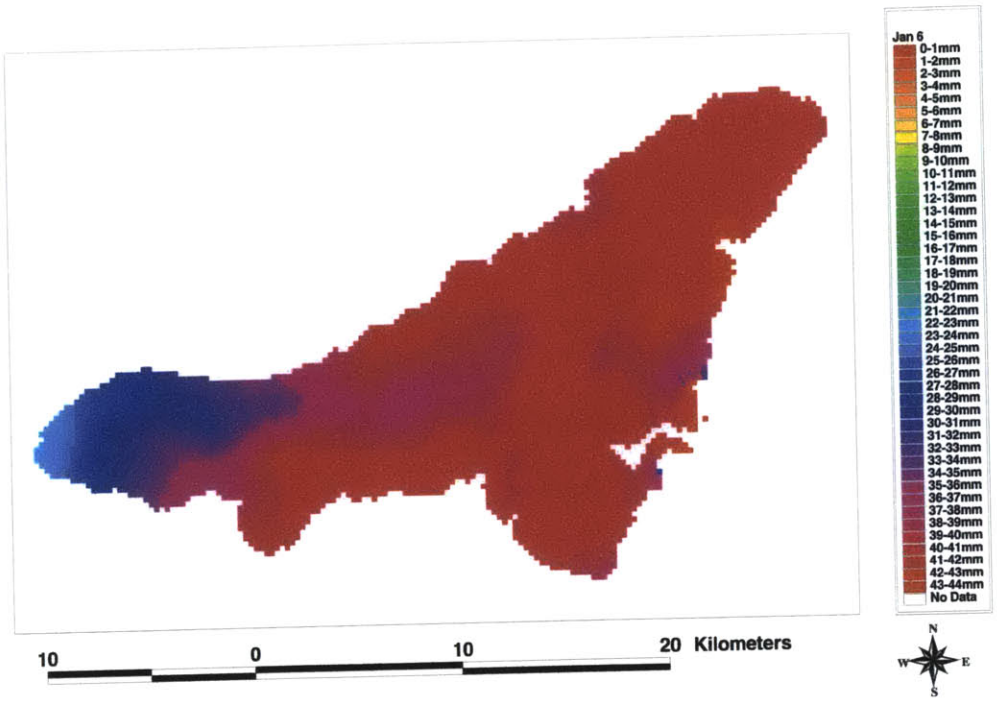

January 7, 1999

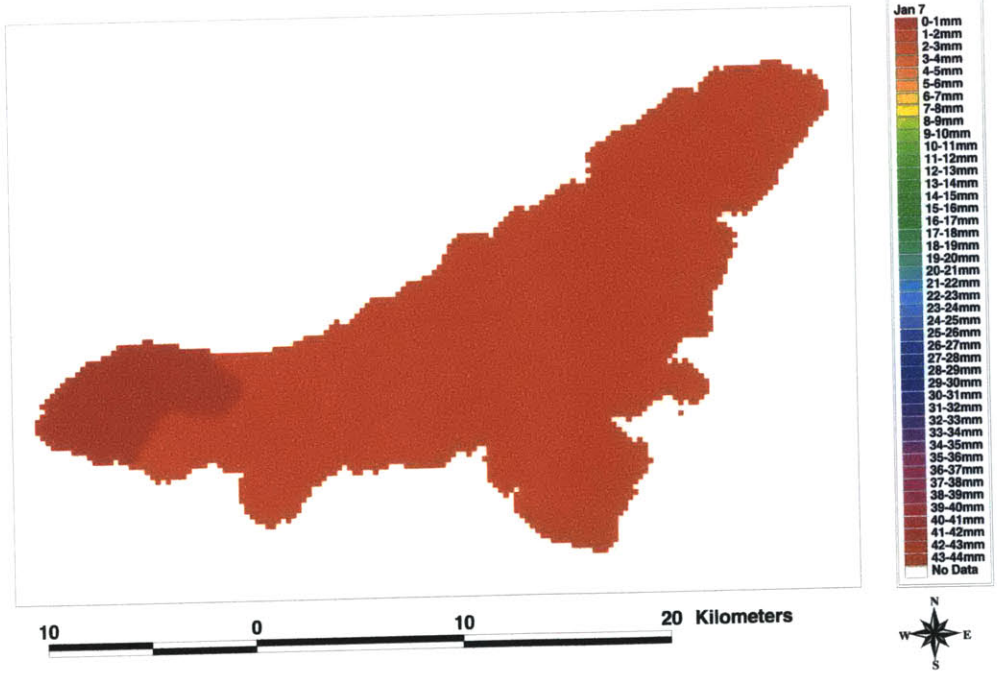

January 8, 1999

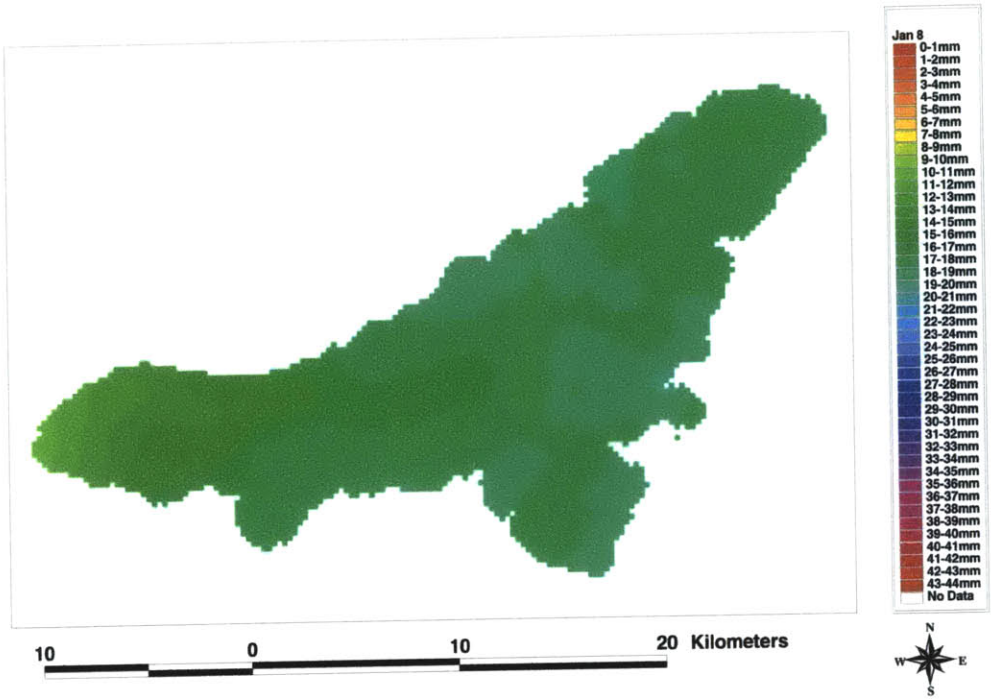

January 9, 1999

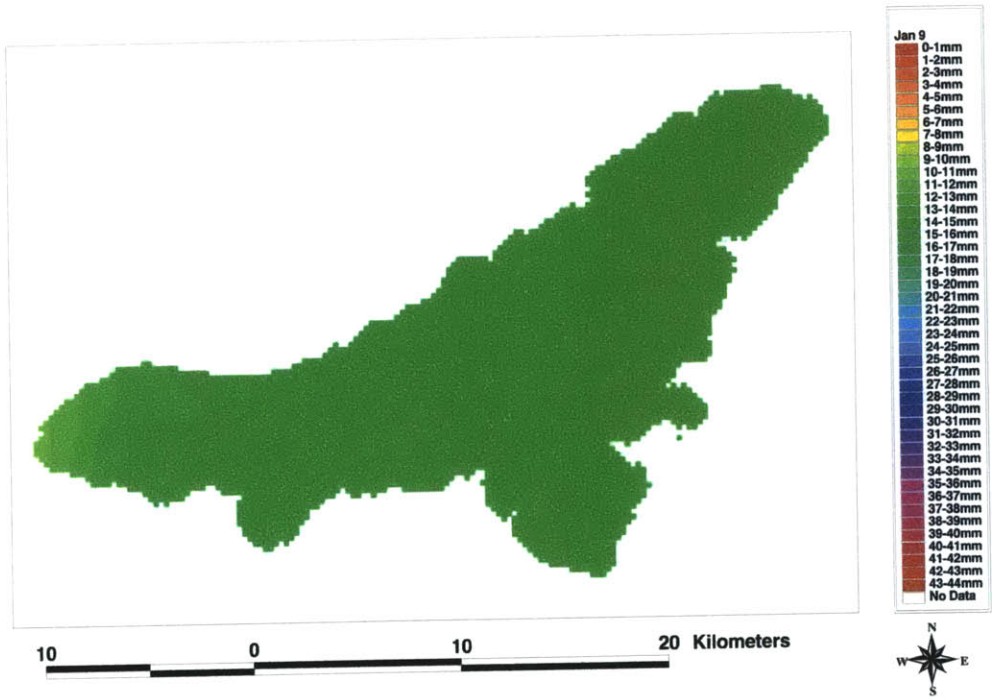

January 10, 1999

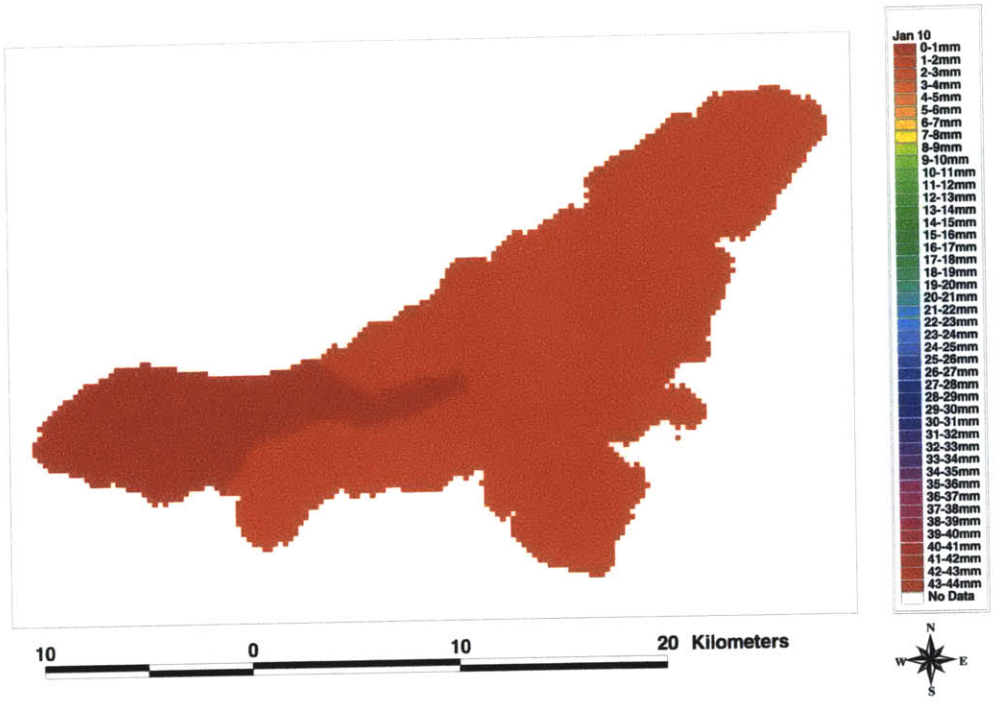

January 15, 1999

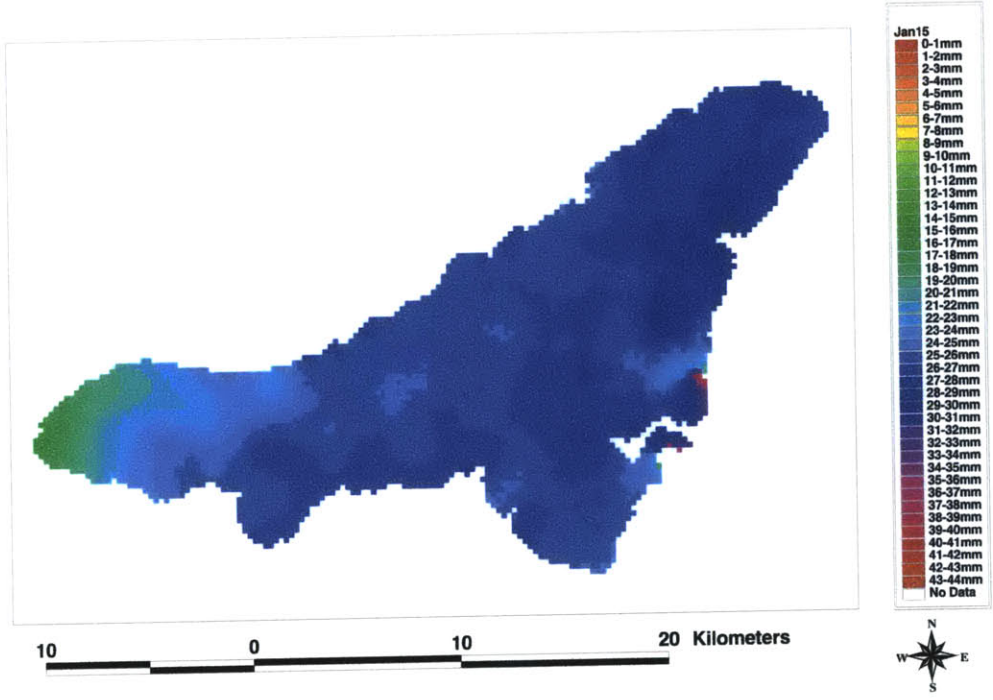

January 17, 1999

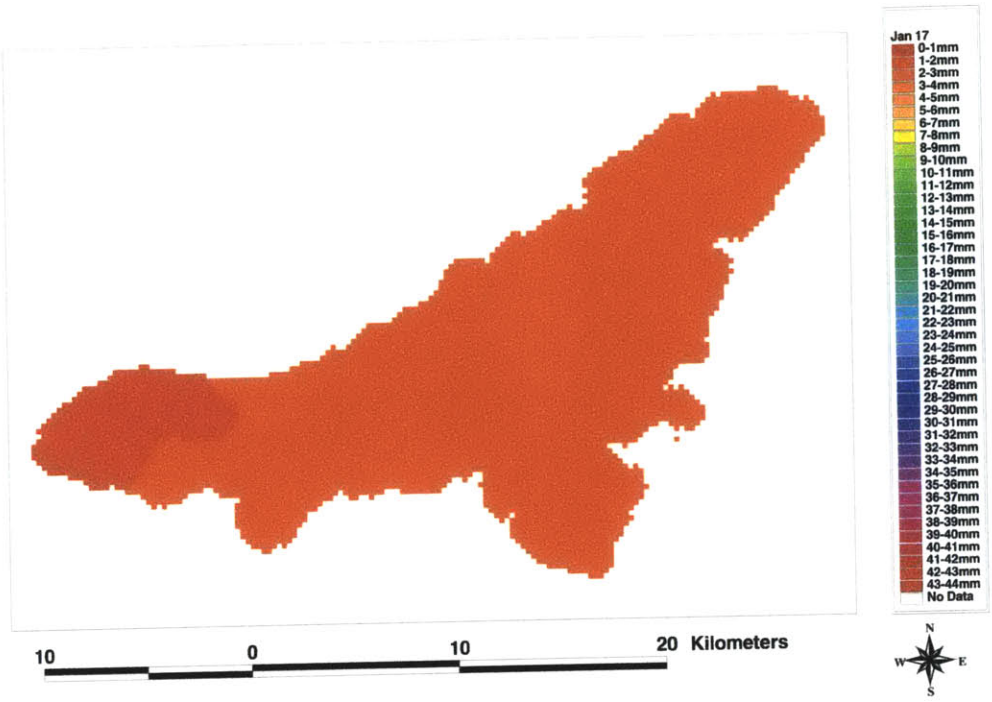

January 18, 1999

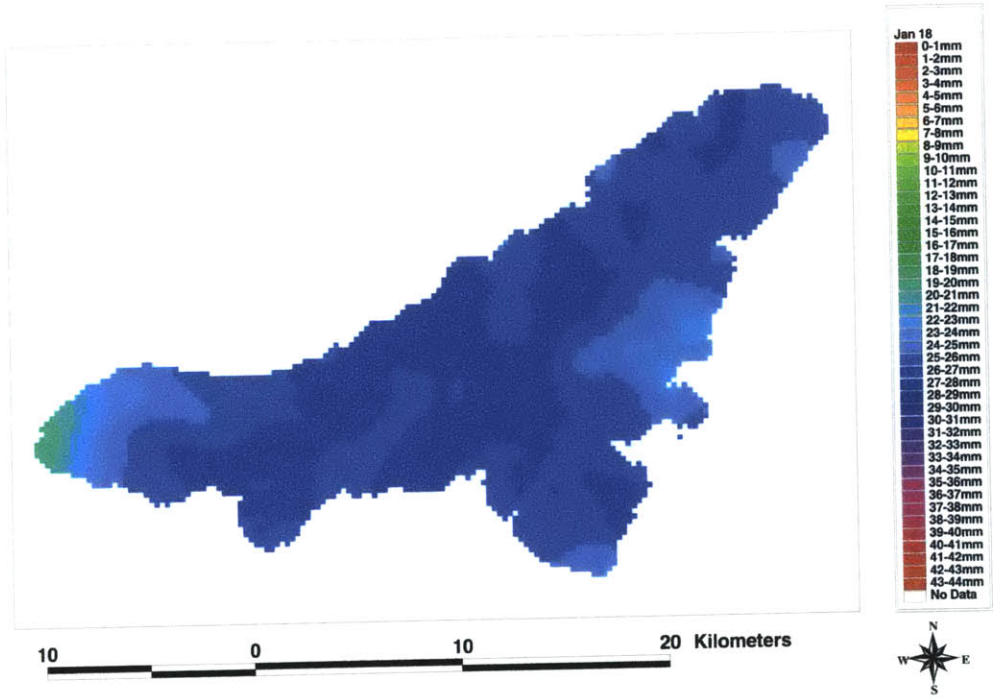

January 23, 1999

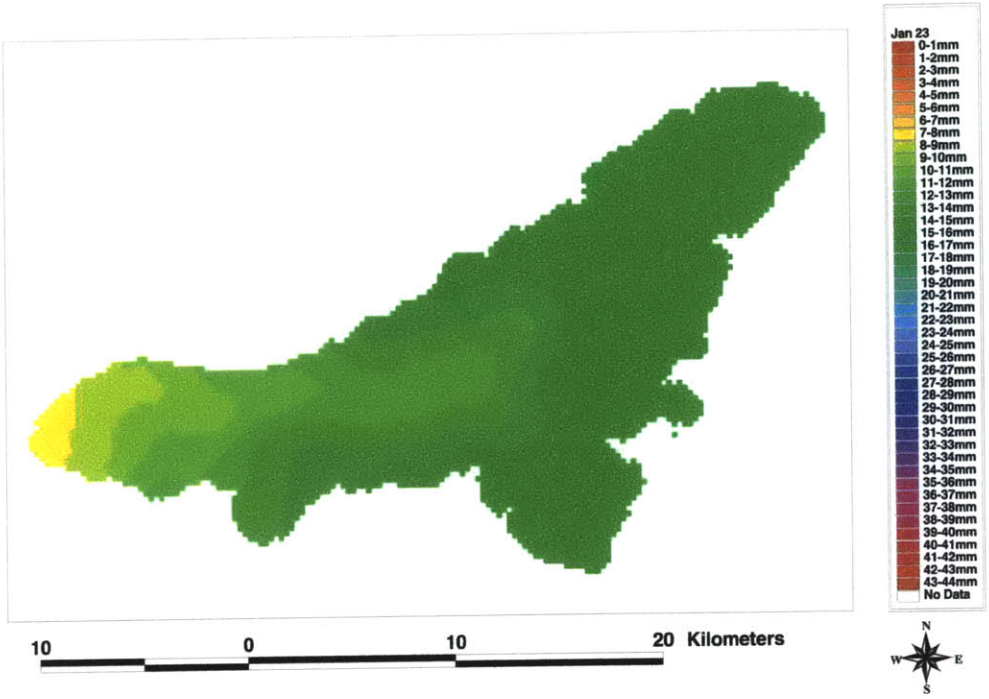

January 24, 1999

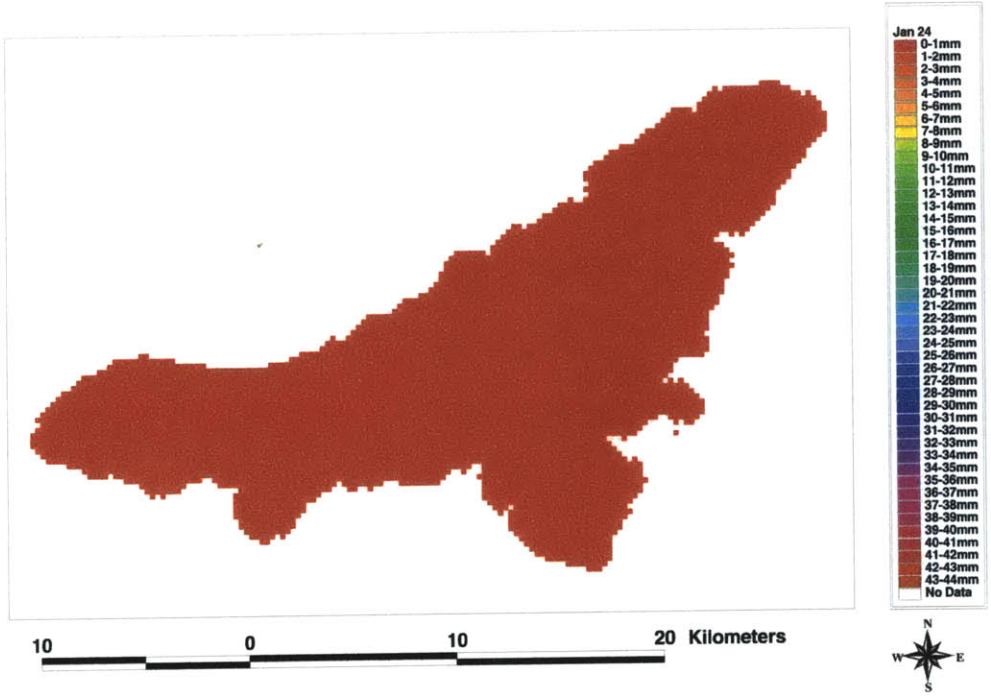

January 19, 1999

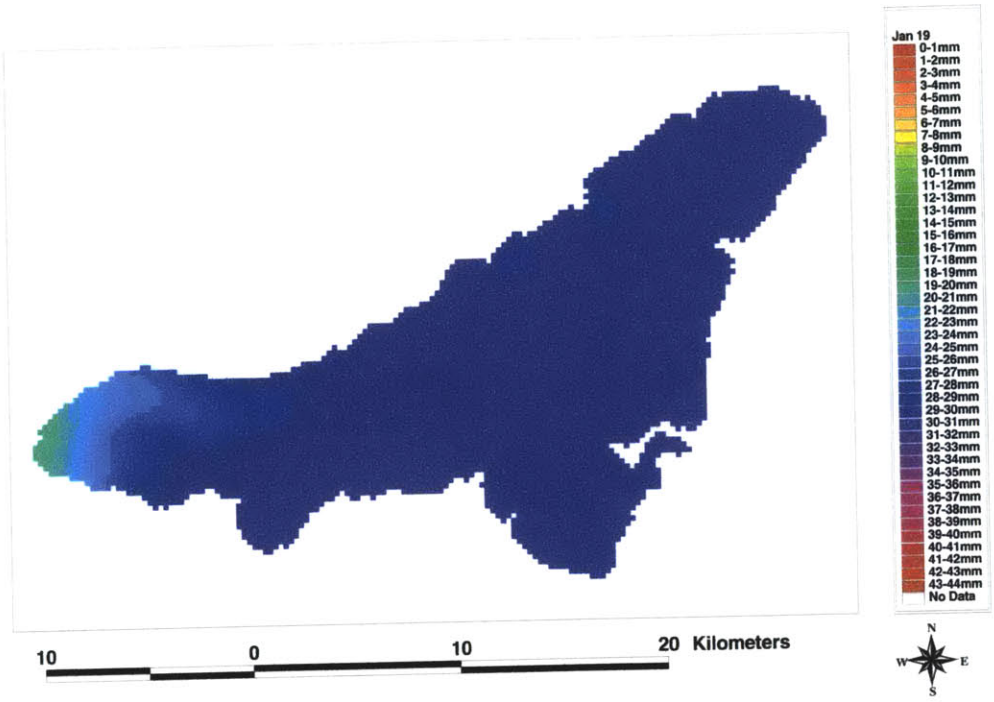

January 20, 1999

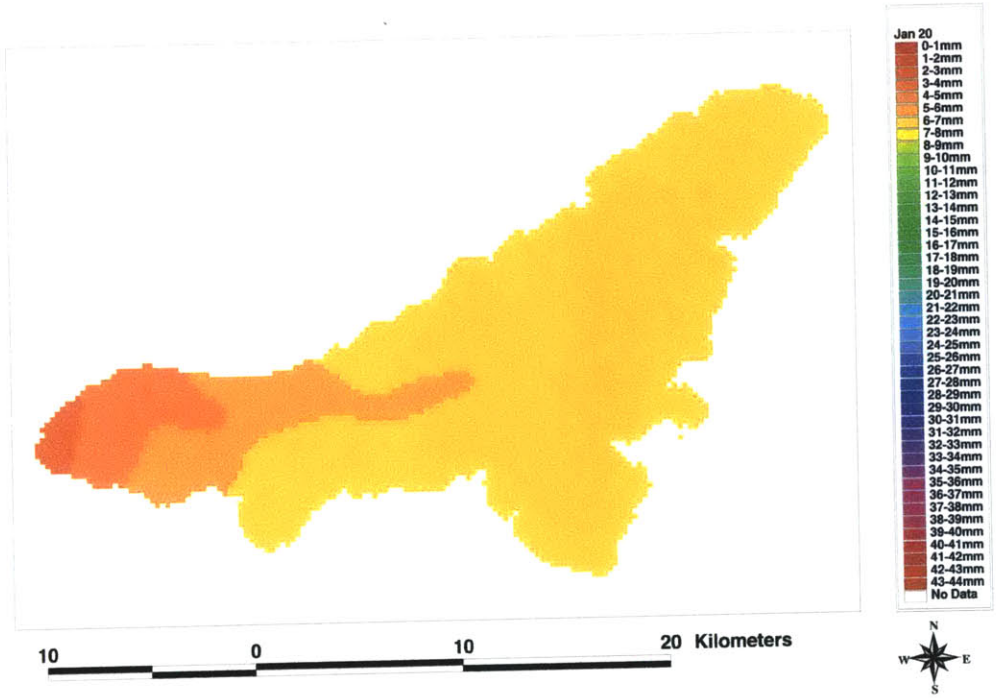

January 23, 1999

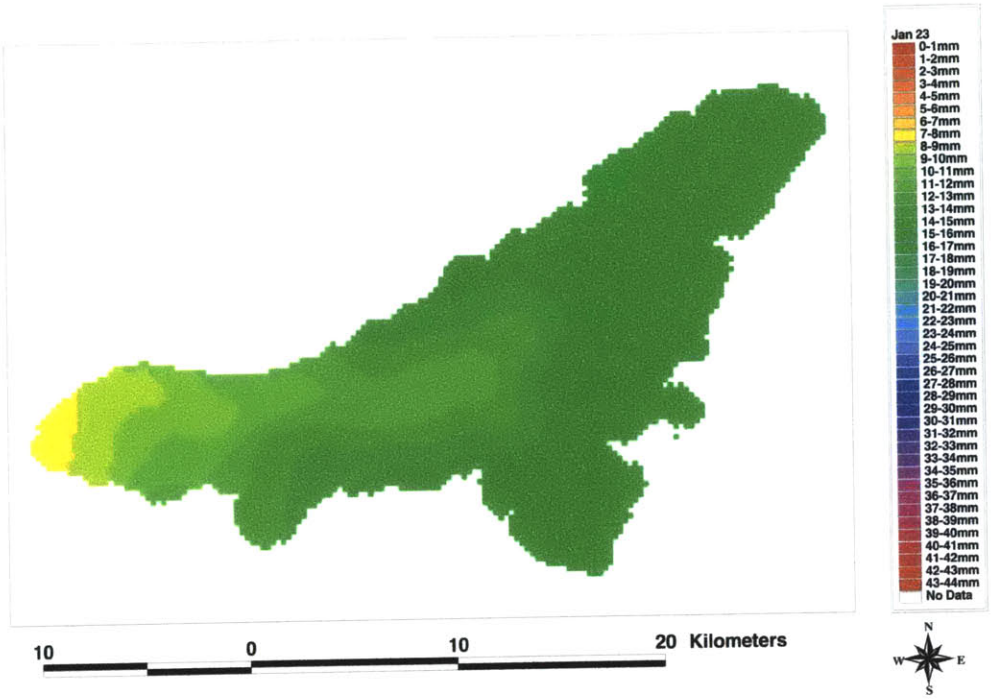

January 24, 1999

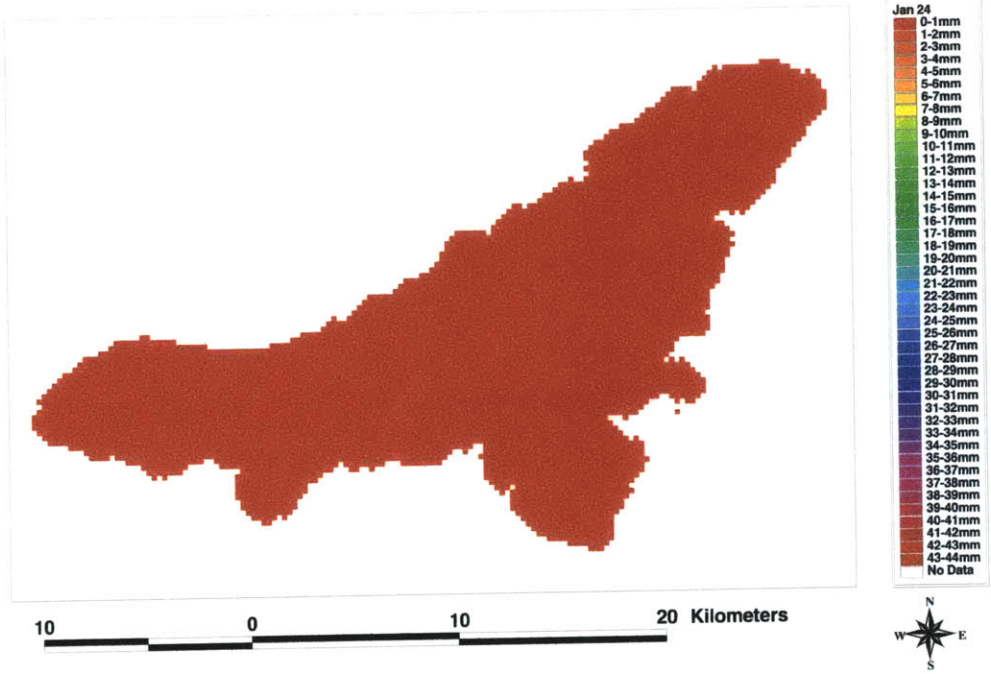

January 27, 1999

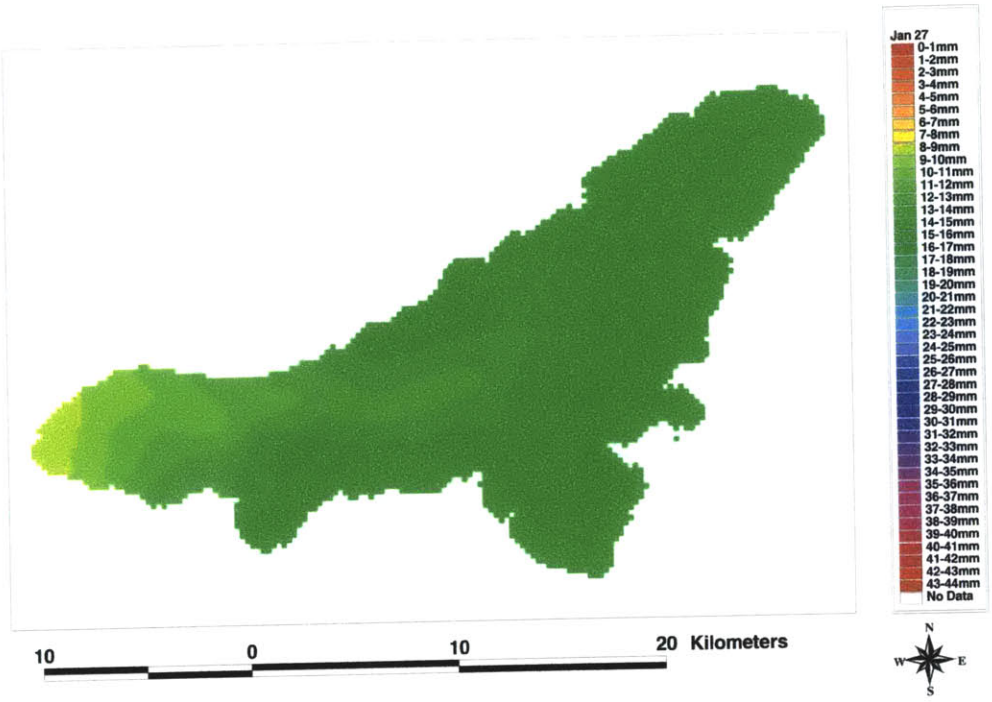

January 28, 1999

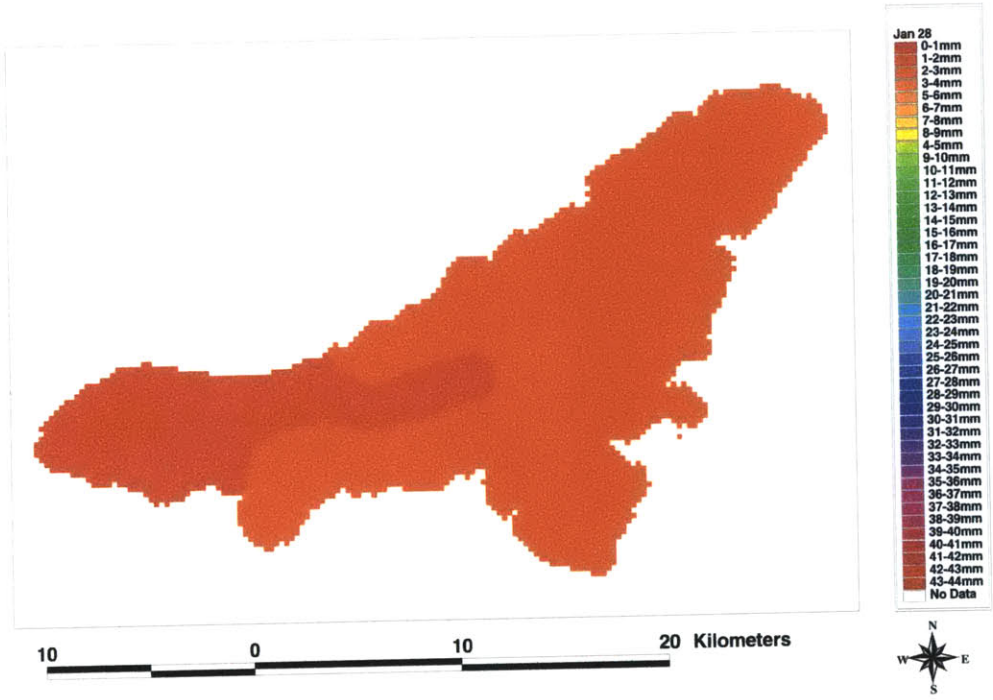

February, 1999
Daily Precipitation Estimation Maps

February 5, 1999

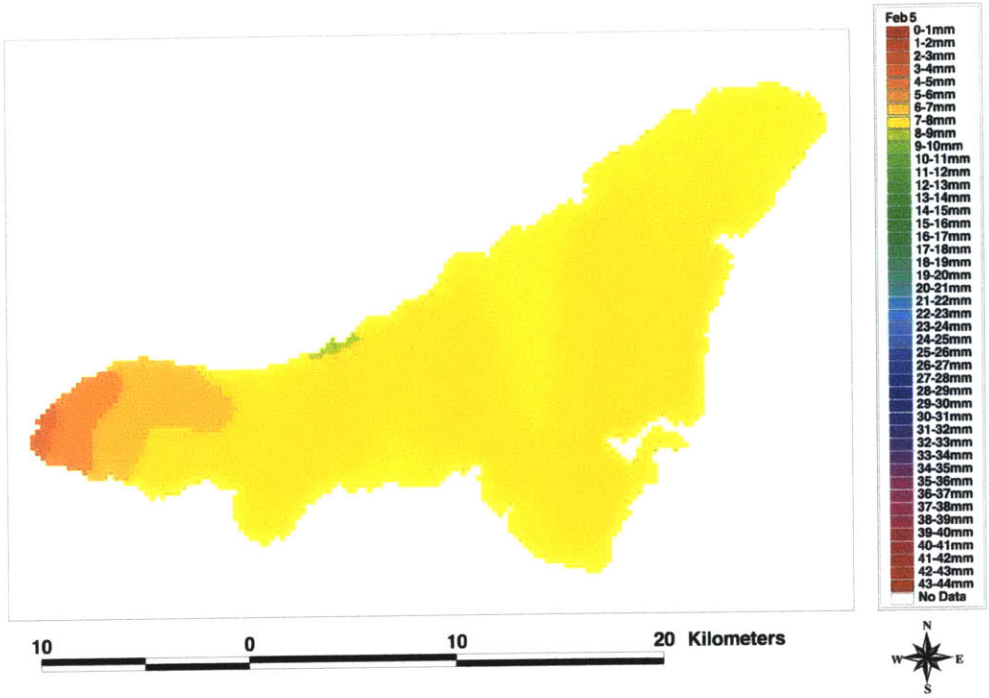

February 6, 1999

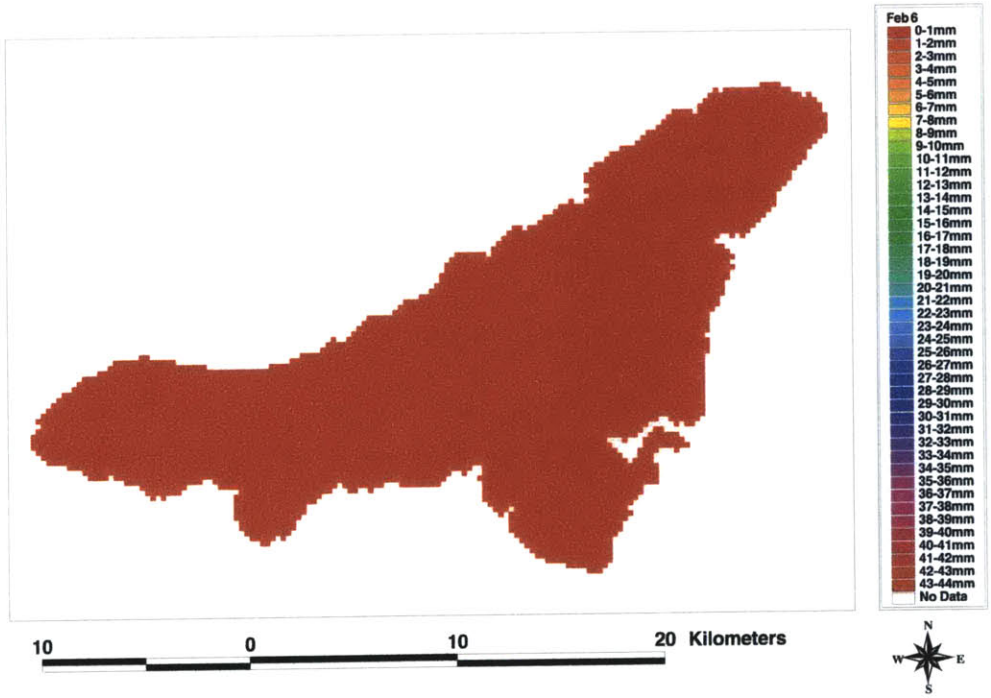

February 7, 1999

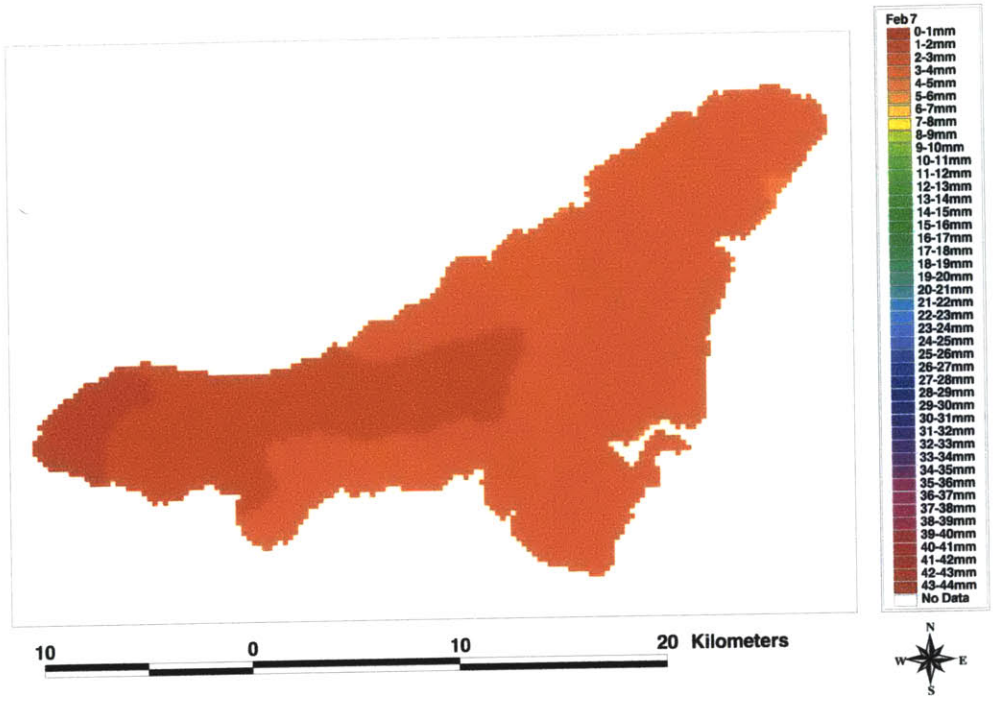

February 8, 1999

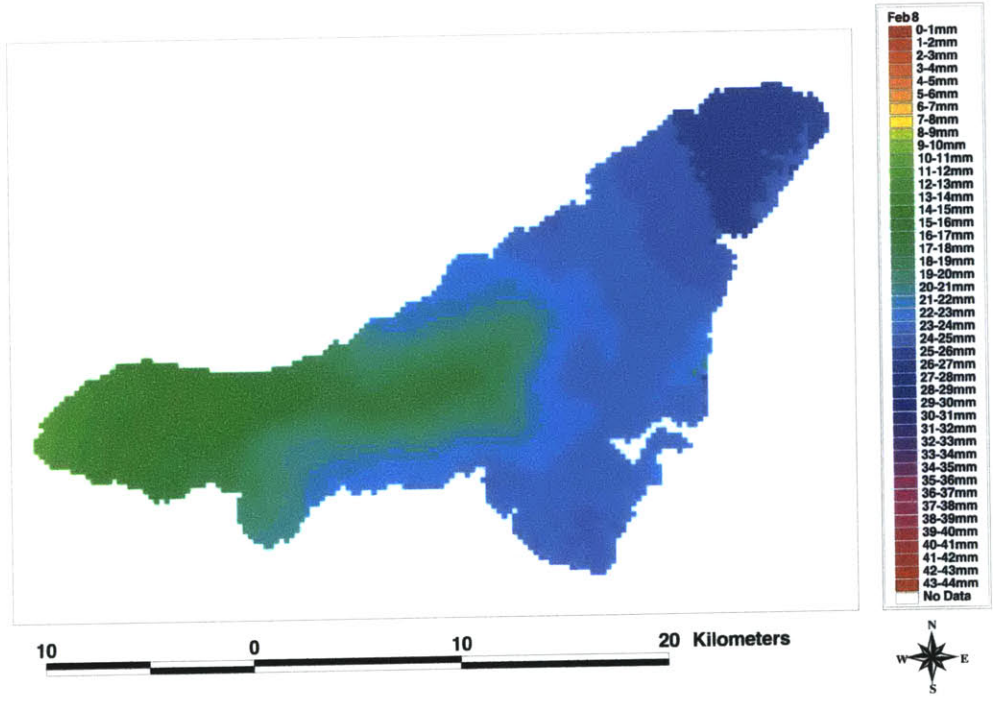

February 18, 1999

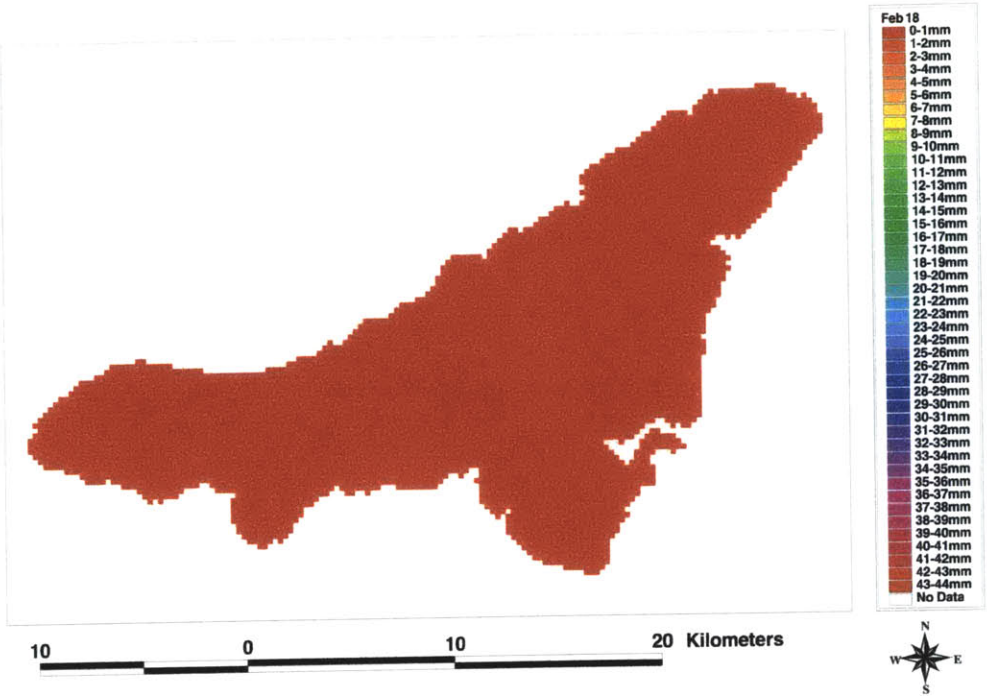

February 19, 1999

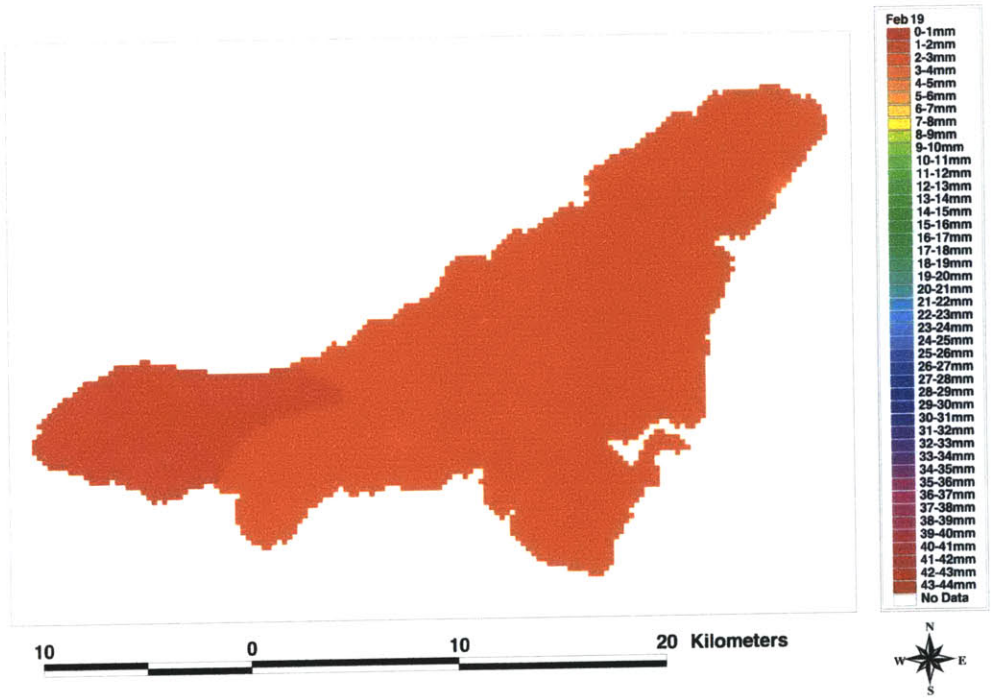

February 20, 1999

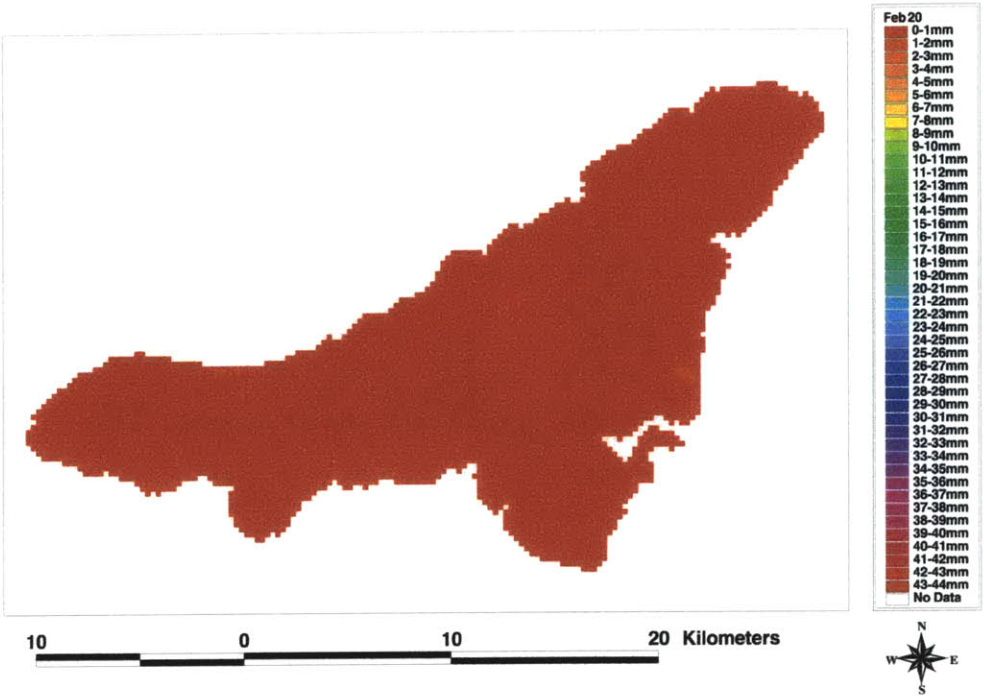

February 25, 1999

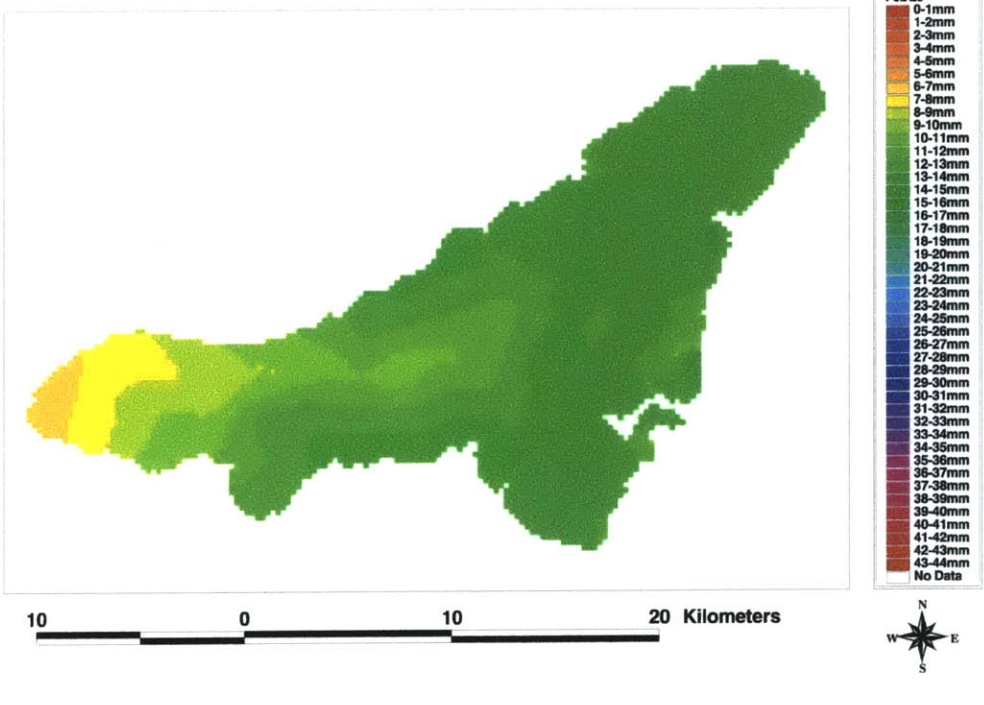

March, 1999
Daily Precipitation Estimation Maps

March 15, 1999

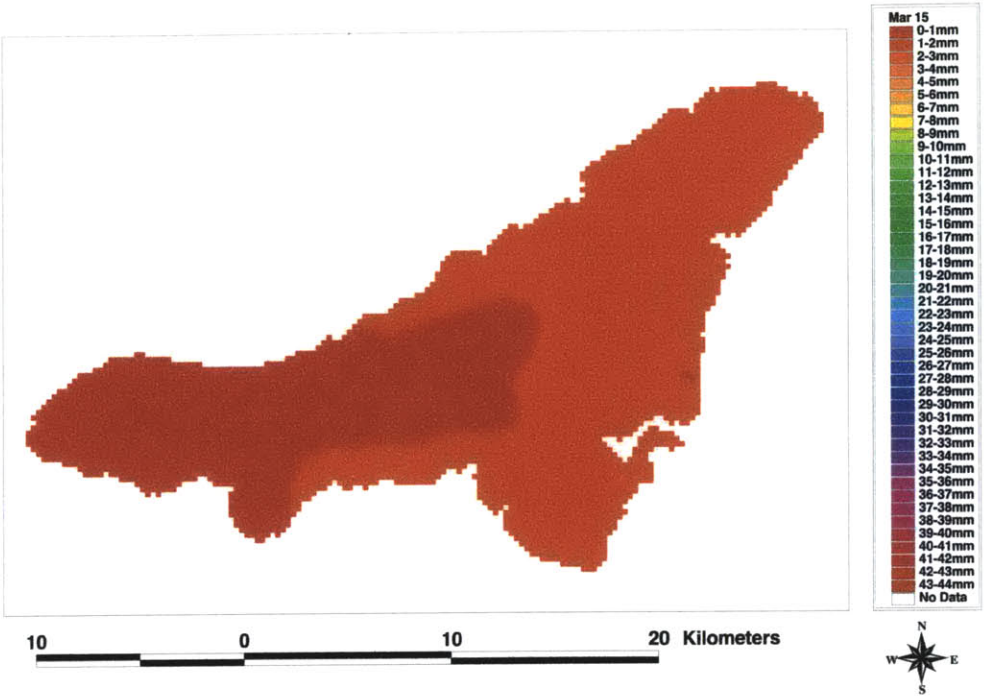

March 20, 1999

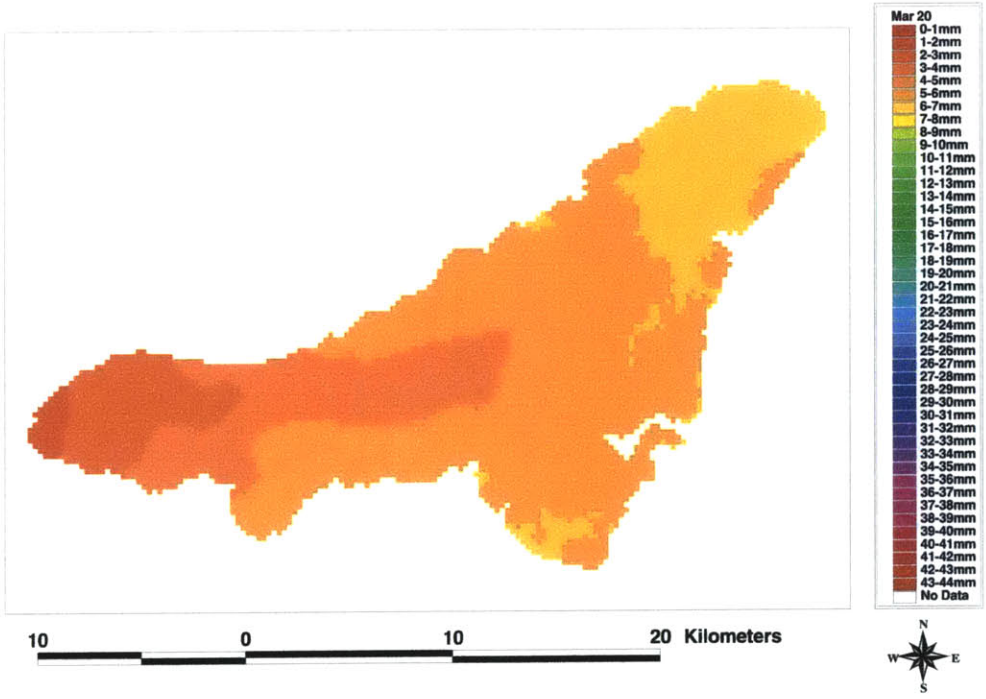

March 21, 1999

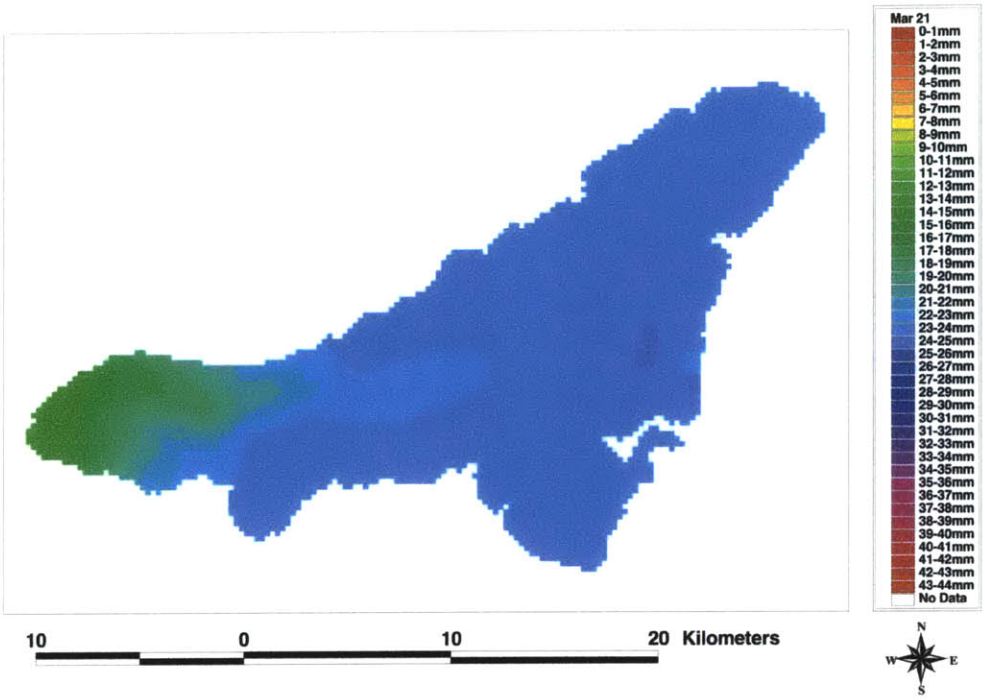

March 22, 1999

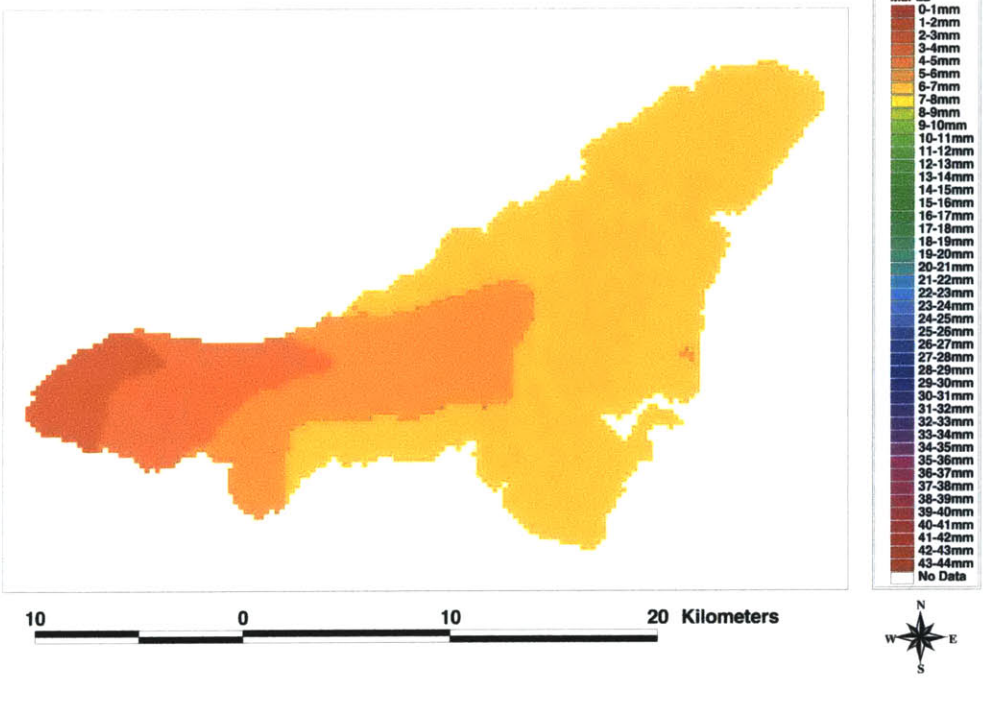

March 23, 1999

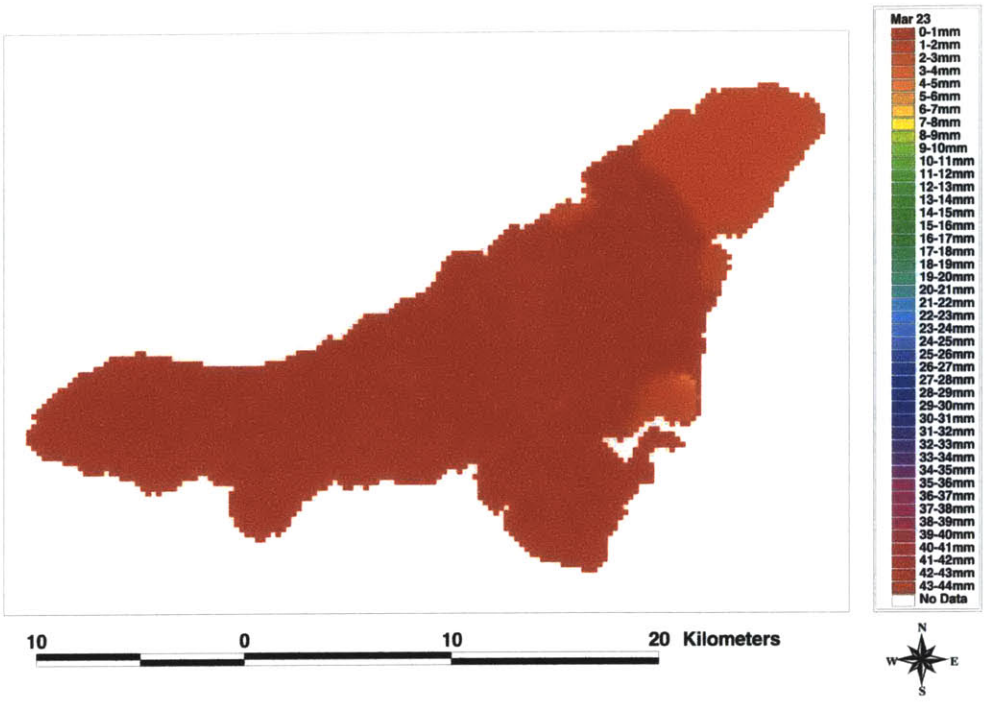

March 25, 1999

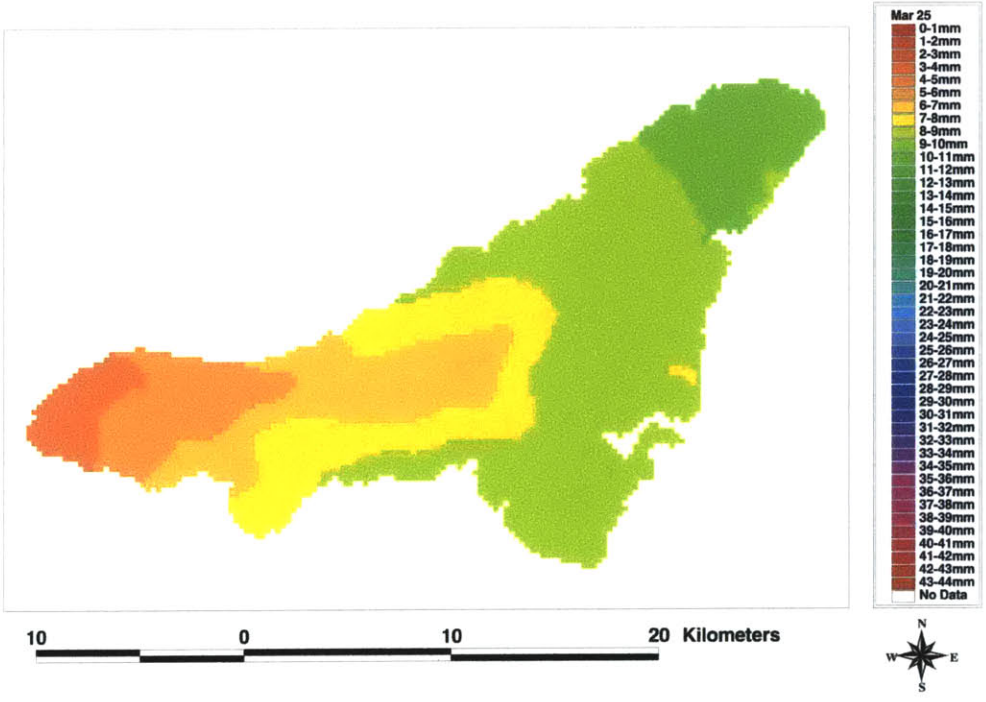

March 26, 1999

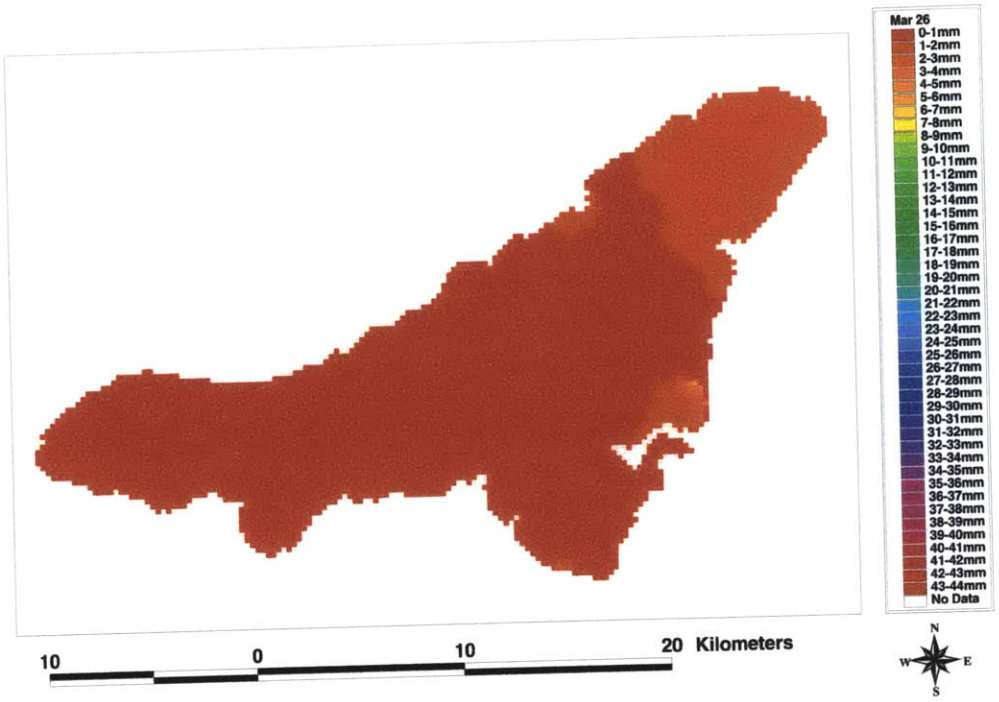

March 29, 1999

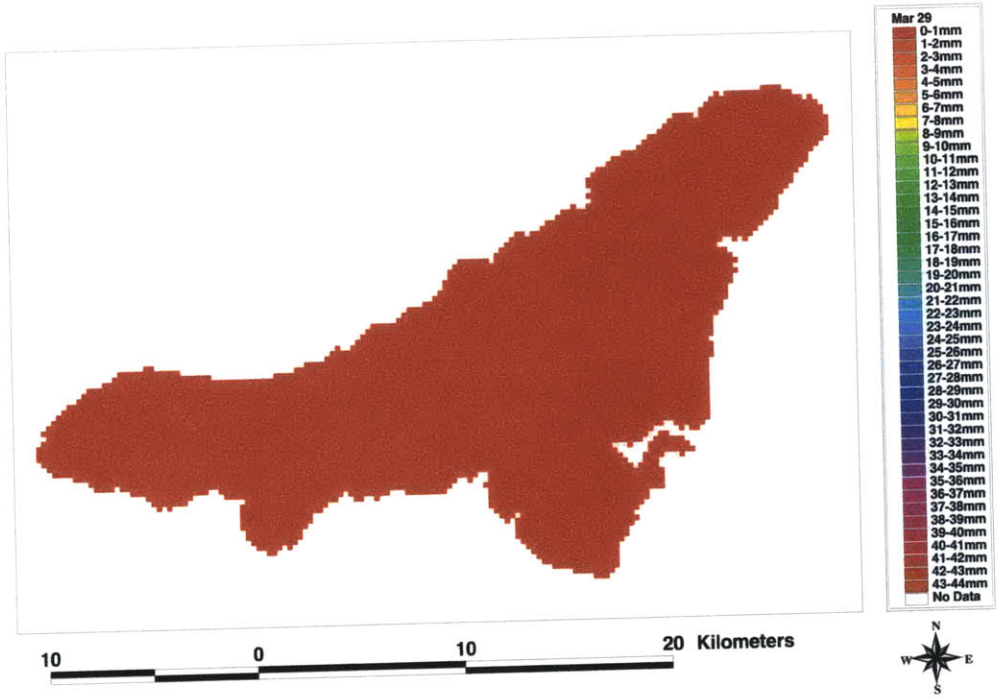

April, 1999
Daily Precipitation Estimation Maps

April 1, 1999

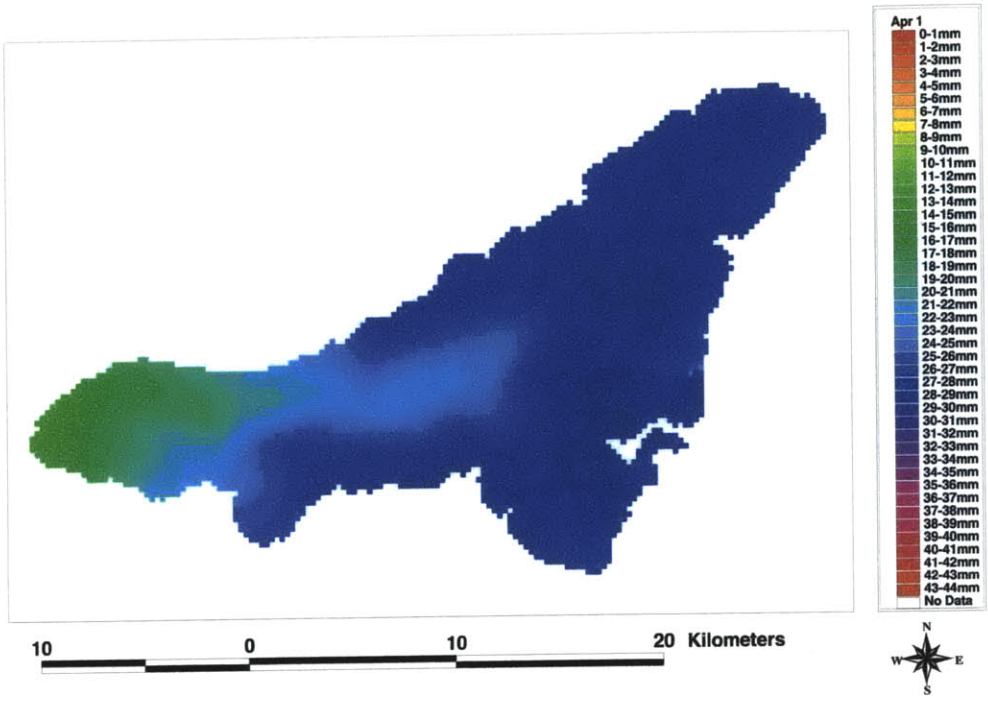

April 2, 1999

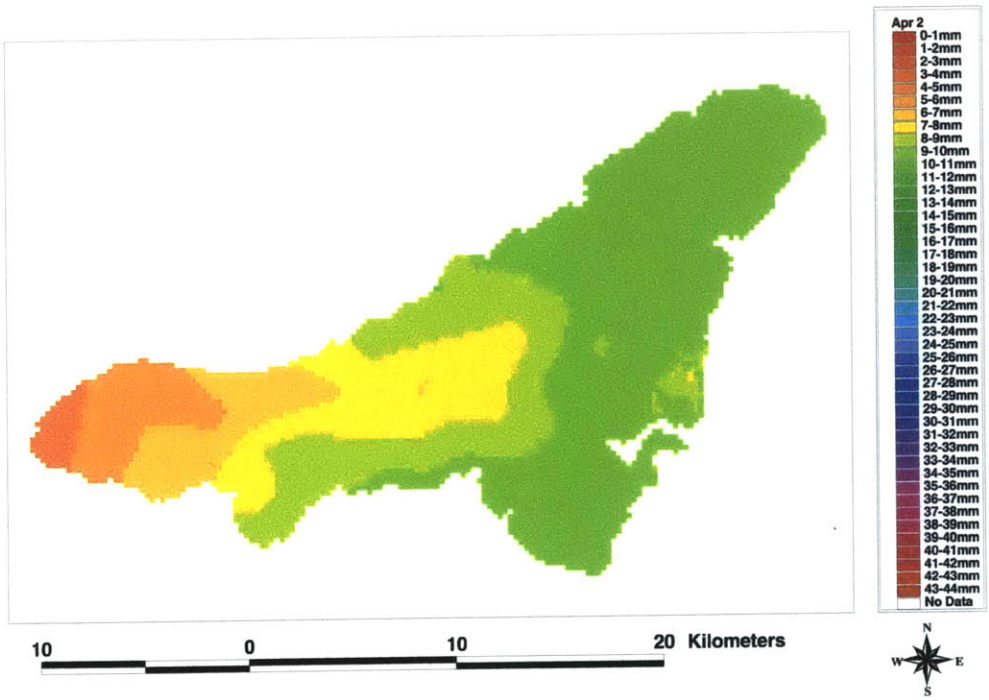

April 7, 1999

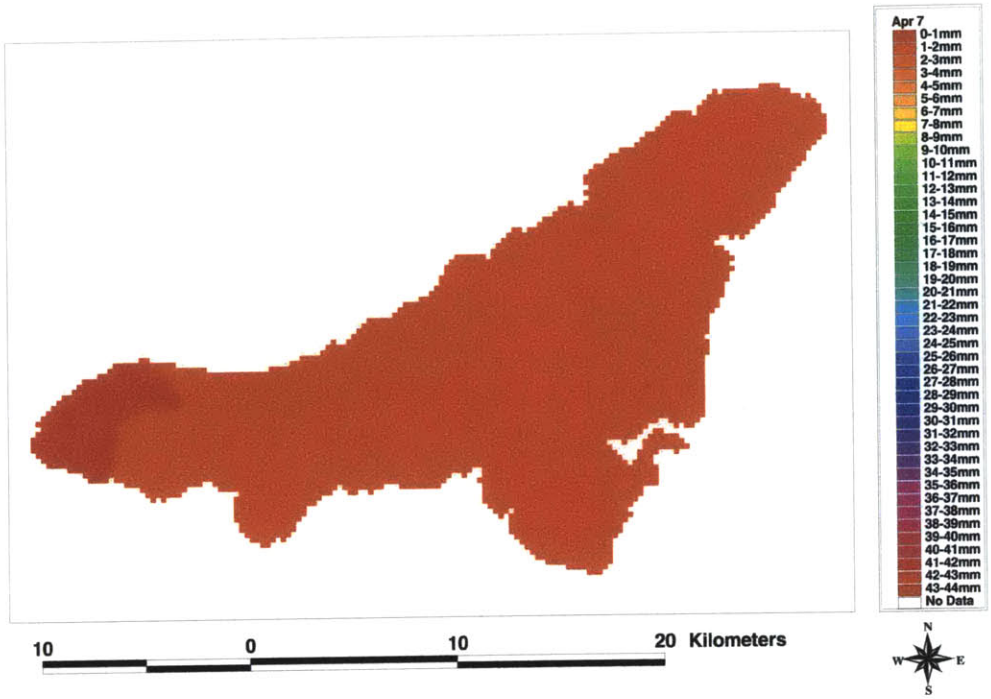

April 8, 1999

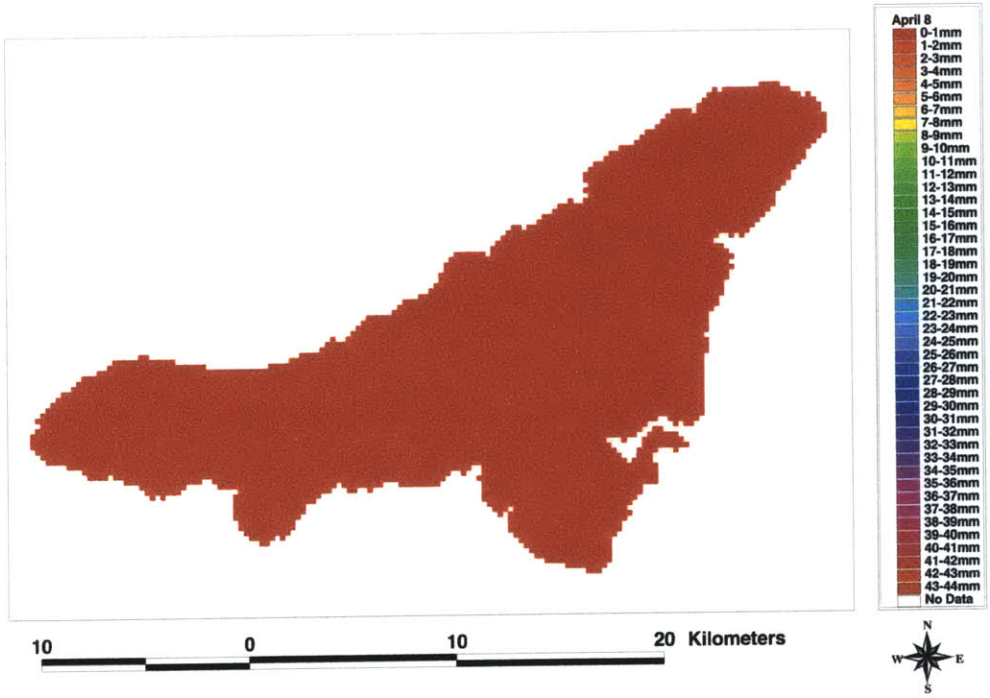

April 12, 1999

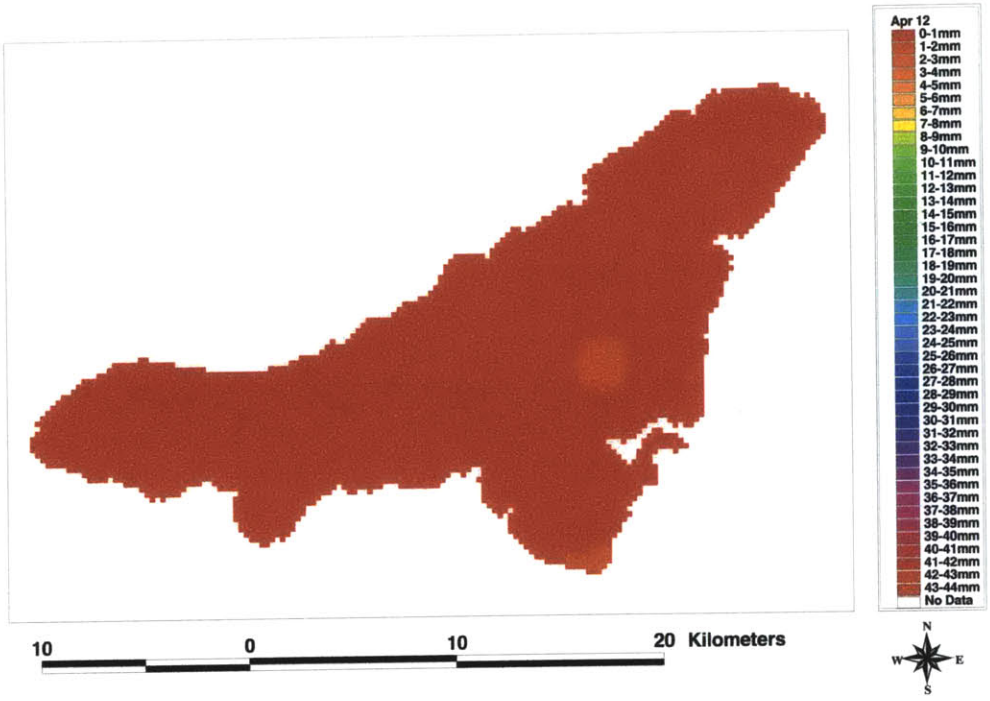

April 13, 1999